



**UNIVERSITA' DEGLI STUDI DI VERONA**

DIPARTIMENTO DI  
MEDICINA E SANITA' PUBBLICA

DOTTORATO DI RICERCA IN  
BIOTECNOLOGIE APPLICATE ALLE SCIENZE BIOMEDICHE

XX CICLO

PHD THESIS

**DEVELOPMENT OF VIRAL VECTOR-MEDIATED RNA  
INTERFERENCE TARGETING SEVERAL P2X RECEPTORS IN  
THE RAT CENTRAL NERVOUS SYSTEM**

S.S.D. BIO/14

Course coordinator: Ch.mo Prof. GUIDO FUMAGALLI

Supervisor: Dr. JOSEPH RIMLAND

PhD student: Dr. CHIARA CAZZIN

## ACKNOWLEDGEMENTS

First of all I would like to thank my course coordinator at the Verona University, Prof. Guido Fumagalli and Dr. Jim Hagan, Head of Biology, Dr. Mauro Corsi, Head of Verona Biology and Dr. Enrico Domenici, Molecular Psychiatry Unit, for giving me the opportunity to carry out this PhD project in collaboration with the Centre of Excellence in Drug Discovery of GlaxoSmithKline Verona (CEDD, GSK).

I would like to thank my supervisor Dr. Joseph Rimland, in the Behavioural Biochemistry Unit, Verona Biology who has followed me during my PhD.

This PhD project was performed in collaboration with several Groups and Institutes whom I would like to acknowledge.

The first part of this project related to the construction and validation of shRNA expressing viral vectors for P2X receptors was conducted in the Gene Interference Group, in the GSK Centre of Stevenage, UK. I would like to thank all the people who have given me the opportunity to work in this fantastic group and who welcomed me with warmth and kindness despite my difficulties with English. In particular, I would like to thank my supervisor in the UK Dr. Christopher J. Ring who has taught me a lot not only professionally but also on a human level.

Thanks Chris for your help and all your kindness: working with you was a great experience!

The second part of this project, related to the *in vivo* viral vector injection in the brain was conducted in Prof. Simonato's Group, in the Department of Clinical and Experimental Medicine, Ferrara University. I would like to thank the entire group and in particular Silvia, Bea, Anna, Manu and Andrea for their friendship and for teaching me a lot.

Part of this work and in particular TaqMan analysis of the injected brain was conducted in the Behavioural Biochemistry Group, Verona Biology, CEDD GSK. I would like to thank Claudio Righetti and Dr. Mario Altieri for their precious technical support.

Infine, il ringraziamento più sentito va a Marco per avermi sempre sostenuto durante questi anni anche nei momenti più difficili ed alla mia famiglia che mi ha accompagnato durante questo lungo percorso.

# RIASSUNTO

L'RNA interference (RNAi) è un meccanismo di silenziamento genico sequenza-specifico, conservato durante il processo evolutivo. Il meccanismo di silenziamento è attivato attraverso la degradazione del mRNA complementare o mediante inibizione del processo trascrittivo o di traduzione. Nelle cellule di mammifero, l'RNAi viene indotto attraverso l'introduzione o l'espressione intracellulare di una molecola di RNA a doppio filamento di 20-22 nucleotidi (chiamata short interfering RNA o siRNA) specifica per l'mRNA bersaglio. Nel passato il processo di ricombinazione omologa in cellule embrionali era il meccanismo più utilizzato per studiare la funzione di un gene di interesse in mammiferi, mediante rimozione o sovraespressione del gene stesso. Questo processo risulta però costoso e non applicabile a molti organismi, inoltre la delezione del gene in esame può portare a processi di compensazione genica o a fenotipi letali. Attualmente l'RNAi è ampiamente impiegato per determinare la funzione di un gene bersaglio sia in sistemi *in vitro* che *in vivo* grazie alla sua elevata versatilità ed efficienza ed è inoltre utilizzato nella ricerca farmaceutica per selezionare potenziali bersagli farmacologici.

Questo progetto di ricerca è stato sviluppato allo scopo di investigare l'applicabilità del meccanismo di RNA interference per il silenziamento genico nel sistema nervoso centrale di ratto sia *in vitro* che *in vivo*. In particolare, il suo impiego nel processo di validazione di un gene d'interesse è stato analizzato in relazione al recettore purinergico P2X7, un gene potenzialmente coinvolto in patologie psichiatriche ed ai due recettori correlati P2X2 e P2X4.

I recettori purinergici P2X2, P2X4 e P2X7 sono membri della famiglia di recettori-canali cationici attivati dall'ATP, permeabili al sodio, potassio e calcio. Questi recettori sono espressi in diverse aree cerebrali nei neuroni, dove sono coinvolti nel rilascio di neurotrasmettitori e nell'attivazione di meccanismi multipli di trasduzione del segnale intracellulare. Il recettore P2X7 risulta inoltre espresso in diverse tipologie di cellule gliali, in cui è coinvolto nella modulazione dei processi neuroinfiammatori e nel rilascio di diverse citochine. Studi farmacologici e di associazione genetica suggeriscono un ruolo potenziale del recettore P2X7 nei disturbi psichiatrici, inclusi la depressione unipolare e bipolare. Nel topo l'inibizione dell'mRNA per P2X7, attraverso RNA antisense, induce un comportamento di tipo depressivo. Studi di associazione genetica indicano una correlazione tra specifici polimorfismi nel gene codificante il

recettore P2X7 e i disordine bipolari (Barden et al., 2004 e 2006). I geni per i recettori P2X2 e P2X4 sono all'interno della stessa regione cromosomica di P2X7 associata con la depressione e i disordini bipolari. P2X2 e P2X4 sono inoltre espressi in specifiche aree cerebrali coinvolte nella depressione, come l'ippocampo, e potrebbero quindi svolgere un ruolo nella patofisiologia della depressione.

Al fine di ottenere la soppressione dei recettori P2X (P2XR), specifiche molecole siRNAs sono state disegnate per ogni gene e sono state poi selezionate per l'attività mediante trasfezione di colture primarie e linee cellulari esprimenti i geni d'interesse. In questo modo la sequenza siRNA più attiva e specifica per ciascun gene è stata selezionata per la produzione di una cassetta esprimente un "short hairpin RNA" o shRNA che porta alla produzione del siRNA di interesse all'interno della cellula. Poiché lo scopo finale di questo progetto era il silenziamento a lungo termine dei recettori P2X nell'ippocampo di ratto, sono stati utilizzati i vettori virali al fine di garantire l'espressione prolungata del siRNA nei neuroni e nella glia. Infatti i vettori virali impiegati possono infettare il tessuto cerebrale con elevata efficienza e persistono episomalmente all'interno della cellula infettata. Per ottenere l'espressione dei siRNAs nei neuroni, i vettori virali Adeno-associati (AAV) esprimenti shRNA (AAV-shRNA) sono stati prodotti per ciascun gene bersaglio, poiché questi vettori possono infettare i neuroni con elevata efficienza. Inoltre, vettori Adenovirali 5 (Ad5)-shRNA sono stati generati per investigare l'effetto della soppressione di P2X7 nelle cellule gliali. Infatti questi vettori virali infettano preferenzialmente la glia. Per selezionare i vettori più attivi e specifici in grado di sopprimere l'espressione dei recettori P2X *in vivo*, i vettori virali sono stati inizialmente testati *in vitro* in colture primarie. I vettori AAV2/6-shRNA sono stati validati mediante infezione di neuroni ippocampali. Una riduzione massima del 80-90% del mRNA dei recettori P2X è stata osservata mediante analisi TaqMan delle cellule infettate. È stato inoltre identificato un vettore Ad5-shRNA in grado di sopprimere del 80% l'espressione del mRNA per P2X7 in astrociti primari di ratto. Dati preliminari hanno dimostrato una diminuzione nel profilo funzionale del recettore P2X7 in cellule microgliali infettate con il vettore Ad5-shRNA. Questi dati hanno indicato una riduzione statisticamente significativa del recettore bersaglio in seguito all'infezione con vettori virali esprimenti shRNA *in vitro*.

Poiché le principali evidenze sperimentali, comprendenti sia studi preclinici che genetici, supportano il coinvolgimento del recettore P2X7 nella pato-fisiologia della depressione, il lavoro *in vivo* è stato focalizzato su questo gene. Pertanto sia i vettori

virali AAV2/6- che Ad5-shRNA-P2X7 sono stati microinfusi in ippocampo di ratto utilizzando aghi di vetro. Questa metodica di microiniezione e' stata selezionata in quanto in grado di indurre un livello minimo di danno anatomico nel sito di iniezione. In seguito all'infusione dei vettori virali, la soppressione del gene bersaglio e' stata investigata. Nel lavoro *in vivo* e' stata dimostrata con successo l'infezione rispettivamente di neuroni e cellule gliali in seguito all'iniezione nella regione ippocampale del giro dentato (DG) con i vettori virali AAV2/6- e Ad5-shRNA. Inoltre una riduzione statisticamente significativa del mRNA per P2X7 e' stata rilevata mediante ibridazione in situ nei campioni iniettati con AAV-P2X7-shRNA rispetto al controllo. Una tendenza simile e' stata riscontrata nei campioni iniettati con vettore Ad5-P2X7-shRNA.

In conclusione, in questo studio sono stati generati e validati vettori virali esprimenti shRNA attivi e specifici, in grado di sopprimere l'espressione del gene bersaglio in cellule neuronali sia *in vitro* che *in vivo*.

# INDEX

<b>ACKNOWLEDGEMENTS</b> .....	<b>2</b>
<b>RIASSUNTO</b> .....	<b>3</b>
<b>1. SUMMARY</b> .....	<b>8</b>
<b>2. INTRODUCTION</b> .....	<b>10</b>
2.1 P2X RECEPTOR FAMILY .....	11
2.1.1 ATP function .....	12
2.1.2 P2Y receptor family.....	13
2.1.3 P2X receptor family.....	14
2.1.3.1 P2XR structure and pharmacology .....	15
2.1.3.2 P2XR localization .....	18
2.1.3.3 P2XR involvement in neuronal function .....	21
2.1.3.5. P2XR in glia .....	23
2.1.3.6 Pathological role of the P2XR in the nervous system.....	24
2.2. RNA INTERFERENCE .....	27
2.2.1 RNA interference discovery.....	28
2.2.2 The mechanism of gene silencing by RNAi .....	30
2.2.3 Designing siRNA .....	32
2.2.4 Delivery of siRNA .....	33
2.2.5 Viral vectors as delivery agents.....	37
2.2.6 Viral vector microinjection into the brain .....	40
2.2.7 RNAi in neurons .....	43
<b>3. MATERIALS AND METHODS</b> .....	<b>50</b>
3.1 IN VITRO WORK .....	51
3.1.1. Cell cultures .....	51
3.1.2 Primary cells .....	51
3.1.3 siRNA design and transfection .....	52
3.1.4 shRNA design, cloning and transfection .....	52
3.1.5 AAV and Ad vector production .....	53
3.1.6 Cell infection .....	55
3.1.7 TaqMan analysis.....	56
3.1.8 Western blot for P2X receptors detection .....	56
3.1.9 Immunocytochemistry (ICC) analysis .....	57
3.1.10 IL-1 $\beta$ release ELISA.....	58
3.2 <i>IN VIVO</i> EXPERIMENTS .....	59
3.2.1 Glass needle preparation .....	59
3.2.2 Animal handling .....	59
3.2.3 Surgery .....	59
3.2.4 Trypan blue visualization .....	61
3.2.5 TaqMan analysis.....	61
3.2.6 Histology and immunohistochemistry .....	62
3.2.7 Non radioactive in situ hybridization .....	63
3.2.7.1 Probe preparation .....	63
3.2.7.2 Perfusion and tissue processing.....	64
3.2.7.3 Hybridization .....	64
3.2.7.4 Post-hybridization and detection .....	65
3.2.8 Oligo radioactive in situ hybridization.....	65
3.3 STATISTIC ANALYSIS .....	67
3.4 TAQMAN PRIMER AND PROBE AND OLIGO SEQUENCES.....	67

<b>4. RESULTS</b> .....	<b>68</b>
4.1 SHRNA GENERATION AND VALIDATION <i>IN VITRO</i> .....	69
4.2 VIRAL VECTOR VALIDATION IN VITRO.....	78
4.3 VALIDATION OF VIRAL VECTORS <i>IN VIVO</i> .....	86
<b>5. DISCUSSION AND CONCLUSIONS</b> .....	<b>100</b>
<b>6. REFERENCES</b> .....	<b>110</b>

# 1. SUMMARY

RNA interference (RNAi) is an evolutionarily conserved process of sequence-specific post-transcriptional gene silencing that is triggered by double-stranded short interfering RNA (siRNA). At present RNAi has become an important and widely used tool for evaluating target gene function both *in vitro* and *in vivo* and has been used for the screening of potential therapeutic targets in pharmaceutical research.

This project has been carried out in order to investigate the applicability of RNA interference for target gene suppression in the rat central nervous system (CNS) both *in vitro* and *in vivo*. In particular its application in the process of target validation has been evaluated focusing on the purinergic receptor P2X7, a putative target for mood disorders and the two related receptors P2X2 and P2X4.

The purinergic receptor P2X7 together with the P2X2 and P2X4 receptors are members of the ATP-gated cation channel family permeable to sodium, potassium and calcium. These receptors are expressed in neurons in many regions of the brain where they play a role in release of neurotransmitters and activation of multiple intracellular signaling pathways. The P2X7 gene is also expressed in several types of glia where it is involved in the modulation of neuroinflammatory processes and cytokine release.

In order to obtain P2X receptor (P2XR) suppression, specific siRNAs were designed for each gene and screened for activity by transfecting both primary cells and cell lines expressing the target genes. In this way the most active and specific siRNA sequence for each gene was selected for the production of a short hairpin RNA (shRNA) cassette leading to intracellular production of the targeting siRNA sequence. Viral vectors have been used for long term siRNA expression in neurons and glia in the brain since these vectors can efficiently transduce brain tissue and persist episomally within the infected cell. In order to drive siRNA expression in neuronal cells, Adeno-associated viral vectors (AAV) containing an shRNA cassette were produced for each target gene, since these vectors can infect neurons with high efficiency. Adenovirus 5 (Ad5)-shRNA vectors targeting P2X7 were also produced to investigate the effects of P2X7 suppression in glia since these viral vectors preferentially infect glia. As a filter to select the most active and specific viral vectors that could down-regulate P2XRs *in vivo*, viral vectors were first tested *in vitro* in primary cells. The AAV2/6-shRNA vectors were evaluated by infecting hippocampal neurons. A maximum of 80-90% down-regulation of P2XR mRNA was observed by TaqMan analysis of the infected cells. An active



Ad5-shRNA vector able to suppress of 80% P2X7 mRNA expression in cultured rat astrocytes was also identified. Preliminary data demonstrated a statistically significant decrease in P2X7 function in Ad5-shRNA infected microglial cells. These data indicate the suppression of target receptor after shRNA viral vector delivery *in vitro*.

Both the AAV2/6- and Ad5-shRNA-P2X7 viral vectors were then microinfused into rat hippocampus through glass needles. Transduction of neurons and glia respectively after infection of the dentate gyrus (DG) region of the hippocampus by AAV2/6- and Ad5-shRNA vectors was demonstrated. Moreover a statistically significant down-regulation of P2X7 mRNA in AAV-P2X7-shRNA injected DG compared to controls was revealed by *in situ* hybridization. A similar trend was observed in the Ad5-P2X7-shRNA injected samples.

In conclusion, in this study active and specific shRNA-viral vectors able to suppress target gene expression in neuronal cells both *in vitro* and *in vivo* were generated and validated.

## **2. INTRODUCTION**

## 2.1 P2X RECEPTOR FAMILY

Adenosine 5'-triphosphate (ATP) is one of the first molecules to appear in the evolution of biological systems as an energy source and as an essential component of nucleic acids. In addition, during the past 25 years, ATP has become accepted as an important neurotransmitter/cotransmitter in both peripheral and central neurons (Norenberg and Illes, 2000). The first report about the potent actions of adenine-based compounds was published by Drury and Szent-Gyorgyi in 1929, who discovered that adenylic acid and adenosine produced sinus bradycardia, complete atrioventricular block, a negative inotropic effect on the atrium and cessation of atrial fibrillation in the mammalian heart. After more than a decade, Burnstock and his colleagues observed a non-adrenergic and non-cholinergic element in the autonomic nervous system and proposed that ATP acted as a neurotransmitter and cotransmitter in the peripheral and central nervous systems. This finding was confirmed and extended over the subsequent two decades, when ATP-evoked synaptic potentials were recorded in neurons in both the central and peripheral systems. Implicit in the concept of purinergic transmission was the existence of post-junctional receptors for ATP. In 1978 Burnstock and colleagues proposed the subdivision of purinergic receptors into P1 purinoreceptors activated by adenosine and P2 purinoreceptors which are preferentially activated by ATP and ADP. The implication deriving from the existence of these two families of receptors is that, during purinergic transmission, ATP released from nerve terminals acts on postsynaptic P2 receptors with an excitatory effect while adenosine generated from the extracellular breakdown of ATP by ectonucleotidases, acts largely via P1 receptors on nerve terminals to inhibit the release of neurotransmitter (Burnstock 1996). At the moment there are four subtypes of P1 receptors cloned, namely A1, A2A and A2B and A3. All P1 receptors couple to G proteins and present the same typical 7  $\alpha$ -helix transmembrane domain structure. The P2 receptors are classified in two types based on their different molecular structure and different activation times and distance of action. Fast excitatory synaptic responses are mediated by P2X receptors comprising a family of at least seven receptor subunits (P2X1-7). Slow changes in membrane potential is mediated by P2Y receptors, a family of G-protein coupled receptors bearing seven transmembrane  $\alpha$ -helices activated by purine and/or pyrimidine nucleotides. This classification of ATP receptors is in line with the receptors of most of other

neurotransmitters such as of acetylcholine (ACh),  $\gamma$ -amino butyric acid (GABA) and glutamate, where ligand-gated and G protein-mediated receptor sub-classifications have already been established.

### **2.1.1 ATP function**

As previously said, there is now considerable experimental support that ATP acts as a cotransmitter with classical neurotransmitters and neuropeptides in the peripheral and central nervous systems. ATP participates in non-adrenergic/non-cholinergic inhibitory neurotransmission in various regions of the gastro-intestinal tract with vasopressin intestinal peptide (VIP) and nitric oxide (NO). Both noradrenaline (NA) and ACh appear to be cotransmitters with ATP in various peripheral and central synaptic terminals (Burnstock, 1996). ATP has also been shown to be a cotransmitter with 5-hydroxytryptamine (5-HT), glutamate, dopamine and GABA in the CNS (Illes and Ribeiro, 2004). Moreover ATP mediates fast excitatory synaptic transmission in some regions of the central nervous system through activation of P2X receptors (Rubio and Soto, 2001).

ATP, mainly through P2Y receptor subtypes, has been shown to regulate ion transport in epithelial cells. There is experimental evidence that both P2Y and P2X receptors inhibit platelet aggregation, while P2X receptors expressed on smooth muscle cells could mediate vasoconstriction (Burnstock, 1996). The involvement of ATP in the initiation of pain is mainly mediated by P2X3 receptors which are predominantly localized in the subpopulation of small nociceptive sensory neurons in dorsal root ganglia. Down-regulation of P2X3 receptors in a model of inflammatory and neuropathic pain leads to inhibition of the development of mechanical hyperalgesia as well as reversal of established hyperalgesia (Dorn et al., 2004). Purines and pyrimidines can both stimulate the progression of cells through the cell cycle and inhibit cell growth, depending upon their concentrations, the target cells and the expression of specific P1 or P2 receptor subtypes. ATP and adenosine have been claimed to play roles in the cytological changes and morphogenetic movements occurring during early embryogenesis not only as a source of energy, but also as key regulators in differentiation and maturation and in the acquisition of highly specialized functions (Burnstock 2001).

Following ischaemic and traumatic insults purines seem to play a role in limiting damage and in favoring repair mechanisms to restore physiological functions. Massive amounts of ATP are rapidly released during ischaemia and hypoxia in the cardiovascular system and CNS. Some of the responses to ATP released during brain injury are neuroprotective but in some circumstances ATP contributes to the pathophysiology initiated after trauma (Neary et al., 2003). It also plays a role in long-term trophic events after ischaemia mainly through activation of glial cells. Multiple P2 receptor subtypes are expressed by glial cells. Both ATP and adenosine induce astroglial cell proliferation and formation of reactive astrocytes. Purinergic receptors are also expressed on inflammatory and immune cells. ATP is involved in the development of inflammation through a combination of actions such as induced release of cytokines from immune cells and histamine from mast cells. In contrast adenosine provokes anti-inflammatory effects (Burnstock, 2001).

### **2.1.2 P2Y receptor family**

Currently, ten P2Y receptor subtypes have been cloned and display 19–55% sequence identity at the protein level. The predicted structure of P2Y receptors includes an extracellular N terminus containing several potential N-linked glycosylation sites, seven transmembrane spanning regions that assist in forming the ligand binding pocket, and an intracellular C terminus that contains several consensus binding/phosphorylation sites for protein kinases. A quantitative RT-PCR study indicated the presence of large quantities of P2Y1 and P2Y11 mRNA in the human brain when compared with other tissues. Like other members of the G-protein coupled receptors superfamily, P2Y receptor stimulation leads to activation of heterotrimeric G proteins and their dissociation into  $\alpha$  and  $\beta\gamma$  subunits that can then interact with a variety of effector proteins. Individual P2Y receptor subtypes have been linked to one or more of the four subfamilies of heterotrimeric G proteins (Gs, Gi/o, Gq/11, and G12/13) (Illes and Ribeiro, 2004).

There are several pieces of experimental evidence for the involvement of P2Y receptors in ATP-mediated neurotransmitter release both in the peripheral and central nervous systems. In particular in cerebral cortical and hippocampal slices it was reported that P2Y-like receptor activation inhibits noradrenaline release. Moreover from experimental results it was suggested that P2Y2 receptor-types couple to recombinant

K<sup>+</sup> channels. In addition to these effects, P2Y receptors are also able to potentiate the conductance of ionotropic glutamate receptors of the N-methyl-D-aspartate (NMDA)-, but not of the α-amino-3-hydroxy-5-methyl-4-isoxazole propionic acid (AMPA)-type in pyramidal neurons of the rat prefrontal cortex (Illes and Ribeiro, 2004).

### **2.1.3 P2X receptor family**

The P2X family is the most ubiquitous ligand-gated channel family yet cloned and these receptor-types have been identified on autonomic nerve endings and on a limited population of neurons in the central nervous system (CNS) both on somatodendritic and presynaptic sites (North, 2002). P2X receptors are ATP-gated cation-selective channels that mediate sodium influx, potassium efflux and, to varying extents, calcium influx, leading to depolarization of the cell membrane. Membrane depolarization subsequently activates voltage-gated calcium channels, causing accumulation of calcium ions (Ca<sup>2+</sup>) in the cytoplasm. Currently, seven human P2X receptor subunits (P2X1–7) have been cloned containing 379 to 595 amino acids and display 30–50% sequence identity at the protein level. The predicted structure of the P2X subunits is a transmembrane protein with two membrane spanning domains (TM1 and TM2) that are involved in gating the ion channel and lining the ion pore, respectively, a large extracellular loop containing the ATP binding site, as well as intracellular N and C terminal tails. Native receptors may occur as homo- or heteropolymers, potentially of trimeric structure. The P2XRs present a low number of conserved aminoacids within the family and with other cationic channel families and also a different cationic permeability between different members.

Within the P2X receptors family, the P2X7 has a distinguished role for several reasons. First, this receptor seems to function only in homo-oligomeric form and is activated by relatively high concentrations of ATP. Second, this receptor was known previously as P2Z receptor, the “cell death receptor”. Its prolonged activation elicits the opening of a transmembrane pore, permeable to large molecular weight molecules up to 800 dalton (Da), leading to cellular death. In addition, in spite of being cloned originally from the rat brain, P2X7 receptor was suggested to be expressed predominantly on antigen-presenting immune cells and epithelia, functioning as an immunomodulatory receptor (Surprenant et al., 1996). Several data confirms that P2X7 receptor regulates many aspects of immune function in immunocompetent cells. It participates in the regulation of the expression and secretion of cytokines and

inflammatory mediators and is involved in the direct effectors function of immune cells, such as multinuclear giant cell formation and mycobacterium killing (Ferrari et al., 1997). However, in the past few years the potential role of this receptor in neuronal functions was suggested. Although debate has emerged on the cell-type specific localization of P2X7 receptor in the nervous system, most data indicate that it is involved in the regulation of several neural functions, such as modulation of neurotransmitter release, as well as microglial and astroglial activation. Moreover, P2X7 receptors have been proposed to play a key role in disorders of the nervous system, such as ischemia-reperfusion injury, Alzheimer's disease, depression and anxiety, spinal cord injury and neuropathic pain (Sperlagh et al., 2006).

### **2.1.3.1 P2XR structure and pharmacology**

The first transmembrane spanning region TM1 of these receptors is involved with channel gating while the TM2 lines the ion pore. The intracellular N- and C-termini possess consensus binding motifs for protein kinases while the large extracellular loop presents 10 conserved cysteine residues forming a series of disulfide bridges. The hydrophobic region H5 is close to the pore vestibule and is the site for possible receptor/channel modulation by cations such as magnesium, calcium, zinc, copper and proton ions while the ATP-binding site possibly involves the region of the extracellular loop adjacent to TM1 and TM2 (see Fig. 1).

P2X receptor family members show many pharmacological and functional differences. Calcium permeability is high for some subtypes, a property that is likely to be functionally important. The kinetics of activation, inactivation and deactivation also vary considerably among the different receptors. P2X receptors can be classified into rapidly (P2X1, P2X3) and slowly desensitizing types (P2X2, P2X5, P2X6, and P2X7). Two P2X2 isoforms differing only in their C terminal regions desensitize at different rates. The P2X2(b) isoform is missing a sixty-nine amino acid segment that is present in P2X2(a), and desensitizes about 5 fold faster than the longer isoform. It was concluded from mutagenesis studies that the rate of desensitization of the P2X receptors is controlled by distinct amino acids located in the C-terminus. Moreover, a protein kinase C phosphorylation site in the N terminus is necessary for the full expression of slowly desensitizing ATP-gated channels (Roberts et al., 2006).

All the P2X receptor subunits have consensus sequences for N-linked glycosylation (Asn-X-Ser/Thr), and some glycosylation is essential for trafficking to the cell surface. In fact, studies of recombinant receptors show that receptors in which any two of the three sites are glycosylated appear at the cell surface and are fully functional. Receptors in which only one site or no sites are glycosylated are not completely functional (North et al., 2002). Heteromultimers as well as homomultimers are involved in forming the trimer ion pore. Biochemical evidence suggests that the protein readily forms stable trimers and hexamers. Heteromultimers were clearly recognized for P2X2/3 in nodose ganglia, P2X4/6 in CNS neurons, P2X1/5 in some blood vessels, P2X2/6 in the brainstem and P2X1/4 and P2X1/2. P2X7 does not form heteromultimers and P2X6 does not form a functional homomultimer.

Although detailed signaling mechanisms have not been established for most P2X receptor subtypes, it is well known that cytoplasmic  $Ca^{2+}$  triggers a variety of intracellular events, in part, through activation of mitogen activated protein kinases (MAPKs), protein kinase C (PKC), and calmodulin. For example, ERK1/2 and p38 are activated by the P2X7 receptor in astrocytes. Activation of these kinases is required for upregulation of monocyte chemoattractant protein. In addition, cytoplasmic  $Ca^{2+}$  is generally important for neurotransmitter release via a calmodulin-dependent process (Erb et al., 2006).

The P2X7 subunit is 595 aminoacids long, having 35–40% homology with the other six members of the P2X receptor family (Surprenant et al., 1996). Although its structure is basically similar to the residual P2X receptor subunits, having two transmembrane domains (M1, M2) and a large extracellular loop, its intracellular carboxy terminal domain is much longer (239 amino acids) than those of other P2X receptor subunits (27–129 amino acids). The long intracellular C-terminal domain has been shown to be critical for the pore-forming property of P2X7 receptors while the ATP binding site is suggested to be located near a cysteine-rich region of the extracellular domain of the receptor, between the M1 and M2 transmembrane regions, similarly to other P2X receptor subunits.

Activation of the P2X7 receptor-gated ion channels leads to two distinct responses, depending on the exposure time of the agonist. Following a single brief application, a non-selective inward cationic current can be recorded, which is similar to inward currents caused by the activation of other P2X receptor subunits, although with different deactivation kinetics. Upon repeated or prolonged application the opening of a



membrane pore can be detected, which renders the membrane permeable to high molecular weight molecules and ions up to 800 Da (Surprenant et al., 1996). Although more recently it has been revealed that the permeability of other P2X subunits, such as P2X2 and P2X4 can also increase as a function of time, the property of pore dilation is generally associated with P2X7 receptors.

A number of variants of the human P2X7 receptor resulting from alternative splicing have been reported, including one that lacks the entire cytoplasmic tail. This finding may explain the fact that properties and functions of P2X7 receptors differ depending on cell type, as recently shown for microglia and astrocytes. For instance, activation of P2X7 receptors on microglia leads to the release of tumor necrosis factor- $\alpha$  (TNF $\alpha$ ), while in astrocytes, P2X7 receptor activation does not induce TNF $\alpha$  release but instead inhibits the release of this cytokine induced by lipopolysaccharide (LPS). Recently, P2X7 receptor gene polymorphisms have been suggested to be associated with several diseases but more epidemiological studies are needed to confirm these results (Barden et al., 2006; Sperlagh et al., 2006).

The pharmacological profile of the P2X7 receptor is relatively well established and distinguishable from other members of the P2X receptor family and this was useful to investigate its function. It has a low affinity for endogenous ATP, which is at least one order of magnitude lower than that of other members of the P2X family, while the agonist 3'-O-(4-benzoyl-benzoyl)adenosine 5'-triphosphate (BzATP) is at least 10–30-fold more potent than ATP at the P2X7 receptor. BzATP can bind to other P2X receptors with similar potency, in particular P2X1, P2X2 and P2X3, but only at P2X1 and P2X7 receptors BzATP is substantially more potent than ATP. The divalent cations Ca<sup>2+</sup>, Mg<sup>2+</sup>, Cu<sup>2+</sup> and low pH inhibit current flow through the receptor ion channel complex. It is only at the P2X7 receptor where Zn<sup>2+</sup> has an inhibitory action. Of various antagonists, Brilliant Blue G is a potent, noncompetitive antagonist displaying remarkable selectivity towards P2X7 receptors in the nanomolar range while the other P2X receptor antagonists, pyridoxal-phosphate-6-azophenyl-20,40-disulphonic acid (PPADS) is a potent antagonist at the human P2X7 receptor but less potent at the rat receptor (North, 2002).

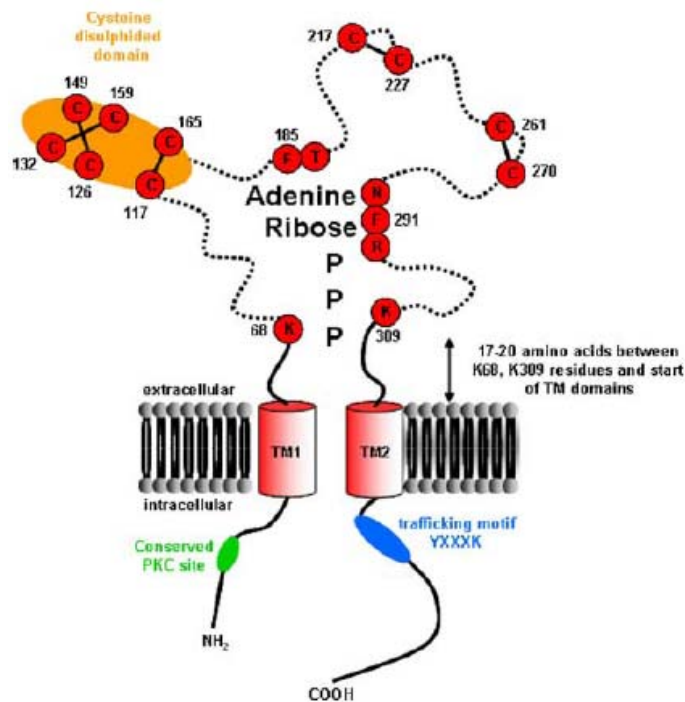


Fig. 1. Model of the P2X1 receptor. The intracellular amino and carboxy termini are associated with conserved protein kinase C (PKC) and trafficking motifs, respectively. The channel has two transmembrane domains (TM1 and TM2). The large extracellular loop is the site of ATP action; residues shown highlighted in red correspond to conserved amino acids that when mutated to alanine resulted in a significant decrease in ATP potency. The proposed disulphide bonds are shown and include a highly disulphided domain between cysteine (C) residues 117–165. Dotted lines correspond to regions of the extracellular domain where their function remains to be determined (Roberts et al., 2006).

### 2.1.3.2 P2XR localization

Since activation of ATP-gated P2X receptor channels induces a depolarizing excitatory input to the neurons bearing them, the understanding of such possible excitatory functions of the co-transmitter ATP under physiological conditions requires the mapping of P2X receptors in the nervous system. In the last 5 years, the use of several techniques such as in situ hybridization by subtype-specific riboprobes, as well as immunolabelling, yielded a wealth of data about the distribution of mRNA and receptor protein for the seven cloned P2X receptor subunits.

In the rat nervous system, P2X mRNA or P2X proteins or both have been detected throughout the neuraxis. The epithalamic region of the medial habenula, the locus coeruleus, the hippocampus, the dorsal horn of the spinal cord, as well as sympathetic coeliac ganglia and the myenteric plexus of the enteric nervous system express receptor proteins for at least one subtype of P2X subunit. In all of these regions

a co-transmitter role of ATP is strongly suggested by electrophysiological evidence. The tissue distribution of the seven P2X receptors ranges from abundant to discrete. P2X2, P2X4, and P2X6 mRNAs or proteins have been detected throughout the brain and spinal cord, as well as in sensory and autonomic ganglia (Norenberg and Illes, 2000). In rat hippocampus P2X2, P2X4, P2X6 subunits have been localized in postsynaptic specializations in CA1 pyramidal cells and Schaffer collateral synapses as well as in the granular cell layer (Rubio and Soto, 2001; Sperlagh et al., 2002). P2X1 receptor, initially believed to be absent in the brain, is expressed in the cerebral cortex, striatum, hippocampus and cerebellum, where P2X1 subunit proteins have also been detected. Outside the brain, P2X1 is found in the dorsal and ventral horns of the spinal cord, sensory ganglia, sensory systems and autonomic sympathetic ganglia. The P2X3 receptor is believed to mostly occur in capsaicin-sensitive sensory neurons involved in nociception and it is mainly restricted to sensory neurons and their termination fields. In addition P2X3 was also found in the hypothalamic supraoptic nucleus and in autonomic sympathetic ganglia in the adult rat nervous system (Norenberg and Illes, 2000). P2X5 also showed a restricted localization in the CNS, in particular in the mesencephalic nucleus of the trigeminal nerve, while in the peripheral nervous system, P2X5 mRNA, P2X5 protein, or both were identified in sensory ganglia.

Regarding the P2X7 mRNA distribution, initial Northern blotting studies revealed a widespread tissue distribution, showing strong expression in the immune system such as the thymus or the spleen, but also in other organs, including the brain, spinal cord, skeletal muscle, lung and placenta (Surprenant et al., 1996). With the high sensitive RT-PCR analysis, strong mRNA expression for P2X7 receptors was observed in several areas of the CNS such as the cortex, hippocampus, brainstem, nucleus accumbens and spinal cord of the rat and human brain. Moreover, it was also evident that at least at the mRNA level, P2X7 receptors may appear both in neurons and in astrocytes or microglial cells (Sperlagh et al., 2006). Immunohistochemical studies showed the P2X7 receptor specific immunoreactivity in several areas of the rat brain such as amygdala, hippocampus, thalamus, striatum, cerebellum, spinal cord and medulla oblongata (Deuchars et al., 2001). Moreover, co-localization studies revealed the co-expression of P2X7 receptor with vesicular glutamate transporter 1 (vGLUT1) and vesicular glutamate transporter 2 (vGLUT2) as well as with vesicular GABA transporter (vGAT) and vesicular acetylcholine transporter (vAChT) in many areas of the brain and the spinal cord (Atkinson et al., 2004). In particular, in rat hippocampus

P2X7 receptor immunolabeling was detected in the nuclear envelope but also appeared at presynaptic nerve terminals in excitatory neurons. Unfortunately, the specificity of the most commonly used antibodies has been debated by two recent studies (Kukley et al., 2004; Sim et al., 2004), which demonstrate a pseudo-immunoreactivity for P2X7 receptors in hippocampal sections of P2X7<sup>-/-</sup> mice. It's still not clear if this immunoreactivity was due to the presence of a neuronal "P2X7-like" protein products from alternatively splicing, or the result of the low dilution of the antibody used in these studies.

Determination of the subcellular localisation of P2X receptors is critical for a clearer understanding of their possible roles as a co-transmitter in ATP-mediated synaptic transmission. The release of ATP from the axon terminals of a presynaptic neuron may activate P2X receptors in the receptive somatodendritic region of a second, postsynaptic neuron and in this way contribute to fast excitatory neurotransmission. However, released ATP may also act at presynaptic P2X receptors, located either at the axon terminal where it is released from or at nearby endings. The activation of such presynaptic P2X receptors may lead to facilitation of ongoing action potential-dependent exocytotic transmitter release through their appreciable Ca<sup>2+</sup> permeability. Several experimental observations provide strong evidence that different P2X receptors, in particular the P2X2, P2X4 and P2X7 subunits are present at some nerve terminals and thus may be involved in the modulation of transmitter release (Norenberg and Illes, 2000). Somatodendritic receptors are usually excitatory (both P2X and P2Y), while presynaptic receptors are excitatory (P2X) or inhibitory (P2Y). Furthermore, the same neuron may bear a combination of P2X, P2Y and adenosine-sensitive P1 receptors which can mediate opposing responses. The final effect depends on the sum of the individual components (Fig. 2).

Regarding peripheral distribution, both P2X1 and P2X2 receptors are expressed in smooth muscle and platelets while P2X4 has been detected in testis and colon. P2X5 is expressed in proliferating cells in skin, gut, bladder and thymus and P2X7 in pancreas and skin (Burnstock, 1996).

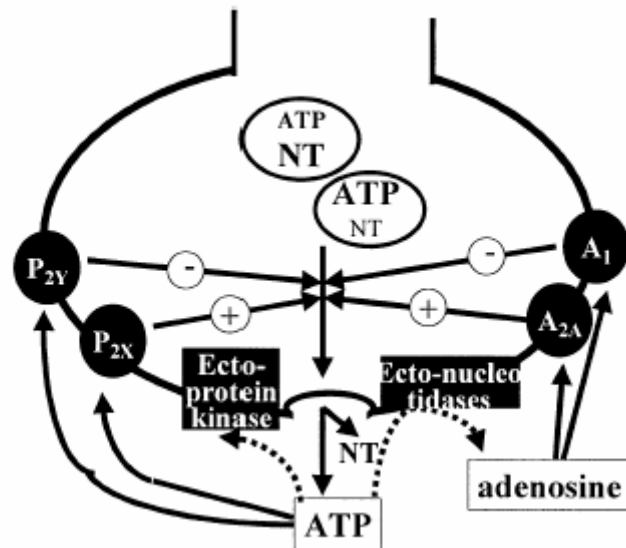


Fig. 2. Purinergic (ATP and adenosine) presynaptic modulation of neurotransmitter release (Cunha and Ribeiro, 2000).

### 2.1.3.3 P2XR involvement in neuronal function

When defining ATP-mediated responses it is necessary to clearly exclude the involvement of adenosine in the presynaptic effects of ATP. This is particularly critical in studies performed in the CNS rather than in peripheral preparations, since the expression of adenosine A<sub>1</sub> receptor mRNA and protein is generally lower in peripheral tissues and higher in most CNS regions. The activation of inhibitory A<sub>1</sub> receptors causes a profound inhibition of synaptic transmission and evoked neurotransmitter release through inhibition of calcium influx. The conversion of ATP into adenosine is mediated by an ecto-nucleotidase pathway, which is present in most regions and cell types in the CNS and present a high catalytic efficiency such that activation of adenosine A<sub>1</sub> receptors can occur within milliseconds after application of ATP. When activated, P<sub>2X</sub> receptors open within a few milliseconds and allow the non-selective passage of cations (Na<sup>+</sup>, K<sup>+</sup>, Ca<sup>2+</sup>) through their channel pore. Hence, measurement of rapidly activating cationic inward currents, evoked either by ATP or some of its structural analogues in neurons voltage-clamped at a negative membrane potential, provides the most direct way to functionally characterize native somatodendritic receptors (Cunha and Ribeiro, 2000).

P<sub>2X</sub>Rs, in particular P<sub>2X</sub>2, P<sub>2X</sub>4 and P<sub>2X</sub>6 receptors seem to be involved in the facilitation of excitatory neurotransmission and in the intracellular Ca<sup>2+</sup> increase in several regions of the brain, in particular in hippocampus. ATP-mediated P<sub>2X</sub>

activation induces fast synaptic currents and an intracellular  $\text{Ca}^{2+}$  increase in hippocampal CA1 neurons and increases the amplitude of the population spike following the stimulation of Schaffer collaterals (Rubio and Soto, 2001, Pankratov et al., 2002). Khakh and colleagues demonstrated that endogenously released ATP facilitates excitatory transmission onto interneurons by the activation of P2X2 receptors in the stratum radiatum of the hippocampus (Khakh et al., 2003). The kinetics of ATP-mediated excitatory post-synaptic currents (EPSCs), the high  $\text{Ca}^{2+}$  permeability of P2X receptors and their localization at appropriate sites suggest an important role for P2XR in the synaptic plasticity of neuronal cells (Rubio and Soto, 2001). Since the level of intracellular  $\text{Ca}^{2+}$  can modulate the functional state of several second messengers involved in important cellular pathways, the P2XR-mediated  $\text{Ca}^{2+}$  modulation suggests their involvement in several neuronal functions and hence neurological disorders (Koles et al., 2005). Moreover, both in hippocampus and in cerebellum, glutamatergic synapses were shown to express several P2XRs, in particular P2X2, P2X4 and P2X6 receptors, indicating that P2X receptors may play a significant role at glutamatergic synapses (Rubio and Soto, 2001).

Regarding P2X7, given the low affinity of the endogenous agonist ATP, a crucial question in the evaluation of the physiological but also pathological role of P2X7 receptor is to identify which conditions result in accumulation of extracellular ATP in concentrations sufficiently high to activate it. Since ATP is ubiquitous, all metabolically active cells of the nervous system such as neurons, astrocytes, endothelial or microglial cells are able to synthesize this nucleotide. In addition, ATP is taken up and stored in synaptic vesicles of nerve terminals and astrocytes. Physiological neuronal activity probably results in a spatially restricted, localized increase in extracellular ATP levels, involved in the synaptic transmission and modulation of pre- and postsynaptic functions within the synaptic cleft. In this limited space, ATP could reach millimolar concentration and activate P2X7 receptors localized near the release site. On the other hand, pathological events such as mechanical or metabolic stress, inflammation, cellular injury or changes in the ionic environment stimulate ATP release, provoking a more widespread activation of the P2X7 receptor. Indeed, several functional data strongly support the role of this receptor in information processing in normal and pathological state of the nervous system. Several experiments report a role for P2X7 in the modulation of glutamate and subsequent GABA release from rat hippocampal slices and an increase in intracellular calcium levels in several isolated neurons (Sperlagh et al.,

2006). Furthermore, the role of P2X7 receptors in these actions has been confirmed by the use of P2X7 KO mice, in which ATP evoked GABA and glutamate release is almost abolished. In contrast, Armstrong et al. (2002) reported that BzATP elicits long-lasting depression of mossy fiber EPSCs underlying the inhibition and not the facilitation of glutamate release. Anyway since this result was not confirmed in knock-out animals, it was probably the result of BzATP breakdown to Bz-adenosine and the subsequent activation of adenosine receptors. Thus, it appears that P2X7 receptors facilitate, rather than inhibit transmitter release in the hippocampus (Sperlarch et al., 2002). However, in view of the unclear cellular localization of P2X7 receptors in the hippocampus, the facilitation of glutamate and GABA release could be mediated by glial cells since this P2X7-mediated neurotransmitter modulation was measured in cultured astrocytes. Since ATP release from brain slices is highly frequency-dependent, P2X7 receptors may serve as molecular sensors of increased neuronal activity and contribute to short- or long-term plasticity phenomena, underlying e.g., memory formation. In addition P2X7 receptors are activated during pathological conditions, when metabolic distress or cellular damage provide an increase in extracellular ATP in the vicinity of P2X7 receptors.

#### **2.1.3.5. P2XR in glia**

P2X receptors, including P2X7 receptors, appear to mediate communication between glial cells and neurons, between different glial cell types, and within glial networks. The main glial cell types of the nervous system are astrocytes, oligodendrocytes and microglia. They play an active role in information processing, control the homeostasis of the neuronal microenvironment, development and differentiation of neural cells and host-defense response. Resident microglia are well known as the immune effector cells of the CNS while Schwann cells are involved in the immune response in the periphery. To realize their diverse roles, glial cells have to communicate with each other and with neurons. P2X7 receptors, besides other ATP receptors, seem to play an essential role in these processes. Both P2X7 mRNA and protein have been found in astrocytes and in several regions of the brains P2X7 protein was co-localized with astrocytic markers as glial fibrillary acid protein (GFAP) (Sperlarch et al., 2006). Astroglial P2X7 receptors participate in a wide array of normal and pathological functions of the astrocyte network. However, the majority of these actions have been described in cultured astrocytes and further experimental work is

necessary to prove that P2X7 receptors indeed play such roles *in vivo*. The primary intracellular signal following the activation of P2X7 receptors is a sustained elevation of intracellular  $\text{Ca}^{2+}$  ( $[\text{Ca}^{2+}]_i$ ), caused by  $\text{Ca}^{2+}$  influx from the extracellular space through the receptor ion channel complex of astrocytes, which is then translated to various signal transduction pathways conveying diverse functions (Fumagalli et al., 2003). In particular, activation of P2X7 receptors elicits the release of several neurotransmitters as glutamate, GABA and purines from cultured astrocytes (Sperlagh et al., 2006).

Astrocytes also participate in neuroinflammatory processes underlying a variety of CNS diseases including trauma, ischemia and neurodegeneration. Inflammatory stimuli rapidly induce the proliferation and hypertrophy of glial cells, a process called reactive gliosis, resulting in the expression and production of cytokines, chemokines and other inflammatory mediators (Di Virgilio et al., 2001). P2X7 receptors are involved in these pathways and receptor activation promotes the expression of MCP1 protein, a critical factor in early monocyte infiltration during the neuroinflammatory process (Panenka et al., 2001), and other proteins involved in gliosis. Furthermore, it increases the phosphorylation of ERK1, ERK2 and p38 MAP kinase, proteins which play a role in the commitment of the cells to apoptosis.

In addition, P2X7 receptor plays an important role in  $\text{Ca}^{2+}$  signaling between astrocytes and microglial cells (Verderio and Matteoli, 2001). Astrocytes communicate by calcium-mediated signaling not only with each other but also with neighboring cells including neurons and microglia. The consequence of this is that astrocyte-derived ATP activates P2X7 receptors on microglial cells and elicits  $\text{Ca}^{2+}$  signals in the microglia, which eventually leads to cytolysis (Verderio and Matteoli, 2001). Interestingly P2X7 receptor-activation in astrocytes usually does not lead to cytolysis, while the same effect might cause cellular death in microglia.

#### **2.1.3.6 Pathological role of the P2XR in the nervous system**

Since the widespread effects of P2X receptors activation on different aspects of neuronal functions and microglial/astroglial activation, their involvement in the pathology of CNS and PNS diseases and their possible role as therapeutic targets has been suggested. Several experimental data, in particular the demonstration of the activity-dependent expression of P2X receptors under pathological conditions and the protective role of P2X receptor ligands in animal disease models, support this



hypothesis (see for example Dorn et al., 2004 and Vianna et al., 2002). Many of these experimental evidences are focused on the P2X7 receptor. Diseases in which P2X7 receptor may play either a harmful or protective role include neurodegenerative and neuroinflammatory diseases, such as ischemia-reperfusion and traumatic injury, Alzheimer's disease, multiple sclerosis, rheumatoid arthritis and retinopathies (Sperlagh et al., 2006). The up-regulation of P2X7 receptors has been observed in a number of pathological models, including *in vivo* ischemia, epilepsy (Vianna et al., 2002), mechanical injury, neuropathic pain and transgenic models of Alzheimer's disease. Nonetheless, it has not been clarified whether the change in their expression pattern and function is a simple adaptive change or plays a more active pathogenetic role. In addition, it is also still unknown whether the final result of P2X7 receptor mediated actions in neuronal, microglial and/or astroglial cells are protective or harmful (Sperlagh et al., 2006).

Regarding the involvement of P2X receptors in psychiatric disorders, there are several experimental evidences for a role of P2X7 in depression and bipolar disorders. Reductions of P2X7 receptor level after stressful handling and an increase after antidepressant treatment (28 day with paroxetine) were measured in mouse hippocampus (Barden et al., 2004). P2X7 mRNA level was found to be down-regulated in the temporal cortex of depressed patients in a post mortem study of suicides, non suicides and non-medicated patients (Aston et al., 2005). In mice, P2X7 inhibition through RNA antisense treatment enhances depressive-like behaviour (Barden, 2004). In contrast hippocampal infusion of BzATP leads to improvement of depressive-like symptoms, evaluated in the Porsolt test or forced-swimming test. This behavioral assay is normally used to test antidepressant drugs. In this assay the animal is forced to swim in a water container and, following initial escape-oriented movements, develop an immobile floating posture in the water cylinder which reflects the animal's state of despair. The total amount of time that the animal demonstrates this immobility behavior, which is reduced by antidepressant treatment, is then measured. Recently genetic linkage and association studies have identified within chromosome 12q the P2X7 gene as a susceptibility factor for both bipolar and major depressive disorders (Barden et al., 2006 and Lucae et al., 2006). Linkage analysis is the attempt to discover predisposing genes by identifying sites (polymorphisms) in the genome at which sequence variations (alleles) travel with illness within families that have more than one affected member. It is a method of locating a disease-associated gene at a specific site

on a particular chromosome. Analysis of different single nucleotide polymorphism (SNP) markers in the pedigrees used for linkage studies and in case-control populations has led to the identification of a non-synonymous SNP lying in exon 13 which show the highest association value. This SNP results in an aminoacid substitution (Gln460Arg) in the P2X7 intracellular C-terminal domain, which is known to be essential for pore formation, intracellular signaling, membrane blebbing and receptor trafficking, and indeed leads to alteration of protein functions (Cabrini et al., 2005). More recently, a new study has confirmed the allelic associations between bipolar disorder and the above SNP marker in a different case-control bipolar collection and shown that a combined analysis of data from bipolar patients and mood disorders increase the strength of the association (McQuillin et al., 2008). The above data suggest that the observed P2RX7 polymorphism might play a causal role in the development of both depression and bipolar disorder. In addition, in the brain, both microglia and astrocytes are stimulated by ATP-induced P2X7 receptor activation, to produce cytokines, chemokines and growth factors and it is now well established that the nervous, endocrine, and immune systems are closely linked. Several works report increased concentrations of pro-inflammatory cytokines and their receptors in depressed individuals (Kim et al., 2002). Consequently, harmful or sustained inflammatory responses could be associated with depressive behavior, and it is possible that the P2X7 receptor plays a key role either directly, or mediated by the regenerative loop at glutamatergic synapses (Bennett MR, 2007).

Since P2X2 and P2X4 receptors are also expressed in specialized areas of the hippocampus and the genes for both receptors are within the region of P2X7 associated with depression and bipolar disorder, they too could be involved. Moreover, changes in intracellular concentrations of  $Ca^{2+}$  have been observed in patients suffering from mood disorders (Wasserman et al., 2004) and these receptors have been shown to play a key role in regulation of calcium intracellular levels in brain areas involved in these disorders, in particular in the hippocampus.

## 2.2. RNA INTERFERENCE

Post-genomic biomedical research has improved the possibilities to uncover disease mechanisms and discover potential target genes relevant to the pathology (Mirnics et al., 2000). Microarray-based genomic analyses permit measuring the complete expression patterns in pathological samples and proteomic platforms enable the identification of proteins with altered expression in a disease state. These techniques permit the systematic identification of a large number of targets with pathophysiological relevance and their involvement in the disease needs to be validated *in vivo*. Pharmacological, immunological and genetic manipulation tools are available for *in vivo* gene validation (Fig. 3). Pharmacological tools are characterized by the use of specific molecules able to directly activate (e.g., agonists, positive allosteric modulators) or inhibit (e.g., antagonists, negative allosteric modulators) the protein product of the gene and provide a rapid means of *in vivo* target validation. Antibodies can be used as immunological tools to inhibit the target protein and validate its function *in vivo* (Salfeld, 2004). These tools have the advantage of rapidly revealing a target-based phenotype but the disadvantage of the difficulty and time-consuming process of finding small molecule compounds or generating antibodies that are selective for the target protein. In addition, the gene product must be identified in order to employ these tools and often many of the resulting genes from microarray or genetic studies are not functionally characterized or are not full-length sequences but just expressed sequence tags (ESTs). The genetic approach requires the production of mutants by homologous recombination in embryonic stem cells (ES) such that the gene of interest is either stably over-expressed or knocked out in animals. This approach is far more selective than pharmacological or immunological manipulation but a major disadvantage is the restricted feasibility of homologous recombination in rodent ES cells. This is further complicated by the phenotypic differences observed among different strains following mutation of the same gene. Other disadvantages of this approach are the enormous amount of time involved in generating stably expressing mutant off-springs, the impossibility to phenotype genes critically involved in the early developmental stages and genetic compensation and developmental adaptations that may mask a clear phenotype. These last disadvantages have been addressed by the use of inducible transgenic animals.

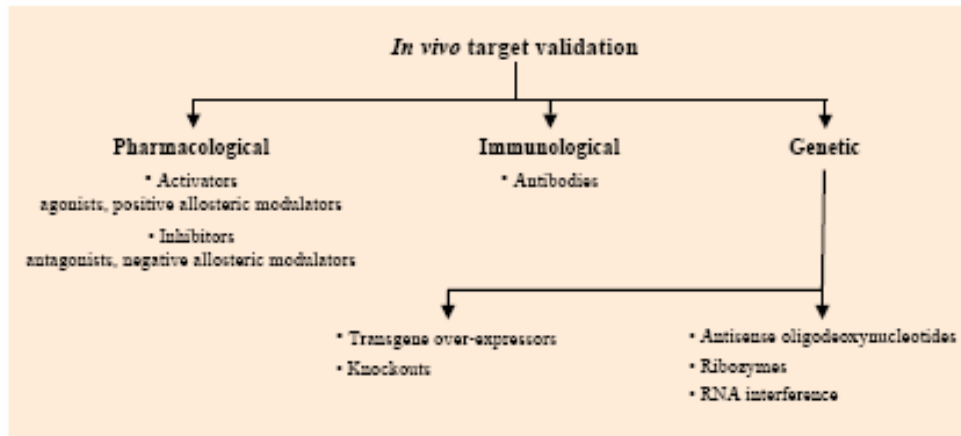


Fig. 3. Tools for *in vivo* target validation (Thakker et al., 2006).

Gene expression in somatic cells can be manipulated using antisense or ribozymes. Ribozymes are RNA molecules that bind the target mRNA in a sequence-specific manner and catalyse the cleavage of the mRNA. Antisense technology uses either DNA or RNA molecules complementary to sequences on the target mRNA, inhibiting protein production. These techniques were successful in some situations but difficult to apply universally.

In this context the advent of siRNA-mediated gene knockdown has allowed an inexpensive and rapid analysis of gene function in mammals. At present RNAi has become an important and widely used tool for evaluating target function both *in vitro* and *in vivo* and has been used for the screening of potential therapeutic targets in pharmaceutical research. The advantages of RNAi over other techniques include its high specificity (in some cases, a single point mutation can abolish a silencing effect), versatility (interfering RNA can be designed virtually against any gene), and efficiency (in many cases, genes can be silenced by over 90%). Moreover the therapeutic application of RNAi is beginning to be explored. Recently phase I clinical trials were initiated to treat two different pathologies, Respiratory Syncytial Virus (RSV) infection and age-related macular degeneration (AMD). These are the first human trials testing the efficacy of this novel approach (Li et al., 2006).

### 2.2.1 RNA interference discovery

RNA interference (RNAi) is defined as the process by which double-stranded (ds)RNA silences sequence specific gene expression, either by inducing the degradation of complementary mRNA or by inhibiting translation. This mechanism was found and

described for the first time by Fire and colleagues in 1998 (Fire et al., 1998), who found that injection of dsRNA into *Caenorhabditis elegans* lead to target gene suppression dependent on hybridization between the injected RNA and endogenous messenger RNA transcripts. The first silencing phenomena were described in plants (post-transcriptional gene silencing or PTGS) and fungi (quelling) (see Sharp, 1999). Evidence of the existence of RNA-silencing pathways first came from experiments in plants. Rich Jorgensen and colleagues engineered petunias carrying transgenic copies of the gene encoding chalcone synthase, the limiting enzyme in the synthesis of the flower's purple pigment. Their intent was to generate more intensely purple flowers, but often their efforts yielded plants with dramatic pigmentation patterns comprising tissue in which chalcone synthase was produced, flanking tissue in which both the transgenic and endogenous chalcone synthase genes were mysteriously turned off. They defined this phenomenon "co-suppression" (Napoli et al., 1990). Studies in *Drosophila melanogaster* similarly reported that the more transgenic copies of alcohol dehydrogenase (Adh) that were engineered into flies, the less Adh mRNA was actually produced. In the mid-1990s, David Baulcombe's laboratory discovered that plant viruses could also trigger sequence-specific silencing and they showed that this viral-induced gene silencing (VIGS) was mechanistically related to the silencing triggered by transgenes. The link between the two silencing pathways was that both required transcription of RNA from the trigger locus, implicating RNA as the initiator of silencing (Ratcliff et al., 1997). Specifically, it was suggested that dsRNA, formed by two RNA molecules annealing or one folding back on itself, might be recognized by plant cells as an activator for the sequence specific silencing of genes. Subsequently Fire and colleagues proved this to be true for RNAi in animals, and other researchers subsequently showed the same for plants.

More recently viral defence has been proposed to be the primary function of RNAi in both plants and animals. In fact the presence of similar RNA interference machinery in several organisms has raised the hypothesis of an evolutionary development of RNAi as a defence system against RNA virus, transposons and other external nucleic acids that can lead to insertional mutagenesis, probably before plants and animals diverged. The development of PTGS and other silencing mechanisms, such as protection from DNA or RNA viral infection, is supported by the presence of counter strategies in many DNA or RNA viruses. Several plant viruses present genes encoding suppressor proteins, which block the development of the PTGS state. In any case the

mechanism of suppression of the dsRNA-induced gene silencing by viral proteins remains to be investigated.

Initially RNA interference was thought not to be useful for targeted gene silencing in mammals, because dsRNA molecules that are longer than 30 base pairs (bp) stimulate the antiviral interferon pathway, resulting in cell death. This process is caused by inhibition of protein synthesis through protein kinase R-mediated phosphorylation of the translational initiation factor eIF2 and non-specific mRNA degradation via the 2'-5' oligoadenylate synthase-RNase L pathway. Tuschl and colleagues in their studies of RNAi processes in *Drosophila melanogaster* embryo extracts showed that long dsRNA substrates could be cleaved into short interfering dsRNA species (siRNAs) of ~22 nucleotides (nt), able to anneal to the target mRNA driving its degradation. They also showed that the introduction of a chemically synthesized 21-22nt siRNA to these extracts facilitated the degradation of the homologous target mammalian genes (Elbashir et al., 2001), evading in this way the interferon response. Another technical advance came from the demonstration that siRNAs could be endogenously expressed in the form of short hairpin RNAs (shRNAs) by a plasmid transfected into a cell. The plasmid contains an shRNA cassette with a promoter that drives the transcription of a fold-back stem-loop RNA structure. This shRNA is then recognized by the RNAi machinery and is therefore able to induce target-gene silencing in mammalian cells.

In addition to its power as a tool for gene silencing in biology, RNAi is thought to be an important system of gene expression regulation due to the discovery of micro RNAs (miRNAs). miRNAs have been cloned from various organism and cells (the first identified was *lin-4* from *C. Elegans*) and are short RNA species (~22nt) produced by cleavage of longer (~70nt) endogenous precursors with imperfect hairpin RNA structure. miRNAs have been showed to be developmentally regulated and to share much of the same machinery of siRNA-induced gene silencing. Recently several miRNA genes have been discovered in mammals, confirming the prospect that the cellular machinery necessary for RNAi in mammalian cells is linked to normal process of gene regulation (Grosshans and Slack, 2002), mainly during development.

### **2.2.2 The mechanism of gene silencing by RNAi**

RNAi can be triggered by various types of molecules, including long dsRNAs and plasmid-based shRNAs. These molecules are processed in the cytosol by the ribonuclease-III activity of the evolutionary conserved Dicer enzyme to generate 21-

22nt siRNAs (initiation step). The siRNAs are characterized by 2-3-nt 3' overhangs and 5'-phosphate and 3'-hydroxyl groups. The Dicer enzyme is part of class III enzyme family characterized by the presence of two RNaseIII catalytic domains, a helicase domain and a PAZ (Piwi/Argonaute/Zwille) domain. The siRNAs produced are then incorporated into a protein complex, known as the RNA-induced silencing complex (RISC) mediating the effector step. RISC uses an ATP-dependent RNA-helicase activity to unwind the duplex siRNA into single stranded siRNA. The antisense strand of the duplex guides the RISC complex to the homologous mRNA, where the RISC-associated RNaseH enzyme Argonaute 2 (Slicer) cleaves the target mRNA at a single site in the centre of the duplex region, 10nt from the 5' end of siRNA. This results in the silencing of the target gene through a reduction in the level of target mRNA and subsequently of the protein. As previously described RISC is characterized by a multi-protein complex that can vary in composition and size. Central to this complex is a member of the Argonaute family, a gene family conserved in most eukaryotic and several prokaryotic genomes. RISC complex may also facilitate the modification of chromatin through recruitment of enzymes responsible for chromatin modification (e.g., methylation) as well as other proteins, such that RNAi can induce silencing at the transcriptional level (Verdel et al., 2004).

In the case of endogenous hairpin micro RNAs, the mechanism of RNAi starts with nuclear transcription of long primary miRNA precursor with a stem-loop structures containing the miRNAs. The RNase III enzyme Drosha cleaves this structure away from the miRNA precursor to generate pre-miRNA intermediates. These pre-miRNAs are transported from the nucleus to the cytoplasm by the nuclear export factor, Exportin-5, where the pre-miRNAs are cleaved by Dicer to generate miRNAs which are then incorporated in the miRNA-protein complex (miRNP). The miRNAs are believed to suppress the expression of partially complementary target mRNAs by translation inhibition rather than mRNA degradation: anyway dsRNA, shRNA and miRNA elicit RNAi through common biochemical pathways (Fig. 4). The translational inhibition mechanism droved by miRNAs has not been completely elucidated: one recent hypothesis is that microRNA/RISC complex blocks cap-dependent initiation of translation. Drosha and Dicer activity is supported by dsRNA binding domain proteins (dsRBD) which acts as co-factors helping for example strand specific incorporation of the siRNA. Reassuming it is possible to identify three different mechanisms of silencing: the cytoplasmatic degradation of target mRNA induced by siRNAs (produced

from long dsRNAs or shRNAs), miRNA-induced translation inhibition of partially complementary mRNAs and nuclear transcription blockage through chromatin modification.

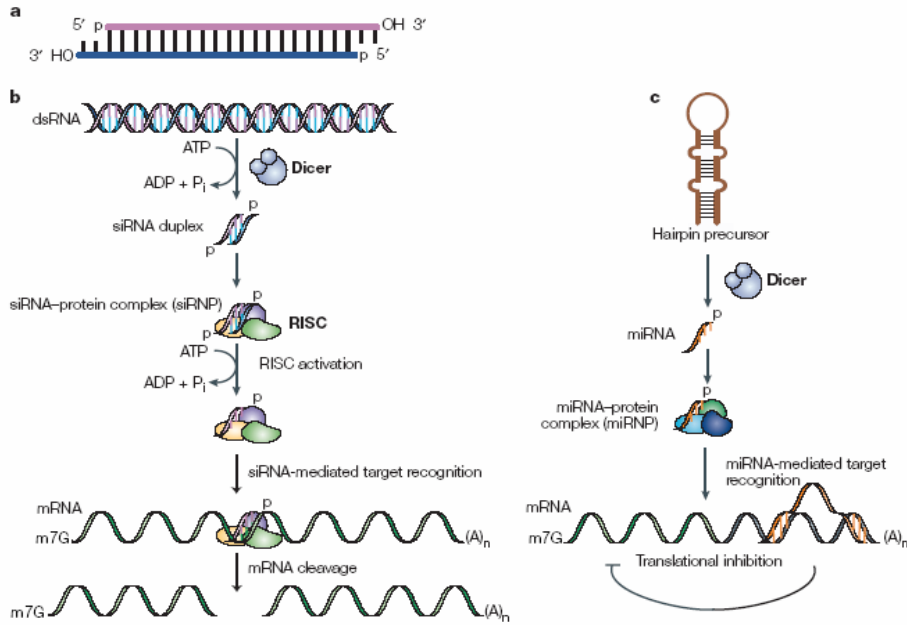


Fig. 4. The RNA interference pathway. a. Short interfering RNA. b. Long double-stranded RNA. c. The microRNA pathway.

### 2.2.3 Designing siRNA

Target gene silencing can be induced by the introduction of siRNA into the cell or siRNA production inside the cell. As shown by Tuschl and colleagues, synthetic siRNAs of 21-22nt can effectively suppress target gene expression in mammalian cells. In order to achieve efficient and specific gene silencing, it is important to optimize design, identification and delivery of effective siRNAs, where effective is defined as >90% specific reduction in protein levels when a siRNA is used at 1-20nM. Several groups have proposed basic empirical guidelines for designing effective siRNAs based on the understanding of RNAi biochemistry and miRNA function. The criteria for siRNA design are thermodynamic and structural parameters like a low to medium guanosine-cytosine content (30-50%), low internal stability at the 5' antisense strand and high internal stability at the 3' sense strand to facilitate interaction with RISC. Base preference at specific positions in the sense strand is required to promote antisense-strand selection by RISC and efficient unwinding. Stringent homology searches are



needed to minimize potential non-specific gene silencing. Moreover, from studies of RISC complex structure, an effective siRNA (or microRNA) sequence needs to begin with an adenosine or uridine and have a mismatched guanosine or cytosine at the 5' end. The application of these rules significantly improved effective siRNA selection. The same rules can be applied to plasmid-encoded shRNAs. The secondary structures of the target mRNA which might limit the accessibility of the siRNAs also have to be considered. In line with this, the application of an algorithm that can predict the secondary structure of mRNA from its primary sequence helps find an effective siRNA. At the moment several commercial algorithms, such as these available on the Ambion and Dharmacon web site, have been designed that predict the most successful siRNA for a particular target gene. Moreover a pool of different siRNAs targeting the same gene can be used, which lowers the amount of a single siRNA required to achieve successful gene suppression, enhancing RNAi specificity.

#### **2.2.4 Delivery of siRNA**

##### ***In vitro delivery***

For RNAi to be effective and elicit gene silencing, the double-stranded RNA must be delivered to the target cell and in some occasions this can be quite difficult. siRNA introduction intracellularly could be requested for gene function studies *in vitro* or to select the active siRNA sequence for *in vivo* work. Synthetic siRNAs can be delivered to mammalian cells by viral and non-viral methods.

Among the non-viral methods, injection of pure, unmodified siRNA or chemically stabilized and modified RNA has been successfully developed. Moreover the encapsulation of siRNA into microparticles or liposomes, the binding of siRNA to cationic or other particulate carriers and the electroporation of siRNAs into cells have been recently used for many targets and for several cell types. Several lipophilic agents are commercially available for the delivery of siRNAs into cells, with different formulations optimized for each cell type. The limit of this system is the transient nature of the RNAi response and in some cases, the lipid-mediated cellular toxicity, which can be a major hurdle for phenotype identification following target gene suppression. Chemical modification of siRNA, in particular on the phosphate backbone, can facilitate siRNA entry into the cell but even if modified, siRNA can be rapidly degraded by nucleases.

These limitations can be overcome by the use of plasmids that harbour siRNA expression cassettes, providing continuous expression of shRNAs into the cell. The shRNA is predicted to contain a perfectly double-stranded stem of 19-29 bp, characterized by the antisense strand, which is identical to the target sequence in the mRNA and the complementary sense strand. The 2 strands of the stem are connected by a loop of 6-9 bases. The loop of the hairpin can be digested in the cytosol by the RNAi enzymatic machinery to form the active siRNA. This will enter in the enzymatic RISC complex in order to be unwound and annealed with the target mRNA driving its degradation. In general, chemically synthesized siRNAs that are effective in gene silencing are also effective when expressed from an shRNA. However the length of the stem and the size and sequence of the loop seem to affect the silencing efficiency. Stem lengths of 19 to 29 nt have been described, demonstrating that the stem size is not the limiting parameter. On the contrary, the dimension and sequence of the loop seems to be critical. In a direct comparison of loop sequence and size, the 9 nt loop sequence 5'-UUCAAGAGA-3', also called the Brummelkamp loop, was the most efficient silencer using a constant 19 nt duplex (Brummelkamp et al., 2002). This loop is frequently used by researchers. Another important parameter in the design of the shRNA vector is the promoter. RNA polymerase III (pol III) promoters, mainly U6 and H1 small nuclear RNA (snRNA) promoters, are widely used to drive shRNA expression, because they are active in almost all cell types and efficiently direct the synthesis of small non-coding RNA with well defined ends. The U6 promoter requires a guanosine at the +1 position, while the H1 promoter is much more permissive. RNA pol III efficiently recognizes a cluster of 4 or more thymidine residues as a termination site. Transfer RNA (tRNA) promoters and RNA pol II-based cytomegalovirus (CMV) promoters have also been used. Generally, a single promoter drives the expression of the shRNA, which is subsequently processed by Dicer into siRNA, but it is also possible to use different promoters to drive the expression of the sense and antisense strands.

The use of plasmid shRNA vectors *in vitro* might be ineffective when the target cells are difficult to be transfected, such as freshly isolated primary cells, neuronal cells and stem cells. In order to overcome this problem, viral vector expressing shRNA cassettes can be used. The various viral vectors ensure broad tropism and efficient transduction of both transformed and primary mammalian cells. These will be described in more detail later. Briefly, the five types of viral vectors that are mainly used for RNAi include retrovirus, lentivirus, adenovirus, adeno-associated-virus (AAV) and

baculovirus. To achieve stable integration of the shRNA-expression cassette into the host genome, lentiviral vectors, retrovirus vectors based on the Moloney murine leukaemia virus (MoMuLV) or the murine-stem cell virus (MSCV) can be used. A disadvantage of lentiviruses and retroviruses is that they can integrate into the host genome causing insertional mutagenesis. To avoid integration, adenovirus or adeno-associated viral vectors are preferred.

### ***In vivo delivery***

*In vivo* RNAi can be useful to elucidate gene function or to achieve therapeutic gene silencing. Several methods are available for RNAi in the live animals such as non-viral local or systemic delivery of siRNA, viral or plasmid delivery of shRNA and the constitutive or inducible expression of shRNA in transgenic animals.

Non-viral delivery of siRNA *in vivo* is challenging since small RNA molecules like siRNAs are relatively unstable in the extracellular and intracellular environment due to the presence of RNA degrading enzymes (RNAses) in serum. Even if chemically modified to increase stability, when systematically administered they are rapidly excreted or diluted. A large amount of siRNA is therefore necessary to obtain an effective silencing. Actually few papers have reported successful silencing of genes *in vivo* using naked siRNAs or shRNA encoding plasmid DNA (Ocker et al., 2005). The duration of siRNA activity *in vivo* and any possible therapeutic effect will depend on its stability in serum. Double stranded RNA is more stable than single strand RNA but it will still be degraded within a few hours. Chemical modifications which increase stability of siRNA molecules without affecting RNA interference have been investigated. Ideally, chemical modifications could also increase thermal stability, cellular tropism, silencing activity and pharmacokinetic properties of the siRNA. Locked nucleic acid (LNA) residues that increase stability of oligonucleotides have been used successfully to enhance the effect of antisense RNA and ribozyme RNA (Li et al., 2006). Another way to chemically stabilize RNA molecules is via phosphothioates (PS) in which phospho-sulfur replace phosphodiester linkages in the sugar backbone of the RNA. PS linkages increase the half-life of oligonucleotides *in vivo* and were used with antisense nucleotides in several clinical trials to increase stability (Crooke, 2000). Other reported chemical alterations include modifications of residues added at the 2' position of the ribose since the 2'OH group is not required for silencing in siRNA. Several cationic lipids and polymers have been developed to deliver normal or modified siRNAs. The most popular envelopes include liposomes and other

nanoparticles. Liposomes made of a mixture of cationic and neutral lipids have been formulated, covered with a hydrophilic polyethylene glycol (PEG)-lipid which facilitates formulation and administration in the aqueous phase (Li et al., 2006). In an attempt to confer more specific tissue tropism to liposome-carried RNAi, some groups established methods to increase affinity for defined cell types using either ligands for specific receptors or antibodies against cell surface markers. Successful applications have been obtained either by local application to organs such as brain, lung, muscle and tumors or systemically by intravenous or intraperitoneal administration (Xie et al., 2006; Li et al., 2006).

Another approach for interfering with gene expression *in vivo* is shRNA-mediated transgenic RNAi that, through electroporation of the shRNA expression vector into mouse ES cells, offers a prolonged, stable, loss-of-function phenotype *in vivo*. Stable integrants demonstrating significant gene knockdown are then injected into blastocysts. With this method, it has been demonstrated stable passage of the RNAi-induced gene knockdown from the ES cells to adult mice by germline transmission of the shRNA-expressing vector in the F1 progeny (Carmell et al., 2003). Since lentiviral vectors can infect mouse ES cells and are resistant to proviral silencing during development, they have been used for transducing ES cells with shRNA-expressing vectors (Rubinson et al., 2003). Alternative methods have been developed to generate transgenic RNAi animals, for which homologous recombination is not possible due to the lack of ES cells such as injection of shRNA constructs into the pronuclei of mouse or rat fertilized eggs. However, similar to traditional knockouts, the constitutive and widespread gene knockdown in the whole animal presents serious limitations to the use of transgenic RNAi animals. As a solution, the Cre-loxP recombination system has been recently employed to produce an inducible and cell or tissue-specific expression of shRNAs. In this system, the shRNA-expression vector is modified in order to incorporate a specific sequence that prevents transcription from the vector, flanked by loxP sites. These sites are recognized by the Cre recombinase, therefore only a Cre-mediated recombination event is able to restore the original open reading frame of the vector. The use of inducible Cre expression systems, such as tetracycline or tamoxifen, along with transgenic RNAi, represents a systematic evaluation of organ or tissue-specific gene suppression (Ventura et al., 2004).

### 2.2.5 Viral vectors as delivery agents

Viruses are naturally evolved vehicles to efficiently transfer genes into host cells. This property makes them ideal for engineering viral vectors for the delivery of genes. Viral vectors are commonly used in a wide number of applications, such as gene therapy to restore normal function or to treat diseases such as cancer. They are employed for gene expression modulation to investigate the function of a target gene or to confirm the involvement of a gene in a disease mechanism as part of the target validation process. The viral vectors normally used in laboratory or clinical research are based on RNA or DNA viruses with different genomic structures and host ranges and are characterized by an ability to efficiently deliver and express foreign sequences into host cells. These are mainly retroviruses, adenoviruses, adeno-associated viruses, herpesviruses and poxviruses. Retroviruses are most widely used since these viruses have high gene transfer efficiency and mediate high expression of target genes. More recently members of the DNA virus family, such as adenovirus-, adeno-associated virus and herpes virus (HSV) have also been used for efficient gene delivery. Moreover, numerous new viral vectors are being developed based on vaccinia virus, human cytomegalovirus, Epstein-Barr virus and others (Walther and Stein, 2000). From the beginning of the development and utilization of viral vectors, efforts have been made to increase infection, viral targeting, cell-type specific expression, duration of expression and safety, to develop efficient and safe RNA- and DNA-viral vectors. This is particularly important when using viral vectors for *in vivo* applications, which require limited toxicity derived from viral infection, immuno-responses towards viral antigens or potential homologous viral recombination.

Retroviral vectors are derived from RNA viruses which reverse-transcribe their RNA viral genome into double stranded DNA, which is then stably inserted into the host DNA. Members of this class of virus are the murine leukaemia virus (MuLV) and lentivirus. These viruses are characterized by three structural genes, *gag*, *pol* and *env*, flanked by viral long terminal repeats (LTR), which are responsible for the regulation and expression of the viral genome and the integration of the pro-virus into host DNA. Removal of structural genes and the packaging signal (*psi*-site) are performed to produce safe and efficient recombinant viral vectors. Helper cells are required to replace the viral structural genes. The advantages of these viral vectors are determined by their characteristics of stable integration into the host genome, generation of viral titers

sufficient for efficient gene transfer, infection of a broad variety of target cell types and the ability to carry foreign genes of reasonable size ( $\leq 8$  kilobases, kb). Thanks to these properties, they lead to persistent expression of the transgene in the transduced cells and their progeny cells with a high level of expression, which is essential to obtain a therapeutic effect or modify a phenotype. For efficient gene expression the transgene is placed in opposite orientation in relation to the viral LTR. It is possible to insert an entire gene cassette of a functional gene, including its own regulatory unit. These vectors are characterized by several disadvantages including the instability of some retroviral vectors, possible insertional mutagenesis by random viral integration into host genome and the requirement of cell division for the infection of MuLV-derived vectors. Nonetheless, retroviral-derived vectors and in particular those based on Moloney MuLV, are currently used *in vivo*. Among the lentiviral family the most widely used for the production of viral vectors is the human immunodeficiency virus (HIV) which can infect both dividing and non dividing cells.

DNA viruses contain a single- or double-stranded DNA viral genome. The most predominant viruses used are the Adenovirus, AAV and HSV thanks to their large packaging capacities, broad range of target cell tropism and efficient infection and gene transfer. Adenoviruses are non-enveloped DNA viruses carrying linear double-stranded DNA of about 35kb. There are at least 49 serotypes known, which can be further classified by haemagglutination properties. The most characterized, which is used for engineering work, are the adenovirus type 2 (Ad2) and type 5 (Ad5), since these are not associated with severe diseases in humans and are therefore suitable for *in vivo* use. Adenoviral genome is modified by deleting the early gene 1 (E1A), essential for virus replication, to create replication incompetent vectors and to provide sufficient space to carry exogenous genes. Partial deletions of E1B and E3 genes are also made to create more space for gene insertion, producing vectors with packaging capacities of 7 to 8kb. Helper cells, which provide the essential E1A protein *in trans* for efficient viral encapsulation are needed for the production of infectious viral particles. The human embryonic kidney cell line (HEK) 293 with the E1A gene stably inserted is normally used for generation of recombinant viral stock since these cells are easy to transfect and produce high virus titres. Viral titres of  $10^{10}$  colony forming units (cfu) /ml can be achieved using this system, which is a great advantage over retroviral vectors, since these titres ensure efficient *in vivo* gene transfer. Furthermore, adenoviruses have a broad cell tropism and can infect non-dividing cells. On the other hand, they allow only

a transient expression of a transgene, since they persist in infected cells as an episome and expression of the E2 viral protein provokes inflammatory reactions and toxicities that limit repeated application of the viral vectors. To prevent immunogenic reactions, second generation vectors were established with lack of E2A functions in addition to a mutation or deletion of the viral E4 gene (Morsy and Caskey, 1999). These vectors require helper cells which can provide the E4 function required for transcription regulation, transition from early to late viral gene expression, mRNA transport, viral DNA replication, shut-off of host gene expression and assembly of the virion. More recently defective adenoviral vectors were created in which all viral coding regions were removed, leaving only the inverted terminal repeats (ITR), the transgene and *psi* packaging sequences in these vectors (Kochanek et al., 1996). The advantage of such vectors is that they are less immunogenic and produce high viral titres in the HEK293 cell line but their separation from helper virus is difficult. Many strategies are currently being investigated to combine the advantages of adenoviral vectors with reduced immunogenicity and long lasting, high level expression of transgenes typical of other viruses, through the creation of chimeric vectors such as adenovirus-AAV or adenovirus-retrovirus chimera to achieve viral integration into host DNA coupled with efficient infection and high level gene expression. Since adenoviral vectors are very efficient gene transfer vehicles mediating transient but high level expression of the target gene, these vectors are frequently used in clinical gene therapy studies (Walther and Stein, 2000).

AAV is a single stranded DNA dependovirus belonging to the family of Parvoviruses that can infect a broad range of cell types. No pathology has been observed with viral infection although the majority of the human population is seropositive for AAV. AAV contains 2 genes, *rep* and *cap*, encoding polypeptides essential for the replication and encapsulation of AAV and flanked by viral ITRs. AAV requires an adenovirus or a herpes virus for viral replication and needs stimulation by, for example, adenoviral E1 and E4 proteins. In addition, adenoviral E1B and E4 proteins are required for a productive AAV infection and for the synthesis of the second AAV DNA strand. This process is important for the conversion of the single-stranded AAV genome into the transcription-competent double-stranded DNA molecule. The generation of recombinant AAV (rAAV) particles requires super-infection with an adenovirus causing difficulties in obtaining high-quality viral stocks. This is also complicated by the difficulty of completely removing helper viruses. Notwithstanding,

newer rAAV production systems circumvent these problems by replacing adenovirus with adenovirus helper plasmids carrying the adenoviral E2A, E4 and VA genes, which are expressed by their endogenous promoters. Co-transfection of rAAV vectors with the adenovirus helper plasmid in HEK293 cells generates rAAV particles at high titres. The wild-type AAV integrates into a specific region of human chromosome 19 after infection, whereas the recombinant virus has lost this site-specific integration, possibly by deletion of the rep gene in rAAV vectors (Xiao et al., 1998). For the construction of rAAV-based vectors, the rep and cap genes are replaced by exogenous genes and internal promoters regulating transgene expression. In contrast to adenoviruses, AAV has low immunogenicity, which is important for the use of rAAV vectors *in vivo*, but has only limited capacity for insertion of foreign genes ranging from 4.1 to 4.9kb. rAAV vectors are suitable for *in vitro* and *in vivo* gene transfer into several organs and cells such as muscle, brain, haematopoietic progenitor cells, neurons and liver cells (Walther and Stein, 2000).

HSV-1 is a DNA virus possessing a linear double stranded genome of 150kb encoding 70 to 80 genes. This feature determines the large packaging capacity of this virus for insertion of foreign genes of 30 to 50kb. The virus has a broad range of target cell types, and can infect dividing and non-dividing cells, where it can establish a lytic or a latent infection persisting for years. The virus does not integrate into the host genome, which is the reason for only transient expression in infected cell populations. HSV is of interest because of its large insertional capacity for foreign DNA, its natural tropism toward neurons, its relative stability and the ability to obtain high titres of up to  $10^{12}$  cfu/ml (Chou et al., 1990). Despite several studies generally demonstrating the applicability of HSV vectors for long term expression of transgenes, particularly in neurons, there are still numerous safety and technical issues to be addressed such as reduction of toxicity after viral infection, possible inactivation of circulating viral vectors by host antibodies and risk of recombination (Walther and Stein, 2000).

### **2.2.6 Viral vector microinjection into the brain**

Different physical methods are available for viral vector delivery into the brain: stereotaxic injection, intrathecal and intraventricular injection and intravascular infusion with or without modification of the blood brain barrier (BBB). The choice of route for viral vectors administration affects neuronal cells transduction efficiency and spatial



distribution, as well as the extent of transgene expression in the infected cells (Rainov and Kramm, 2001). The simplest local approach for viral vectors delivery to a specific brain area is the stereotaxic injection: it offers the advantages of low systemic toxicity, high local vector concentrations and minimal vector loss to the systemic blood and lymph circulation. On the other hand this procedure presents some disadvantages, such as limited vector distribution to a few millimetres surrounding the respective injection site and the need of multiple injections to achieve wide virus distribution in a large brain region. Since the number of injection sites and the single volume of inoculum are limited for practical reasons by length of surgery and increasing risk of haemorrhage, stereotaxically guided viral vectors injections provide adequate vector delivery to spatially limited areas of the brain. Intrathecal virus injection provides minimally invasive approach to access to the cerebrospinal fluid (CSF) spaces and a ubiquitous distribution of vectors in the CNS but does not permit spatial selectivity of delivery. Moreover it requires a large amount of vectors since viruses may be inactivated by CSF. Intravascular viral vector applications, in particular intra-arterial injection or infusion, are not linked to mechanical injury to brain tissue but provoke major loss of vector to peripheral organs, possible systemic toxicity, and need high concentration of vector with low rate of neuronal vector delivery.

In 1994 Nikkhah and colleagues experimentally demonstrated that a minor brain damage is provoked by stereotaxic microinjection compared with conventional macroinjection with steel needles (Nikkah et al., 1994). In particular they compared the effect of injection into striatum with a Hamilton syringe connected to a 0.5mm outer diameter (OD) metal cannula or to a glass capillary with an OD of 50-70 $\mu$ m. The results showed that glass needle minimized injection trauma and was associated with a more extensive functional recovery after surgery. Whittemore and colleagues explored the effect of various OD glass tips as well as configuration of the tip (broken, bevelled, fire polished) on the deformation of the spinal cord before the tip penetrated the cord parenchyma, an indication of the degree of the host tissue damage (Whittemore et. al., 2002) (Fig. 5). In addition they investigated the effect of a 1 $\mu$ l Hamilton syringe injection since it is widely used in research for injection into the CNS. The results showed that injections with Hamilton syringe connected to steel needle caused substantial deformation of the spinal cord and a 10% lower cell viability compare to glass needle injection, while among the glass needles, bevelled tips performed better than broken or polished tips (Table 1).

**Table 1**  
**Micropipet Parameters**

Pipet size (OD)	Tip type	Spinal cord deformation (mm)
25 $\mu\text{m}$	Beveled	$0.24 \pm 0.02$
40 $\mu\text{m}$	Broken	$0.65 \pm 0.03$
40 $\mu\text{m}$	Beveled	$0.35 \pm 0.03$
90 $\mu\text{m}$	Broken	$0.93 \pm 0.04$
90 $\mu\text{m}$	Beveled	$0.72 \pm 0.04$
90 $\mu\text{m}$	Fire polished	$1.08 \pm 0.03$
1 $\mu\text{L}$ Hamilton syringe		$>1.00^a$

Table 1. Spinal cord deformation provoked by several type of glass micropipetes or 1 $\mu\text{L}$  Hamilton syringe (Whittemore et al., 2002).

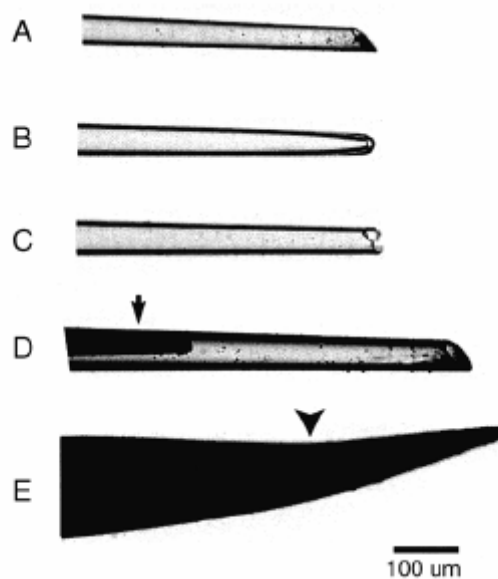


Fig. 5. Example of micropipet tip configurations. (A) beveled, (B) fire-polished, (C) broken, (D) beveled with tungsten filament partially lowered (arrow), (E) tip of 1 $\mu\text{L}$  Hamilton syringe. The arrowhead indicates the center of the opening in the syringe (Whittemore et al., 2002).

They also tested both manual and motorized injection procedures and reported the advantages of motorized over manual microinjection to deliver precise small volumes. In the motorized procedure the syringes connected to the micropipette is mounted on a programmable infusion pump. Some disadvantages are associated at this delivery system since it relies on pressure for delivery and the injection volume could be influenced by changes in tip and tissues resistances. Moreover small OD diameter needles have the potential to become clogged as the tips is lowered in the tissue but this problem can be overcome by using a high flow rate while lowering the needle within the tissue.

### 2.2.7 RNAi in neurons

Thanks to its feasibility in target gene suppression, RNA interference has been used in the last few years to explore the patho-physiology of several diseases. The use of RNAi in neuropsychiatric diseases faces the problematic task of targeting gene expression in the mammalian brain. Mammalian neurons are non dividing- terminally differentiated cells more difficult to transfect *in vitro* and more sensitive than other primary cells to some transfection systems such as lipophilic agents or electroporation. Despite this, there are several reports in literature of the ability of siRNA to reduce gene expression in mammalian neurons (Numakawa et al., 2004). Moreover, there are peculiar characteristics of the brain that can hinder RNAi successful application. Since the blood-brain barrier restricts the passive entry of materials from the peripheral circulation, systemic administration of siRNAs is almost ineffective to obtain RNAi-mediated gene suppression in the brain. In addition, a high level of complexity and connections in the cellular population are obstacles to achieve the desired gene knockdown within a specific set of cells in a particular brain area. Nonetheless in the past few years an intense exploration of possible RNAi applications in mammalian brain not only in neuroscience but also as a potential therapeutic tool for otherwise untreatable neurological diseases was reported (Federici and Boulis, 2007; Hoyer D, 2007).

The methodologies for RNAi application in the brain are essentially two: direct pre-synthesized siRNAs using several delivery systems or short-hairpin RNA-mediated gene knockdown. After their *in vitro* success in down-regulating gene expression in neurons, chemically synthesized siRNAs were tested for their ability to knockdown gene expression in the brain. The simplest way to deliver siRNAs is to locally inject them in the desired region of the brain. Successful gene knockdown in brainstem and hypothalamic nuclei was reported with this method, but only a transient and highly restricted injection site suppression was achieved (Makimura et al., 2002). Transfection reagents able to efficiently deliver siRNA in the brain have been recently described (Hassani et al., 2005). Cationic vehicles, using either polyethylenimine or a mixture of lipids and alcohol as well as an aqueous formulation, were tested for their ability to deliver siRNA into the cerebral hemispheres of neonatal mice. Only with the aqueous formulation of the lipoplex-neutral lipid mixture gene suppression was achieved. Since neurons are sensitive to liposomal toxicity, when using a cationic lipid-based

transfection reagent it is necessary to investigate the potential metabolic effect on these cells (Lingor et al., 2004). Electroporation is able to effectively introduce exogenous DNA, RNA or low molecular weight compounds into neurons. This method was recently used to regulate the target area of siRNA-induced gene knockdown in the brain. Cellular introduction of siRNA was facilitated with local electroporation via electrodes implanted 5 mm apart, placed on either side of the siRNA injection site. Following electroporation, siRNA-mediated down-regulation of target mRNA was found to be transient, with maximal knockdown of 80% obtained after 6 days, returning to basal levels in a 2- to 4-week period. The target region did not show any signs of cytotoxicity occasionally found with this method (Akaneya et al., 2005). Indeed electroporation may be a powerful technique for investigating regionally defined neuronal circuits involved in disease pathology in animals.

The previously discussed methods, in conjunction with the use of short-hairpin RNA, can be used for phenotyping of genes expressed in specific brain regions. These approaches are not ideal for the suppression of broadly expressed genes and for genes in which their mRNA processing events or the brain regions relevant to their physiological actions are lacking. To address this, prolonged siRNA administration, using osmotic mini-pumps was used to efficiently produce gene silencing throughout the whole brain (Davies, 2005) without neurotoxic effects possible associated with the use of transfection and electroporation.

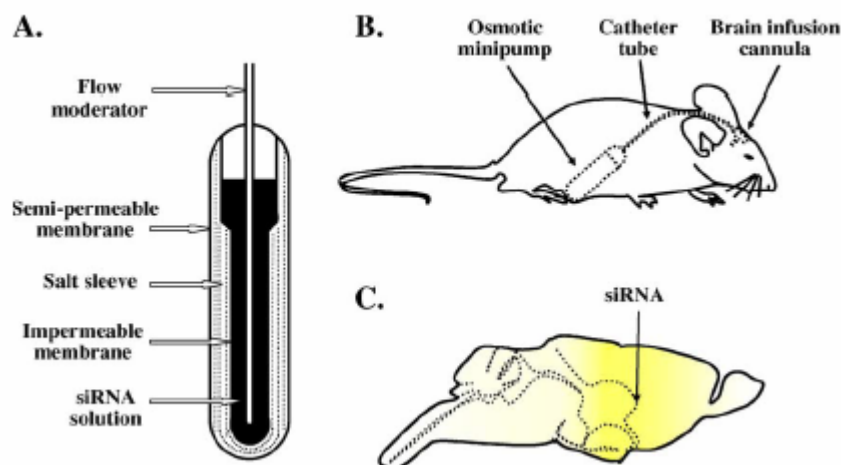


Fig. 6. siRNA infusion, using osmotic minipumps, for widespread knockdown of gene expression in the brain. (A) Cross-sectional view of an osmotic minipump (<http://www.alzet.com>). (B) The osmotic minipump is subcutaneously placed on either side of the mouse, with its flow moderator connected to a catheter that is attached to a brain infusion cannula on the other end. The brain infusion cannula is stereotaxically placed so as to infuse the siRNA into the brain. Subsequently, siRNA is directed via the

catheter to the brain infusion cannula and infused into the dorsal third ventricle. (C) A schematic is shown, illustrating the extent of gene knockdown obtained upon infusing siRNA for 2 weeks into the dorsal third ventricle. The intensity of yellow color roughly denotes the magnitude of knockdown attained in various brain regions for a number of genes (Thakker et al., 2006).

An osmotic minipump contains a high-osmolality chamber that surrounds a flexible and impermeable, reservoir filled with the siRNA containing vehicle (Fig. 6). Subsequent to the subcutaneous implantation of this minipump, extracellular fluid enters through an outer semi-permeable membrane into the high-osmolality chamber, thereby compressing the reservoir to release siRNA at a controlled, pre-determined rate. siRNA, released from the pump, is directed via a catheter to a stereotaxically placed cannula for infusion into the brain. There are several examples in the literature of successful and widespread gene suppression in the brain achieved with the minipump method such as the knockdown of P2X3, which is implicated in pain, in the rat dorsal root ganglia after chemically modified siRNA intrathecal infusion (Dorn et al., 2004). No signs of neurotoxicity, with respect to neuroanatomical damage, spinal inflammation, or hind-limb paralysis, were noted after intrathecal siRNA infusion even if at rates very high (0.4 mg/day for up to 6 days). Similar results were achieved by Thakker and colleagues, who demonstrated that intracerebroventricular (i.c.v.) infusion of siRNA, using osmotic minipumps, lead to a specific knockdown of gene expression in the brain (Thakker et al., 2004, 2005). They obtained a significant reduction of mRNA for the dopamine transporter (DAT) of 33% in the substantia nigra compacta and ventral tegmental area, following infusion of an unmodified siRNA into the dorsal third ventricle over 2-weeks. Down-regulation of the DAT protein was also demonstrated. Concomitant to the siRNA-induced knockdown of DAT, a time-dependent hyperlocomotor phenotype developed in the mice, similar to that obtained after infusing a pharmacologically selective DAT inhibitor. More recently, suppression of the serotonin transporter (SERT) gene, implicated in the etiology of anxiety and depression, was achieved after a 2-week siRNA infusion into the dorsal third ventricle. This decrease in mRNA levels was reflected in a widespread and specific reduction in the levels of the SERT protein in the brain and in an antidepressant-like behaviour in the mouse forced swim test, an effect identical to that obtained from mice receiving a pharmacologically selective SERT inhibitor. siRNA infusion into the dorsal third ventricle using osmotic minipumps is an effective means for producing specific and

bilateral knockdown of gene expression in the brain, evading the need for repeated siRNA injections and permitting the prolonged siRNA infusion over time by replacing the empty minipump with newly filled pumps. However, a disadvantage in the use of this system is the cost associated with the synthesis of siRNA, depending on the concentration and infusion period required in order to achieve a stable and significant gene knockdown and the technical difficulties in the use of minipumps.

As previously seen, one of the major disadvantages of using pre-synthesized siRNA *in vivo* is the transient nature of gene knockdown. Consequently, DNA vectors have been developed to constitutively express shRNAs in order to achieve a long-lasting siRNA production intracellularly. These DNA vectors incorporate either the RNase P H1 (H1) or the U6 small nuclear RNA (U6) polymerase (Pol) III promoters to express shRNAs with well-defined 5' and 3' ends. At the moment, only one study has reported the suppression of target gene expression after liposomal transfection of an H1 promoter-driven shRNA expression vector, but this suppression was transient (Makimura et al., 2002). It is unclear if liposomes would further enhance the duration of RNAi-mediated gene silencing and subsequent phenotyping, without eliciting cytotoxic or off-target effects. More successful was the application of electroporation to deliver shRNA-vectors (see Konishi et al., 2004). In any case the most investigated technique to deliver and express shRNA in the brain is through recombinant viral vector. Among the retroviral vectors, lentiviral vectors have been used to deliver shRNA in the brain thanks to their ability to infect actively dividing as well as non-dividing, post-mitotic cells such as neurons and achieve extended expression of shRNA. However, the fact that retroviruses integrate their genetic material into the host genome also enhances the risk of insertional mutagenesis. In the first proof-of-concept study, an HIV-1-derived lentiviral vector expressing an enhanced green fluorescent protein (eGFP) targeting shRNA under the control of a U6 promoter was injected into the striatum of adult mice (Van den Haute et al., 2003). One week after injection, eGFP expression from a co-injected eGFP-encoding lentiviral vector was completely silenced. HIV-1-based lentiviral vectors have been used also for extended knockdown of endogenous gene expression in motor neurons of the brainstem and spinal cord. In mice expressing a mutated form of the human Cu/Zn superoxide dismutase (SOD1) (SOD1G93A), increase in the survival and function of motor neurons and a marked reduction in the muscular atrophy was observed after SOD1-shRNA expression driven by HIV-1-based lentiviral vector (Gurney et al., 1994).

Adenoviruses, which do not integrate into the host genome, exhibit comparable transduction efficiencies in neuronal cells to lentiviruses. A substantial knockdown of eGFP expression has been demonstrated in the striatum of adult eGFP-expressing mice 5 days following local injections of recombinant adenoviral shRNA constructs (Xia et al., 2002). However, the *in vivo* use of adenoviruses has been limited by the possible activation of immune response.

In contrast, recombinant adeno-associated viruses are weakly immunogenic and are episomal, not integrating into the host genome. They also transduce both dividing and non-dividing, post-mitotic cells such as neurons. Thanks to this property, they present an attractive alternative for the delivery of shRNAs into the brain, particularly the AAV serotype 2 (AAV2). Infection of specific neurons in the brain has been achieved with pseudotyping, using capsid proteins from AAV1 along with those of AAV2 for cross-packing the shRNA-expressing vector containing AAV2 inverted terminal repeats (Cao et al., 2004) to create recombinant AAV1/2 chimeric vectors. These vectors have been demonstrated to efficiently deliver an shRNA to hippocampal neurons of young rats (Cao et al., 2004). AAV expressing vascular endothelial growth factor (VEGF) shRNA specifically suppress mRNA by 50% as well as protein by 15%. Tropism for midbrain dopaminergic neurons was also revealed after injecting AAV-shRNA vectors targeting the mRNA of tyrosine hydroxylase (TH), a rate-limiting enzyme in the biosynthesis of catecholamines, into the substantia nigra compacta or ventral tegmental area of adult mice (Hommel et al., 2003). shRNA-mediated downregulation of TH was persistent for a period of up to 50 days post-transduction and rostrocaudally spread across the substantia nigra compacta. In addition reduction in protein levels and decrease in a motor-deficit was demonstrated. Recombinant AAV-shRNA vectors were also used to treat polyglutamine disorders, such as Huntington's disease (HD; Harper et al., 2005) and spinocerebellar ataxia type 1 (SCA1; Xia et al., 2004). The mutant huntingtin was targeted by AAV-shRNA vectors in the striata or cerebellar lobules of a murine model of HD, achieving successful target gene and protein suppression and a significant reduction in the HD neuropathology. Similarly, recombinant AAV vectors expressing a human ataxin-1-targeting shRNA from the H1 promoter (Xia et al., 2004) were injected at multiple sites in the midline cerebellar lobules of SCA1 mice, expressing the human ataxin-1 disease allele in cerebellar Purkinje cells. Also in this study, successful target suppression was achieved, associated with a reduction in the typical phenotypic characteristic of this pathology. These results

confirm the ability of AAV-shRNA vectors to mediate sustained and prolonged suppression of target gene in specific brain area.

A non-viral transvascular delivery of shRNA-expressing DNA vectors was explored by Pardridge and colleagues (Zhang et al., 2003) to suppress genes broadly expressed in the brain. Their approach consists of intravenous (i.v.) injections of vector-encapsulating liposomes (PILs) that are externally conjugated to PEG to restrict the uptake to the reticuloendothelium and extend their half-life in the bloodstream. In addition, PEG also binds to receptor-specific peptidomimetic monoclonal antibodies that facilitate organ- or tissue-specific delivery. Antibodies directed against the insulin or transferrin receptors enable a receptor-mediated transcytosis of PILs across the BBB and endocytosis into the brain cells. PIL-mediated RNAi delivery into brain was tested by targeting human epidermal growth factor receptor (EGFR), in brain tumors of adult rats (Zhang et al., 2004). Consequent to the weekly i.v. injections of PILs, a marked decline in the target protein levels was noted in cancer cells, correlated with an approximate doubling in the survival time of shRNA-expressing mice. Despite that, the impossibility to restrict gene knockdown to specific cell populations within the brain and the limited longevity of the PIL-mediated RNAi response restricted the use of this approach.

An alternative method to investigate neuronal gene function *in vivo* is represented by the development of constitutive and inducible transgenic RNAi animals. In fact using accurate inducible Cre expression strategies for transgenic siRNA expression, it is possible to study neuronal genes (Ventura et al., 2004).

To choose the appropriate RNAi approach for evaluating neuronal gene function *in vivo*, it is important to consider the proprieties of the target gene itself such as the stability and/or turnover rate of the encoded mRNA, and protein. Genes with short mRNA and/or protein half-lives (hours to days) can be effectively silenced using transiently effective approaches, such as local injections or transfection of si/shRNA. In contrast, genes with longer half-lives (days to weeks) require an extended knockdown, that can be achieved either by repeated electroporation of siRNA, by injecting PIL encapsulating shRNA-expressing vectors, by minipump infusion of siRNA or by injection of recombinant viral shRNA-vectors. Stable knockdown of gene expression can be obtained using transgenic RNAi mice. Another consideration that needs to be taken into account is the local or widespread application of the siRNA required. RNAi offers an immense potential in not only investigating the patho-physiological role for



genes that are expressed in the brain, but also for generating the relevant animal models of neurological and psychiatric disorders. RNAi holds promise for the development of novel therapeutic strategies to treat neuron-based disorders that are at present yet difficult to treat, such as neuropathic pain and depression (Dorn et al., 2004; Thakker et al., 2005), as well as dominantly inherited neurological diseases that result from gene mutations like HD, even if more studies are needed to explore the effective benefit of the RNAi therapeutics.

### **3. MATERIALS AND METHODS**

## **3.1 IN VITRO WORK**

### **3.1.1. Cell cultures**

The rat pheochromocytoma PC12 cell line and a sub-clone thereof, PC12NS1 were grown in F-12 and F-10 respectively medium with 15% horse serum, 2.5% fetal bovine serum, 2mM Glutamine, penicillin and streptomycin (both 100U/ml). Human HEK293A cells were grown in D-MEM with 10% fetal bovine serum (Sigma, UK), 2mM Glutamine, penicillin and streptomycin (both 100U/ml) and rat P2X4 and P2X7-HEK recombinant cells were grown in the same medium with G418 geneticin 0.3mg/ml for selection. All the cells were grown at 37 °C in a humidified atmosphere of 95% air and 5% CO<sub>2</sub>. All reagents were provided from Gibco, UK.

### **3.1.2 Primary cells**

Rat astrocytes were by Steve Skaper (GlaxoSmithKline, Harlow) and have been growth in D-MEM with 10% fetal bovine serum, 2mM Glutamine, penicillin and streptomycin (both 100U/ml) at 37 °C in a humidified atmosphere of 95% air and 5% CO<sub>2</sub>.

Primary cultures of hippocampal neurons were prepared as described in previous works (Skaper SD et. al., 1990) from rat hippocampi isolated from E17-19 embryos. Time-mated pregnant rats (Wistar-Han by Charles River, UK) were killed by CO<sub>2</sub> asphyxiation, fetuses were removed by caesarean section and fetal hippocampi were dissected from surrounding brain tissue. After the meninge removal, hippocampi were isolated, enzymatically dissociated and purified with the papain dissociation kit (Worthington, UK). Neurons were plated at  $1.5 \times 10^5$  cells/well in neurobasal medium (NBM) containing B27 supplement with anti-oxidants, 0.5 mM L-glutamine, 100/U penicillin/streptomycin and 1mM sodium pyruvate (Sigma, other reagents from Gibco) in plates pretreated with poly-D-lysine 50µg/ml (Sigma). Cultures were lysate 7 days later and submitted for TaqMan analysis or western blot. This work complied with national legislation for animal handling and with the GSK policy on the Care of Use of Animals and related codes of practice.

### 3.1.3 siRNA design and transfection

siRNA sequences were designed and then synthesized using commercial algorithms (in this case Ambion) based on Tuschl design rules (target sites beginning with AA, 3' UU overhangs for both the sense and antisense siRNA strands,  $\approx$ 50% G/C content) and considering a high number of physical characteristics able to influence siRNA potency and specificity, including  $T_m$ , nucleotide content of the 3' overhangs, siRNA length and nucleotide distribution over the length of the siRNA. Moreover, a key step in the algorithm is a stringent analysis of each siRNA sequence to maximize target specificity (see Fig. 7 for an example of a siRNA sequence).

For the siRNA delivery into the cells, Gemini GSK250910, a GSK proprietary surfactant able to form a complex with DNA and RNA and deliver them inside the cell was used, at final concentration of 3.5 $\mu$ g/ml while siRNA final concentration was 100nM. A modified version of the reverse transfection protocol was performed: each siRNA was mixed with the GSK surfactant at the appropriate concentration in general medium, left for 15min at room temperature and then the cell suspension was mixed with the siRNA/GSK surfactant complex and seeded at 6.3x10<sup>5</sup> cells/ml. After 24hr, the medium was replaced with a second dose of siRNA/GSK surfactant complex. After 48hr cells were harvested for TaqMan analysis (adding 100 $\mu$ l/well of Lyses Buffer +  $\beta$ -Mercaptoethanol).

P2X7 (NM\_019256):

```
1 GGUGACAGAGAAUGUCACGtt
2 GGCCAAGAACAGAAGCUGUtt
3 GGAAA AUGGCAUGGAAAAGtt
```

Fig. 7. Ambion P2X7 siRNA sequences.

### 3.1.4 shRNA design, cloning and transfection

shRNAs were designed based upon siRNA sequences, except these containing stretches of three or more uridine or adenosine, since these sequences could be inhibitory of shRNA expression by increasing the chance of premature termination. A guanine at the 5' end of the siRNA sequence (to increase the transcription efficacy) and the Brummelkamp loop at the 3' were inserted, then the complementary and inverted

sequence to form the stem and at the end of the template the termination site (TTTTT). From this sense strand the complementary strand (or antisense strand) was designed and in this way 4 shRNAs were constructed for each gene. The Brummelkamp loop was chosen because it is one of the most frequently reported loop sequence (Fig. 8). The two complementary oligos were annealed to form the shRNA (a double strand DNA) which was then cloned into a linearized plasmid vector (pENTRΔU6) carrying the human U6 promoter. This promoter has been used because it normally drives the expression of short non coding RNAs with high efficiency. Prior to cloning the shRNA, the vector was linearized with the 2 enzymes EcoRI and BbsI producing four nucleotides overhangs at each 5' end (encoding the last four nucleotides of the U6 promoter and first four nucleotides of RNAPolIII terminator site), to direct the directional cloning of the oligo downstream the U6 promoter. The transfected clones, selected for the antibiotic resistance, were sequenced to identify the vectors carrying the correct shRNA, and then isolated to prepare a large amount of vectors. Three shRNA carrying vectors for P2X2 and P2X4 and all the initial four shRNA vectors for P2X7 were obtained. These U6-shRNA plasmids were transfected in different cell types using the GSK30064 Gemini 8-10µg/ml or the commercial Lipofectamine 2K 1.5ng/µl (Invitrogen, UK). For plasmid transfection of astrocytes, the AMAXA nucleofection system (Amaxa GmbH, Germany) was used: this technique uses a unique combination of electrical parameters and cell-type specific solutions and provides the ability to transfect even non-dividing cells. Different amounts of plasmid DNA were tested (2-5 µg), achieving roughly 80% DNA delivery and good cell viability measured transfecting astrocytes with a GFP expressing vector. Three days after plasmid transfection the cells were harvested for TaqMan analysis or western blot.

#### P2X4-1

```

5' -ACCGTCAGCTCGGTGACAACCAATTCAAGAGATTGGTTGTCACCGAGCTGATTTTTG-3'
3' -AGTCGAGCCACTGTTGGTTAAGTTCTCTAACCACAGTGGCTCGACTAAAACTTAA-5'

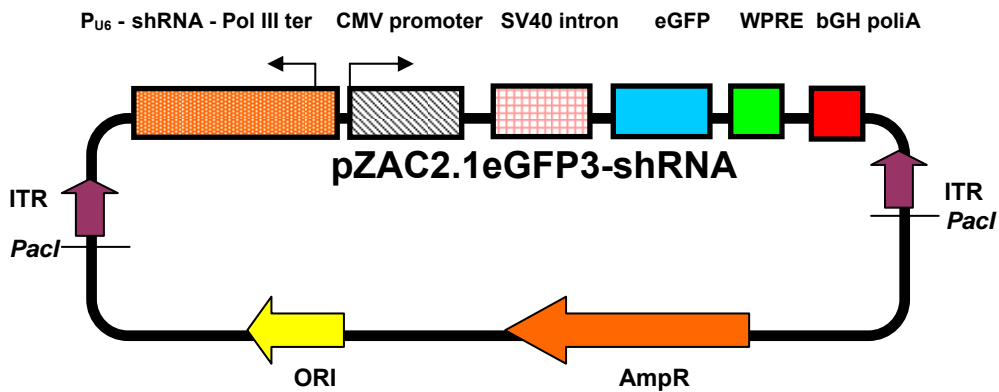
```

Fig. 8. Example of a shRNA sequence.

### 3.1.5 AAV and Ad vector production

For the AAV viruses production, the U6-shRNA cassettes were inserted in a AAV2-based shuttle plasmid, the pZAC2.1eGFP3 vector, carrying part of the wild type

viral sequence (Fig. 9). This vector was then packaged into AAV6 capsids by the Viral Vector Core, University of Pennsylvania for generation of high titer of viral vectors stock. The U6-shRNA cassettes were amplified by PCR from the pENTR-U6shRNA vectors, cut with the XbaI enzyme and purified from the gel band. The DNA fragment obtained presents the 3'-end overhang compatible with the shuttle pZAC vector cut with the NheI enzyme and dephosphorilated at the 5'-end to prevent its closing. After the ligation reaction and *E.Coli* transformation, the clones carrying the pZAC vectors with the correct shRNA cassette were isolated and the vectors produced in large amount. To produce the final viral particles, the recombinant AAV vectors were co-transfected with the adenovirus helper plasmid in 293 packaging cells. Finally the viruses were purified and resuspended in sucrose and the final titer for each viral vector was determined by PCR.

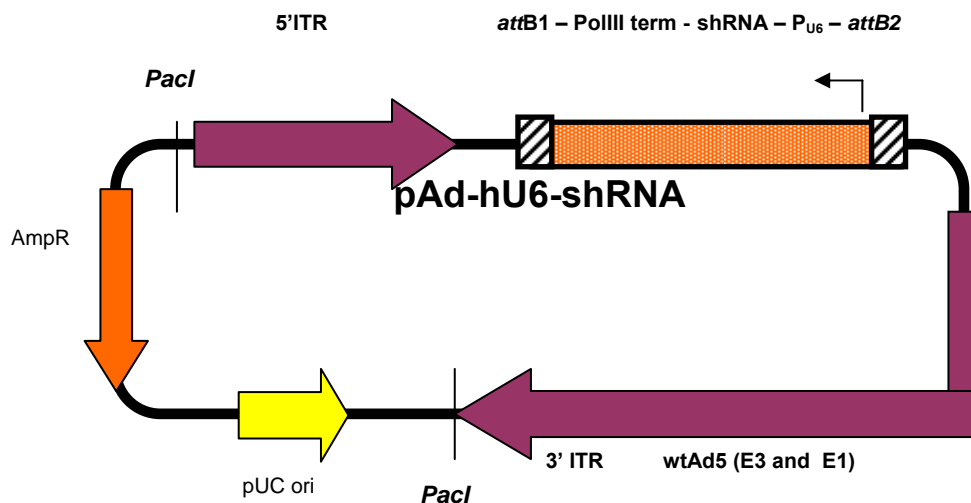


- Legend:
- |  |  |
|--|--|
| ITR:                                   | Inverted terminal repeated                                     |
| P <sub>U6</sub> - shRNA - Pol III ter: | Human U6 promoter + shRNA sequence + Polymerase III terminator |
| CMV promoter:                          | Cytomegalovirus promoter                                       |
| SV40 intron:                           | Simian vacuolating virus 40 intron                             |
| eGFP:                                  | enhanced Green Fluorescent Protein                             |
| WPRE:                                  | Woodchuck Hepatitis Post-transcriptional Regulatory Element    |
| bGH polyA:                             | Bovine Growth Hormon polyadenylation site                      |
| ORI:                                   | origin   |
| AmpR:                                  | Ampicillin resistance site                                     |

Fig. 9. Map of AAV2-shRNA shuttle plasmid.

For the AdV5 vectors production, the U6-shRNA cassettes were cloned in the Ad5 shuttle plasmid through a recombinant reaction (using the Invitrogen clonase enzyme mix) and the vectors carrying the right shRNA sequences were selected for antibiotic resistance and prepared in large amount. The Ad5 shuttle vector contains a part of the human Ad5 wild type sequence, including left and right inverted terminal repeats (ITR),

late genes and packaging signal while the E1 region necessary for the replication, and the E3 region are deleted (Fig. 10). The vector was digested with the *PacI* enzyme to excise the viral genome sequence from the plasmid and allow proper viral replication and packaging when transfected into HEK293A cells (using Lipofectamine 2K as delivery agent). These cells exhibit a flattened morphology, enabling easier visualization of viral plaques (CPE, cytopathic effect) that typically are observed 7-10 days post-transfection. When these are visible, the cells and media are harvested and the viral particles inside the cells released, through several freeze/thaw cycles. These are used to infect a higher number of cells to obtain a large amount of viral vectors. The viral vectors were then purified using the CsCl gradient and the viral titer determined through visualization of the viral hexon proteins (using the Adeno-X Titer kit by BD Biosciences, UK).



Legend:  
 ITR: inverted terminal repeated (5' ITR contains packaging signal)  
 PU6 - shRNA - Pol III ter: Human U6 promoter + shRNA sequence + Polymerase III terminator  
 attB: site for recombination (Invitrogen Gateway system)  
 wtAd5 (E3 and E1): human Ad5 sequences (E3 region deleted)  
 AmpR: Ampicillin resistance gene  
 pUC ori: origin

Fig. 10. Map of Ad5 shuttle plasmid.

### 3.1.6 Cell infection

Rat astrocytes were seeded at  $2 \times 10^5$  cells/ml in 24 or 96 well plates, for western blot or TaqMan analysis, respectively. The following day, the cells were infected with a specific amount of virus, simply by adding the virus to the well and diluting it in 2%

fetal bovine serum medium if necessary. The medium was not replaced (for longer incubations, fresh medium was added.) At the time point chosen the cells were lysed to extract protein or RNA.

Rat hippocampal neurons were supplied in 24 well plates, since the level of P2XR expression in embryonic hippocampal cultures is quite low. The neurons were infected with the virus diluted in 250 $\mu$ l of NBM. The day after additional 250 $\mu$ l of fresh medium were added to each well and an equal volume was added 3 days after infection. At the time point chosen the cell plates were lysed for TaqMan or western blot.

### **3.1.7 TaqMan analysis**

TaqMan primers and probes were designed using the software Primer Express; RNA extraction has been performed using the Promega SV96 kit and the reverse transcription to synthesize cDNA with Applied Biosystem cDNA synthesize kit.

TaqMan analysis was performed using the Applied Biosystem method, using the TaqMan® Universal PCR Master Mix in the 384 well format with the ABI PRISM 7900 sequence detector. For each analysis, the GAPDH normalized copy numbers of P2X2, P2X4 and P2X7 mRNA was measured.

### **3.1.8 Western blot for P2X receptors detection**

The whole cell lysate was obtained by harvesting the cell pellet in SDS + 2.5%  $\beta$ -Mercaptoethanol; hippocampal neurons were lysed with LDS buffer + reducing agent and the protein samples were run on Nupage 4-12% Tris Bis gel with MOPS SDS buffer (all Invitrogen, UK). To obtain the membrane fraction the cell pellet was resuspended in membrane buffer (10mM Tris-HCl, 0.1M EDTA pH 7.5 and protease inhibitors cocktail from Boehringer, Germany), sonicated to homogenize cell suspension and passed through a 25 gauge needle. The nuclei pellet was isolated by centrifugation at 1200xg for 10min at 4°C and resuspended in RIPA buffer and protease inhibitors (0.01M Tris pH 7.2, 0.15M NaCl, 1% Triton X-100, 0.1% SDS, 1% sodium deoxycholate, 0.02% sodium azide and 5mM EDTA) and the supernatant was centrifuged for 20min at 13000rpm to yield the membrane fraction (resuspended in RIPA buffer) (MLA-80, Benchtop Ultracentrifuge). To obtain a crude membrane fraction from whole rat brain, the tissue was dissected with a scalpel, washed in membrane buffer and protease inhibitors, spun briefly to pellet, then resuspended in



membrane buffer and homogenised in a glass potter homogeniser (three cycles of 20 strokes, spinned pellet, re-suspended and re-homogenised). At the end, the homogenised supernatant was centrifuged at 18000rpm for 30min (MLA-80, Benchtop Ultracentrifuge), the pellet washed in 20mM HEPES and re-centrifuged at same speed. The crude membrane pellet was resuspended in RIPA buffer on ice for 1hr and then stored at -80°C.

The protein amount in each sample was quantified using the Coomassie plus Bradford Assay kit (Pierce, UK), following the manufacturer's instructions.

Both whole cells lysate and membrane cell fractions were heated 2 minutes at 85°C prior to loading; a maximum of 25µl of sample was subjected to electrophoresis on Novex 4–12% Tris-Glycine Gel and transblotted onto a nitro-cellulose membrane. Prestained protein standard was used to visualize successful transfer and to measure molecular weight of the subsequent signal (MagicMark™ Western Protein Standard, all Invitrogen, UK). The membrane was blocked with PBS containing 0.1% Tween (PBST) and 5% skimmed milk (Marvel, UK) for 2 hours, and then washed three times at 10 min intervals with PBST. Washed membrane was incubated with the appropriate dilution of the primary antibodies in PBST + 5% skimmed milk overnight at 4°C, then washed 3 x 10 minutes in PBS/Tween and incubated with the peroxidase-conjugated secondary antibody (DakoCytomation) at 1:5000 dilution in PBS/Tween/Milk for 2 hours at room temperature (RT). The membrane was then washed 5 x 10 minutes in PBS/Tween and the proteins visualized after addition of the substrate using the Pierce West-Dura kit (Pierce, UK). The P2X antibodies used were: for P2X2 Alomone Labs APR-003, Santa Cruz (V-17) sc-12211 and the Santa Cruz (S-16): sc-12212; for P2X4 Chemicon AB5226, Santa Cruz (C-15): sc-15190, Santa Cruz (N-15): sc-15187 and for P2X7 Chemicon AB5246, Santa Cruz (L-20): sc-15200, Santa Cruz (H-265): sc-25698. Each membrane was also blotted for the  $\alpha$ -tubulin (Sigma, UK), to assess the amount of protein in each sample.

Western blot bands were quantified with the GeneSnap program, normalizing with  $\alpha$ -tubulin staining.

### **3.1.9 Immunocytochemistry (ICC) analysis**

For this analysis astrocytes were seeded on a 12 well plate, while hippocampal neurons were supplied in a 12 well plate on coverslips. Both culture types were plated at the same concentration ( $2 \times 10^5$  cell/ml). Cells were fixed in 4% paraformaldehyde (PFA)

for 15 minutes under a chemical hood, and then washed 3 x in 100µl PBS. After fixation, the cells were permeabilized with 100µl 0.1% Triton (TTX-100) in PBS for 10 minutes at RT. Non-specific binding was blocked by incubating cells with 100µl 1% bovine serum albumin (BSA) in PBS for 1 hour at RT. The primary anti-P2X antibodies (also used for western blot analysis) were diluted 1:200 in 1% BSA/PBS, applied to the plates and incubated for 1 hour at RT, followed by 3 washes with 100µl 1% BSA/PBS. 50µl of the secondary antibody (anti-rabbit Alexa-488) diluted 1:200 in 1% BSA/PBS was incubated with cells for 1 hour at RT. Plates were then washed 3 times with 100µl PBS, re-permeabilized for 10 minutes, then incubated with the astrocytic or neuronal marker antibody 1:3000 (GFAP Sigma G3893 and β3-tubulin Abcam 7751, respectively). After 3 washes, cells were incubated with the secondary anti-mouse antibody Alexa-594 diluted 1:400 (Alexa, Invitrogen, UK). Results were then visualized with fluorescence microscope.

### **3.1.10 IL-1β release ELISA**

For this assay microglial cells in a 96 well plates ( $2 \times 10^4$  cells/well) were infected with different amounts of Ad5 virus and treated 48 hours later with 1µg/ml LPS (Invitrogen, UK). After 24 hours, medium was removed, cells were washed with HBSS/1mM CaCl<sub>2</sub>. 1mM of the P2X7 antagonist, PPADS (Sigma, UK), in HBSS/CaCl<sub>2</sub> was added at some wells and incubated for 15 minutes at 37°C. 300µM of the P2X7 agonist, BzATP (Sigma, UK), in HBSS/CaCl<sub>2</sub> was then added and incubated for 30 mins at 37°C. The medium was transferred to a new 96 well plate and stored at -80°C. The ELISA was performed using the Quantikine Rat IL-1β kit RLB00 (R&D Systems, UK) following the manufacturer's instructions.

## **3.2 IN VIVO EXPERIMENTS**

### **3.2.1 Glass needle preparation**

For virus injection into specific area of the brain, bevelled micropipette tips were prepared with 30-40 $\mu$ m OD: borosilicate capillary tubes were chosen since this material is a neutral charge glass used for chemistry applications. In particular, thin-walled with internal filament borosilicate needles (Hilgenberg GmbH, 0.15mm filament diameter, 1.5mm OD and 0.315mm wall thickness) were produced using a puller for electrophysiology (Hans Ochozki). The internal filament helps to produce an efficient surface tension of the liquid, avoiding dispersion and glass-adhesion of the viral vectors.

Glass needles were prepared shortly before the surgery with the following parameters: position of carriage 7 and 16 and temperature  $t_1=3.0$  e  $t_2=8.5$ . The OD of the needles produced with these parameters is roughly 20-40 $\mu$ m at the tip and approximately 100-200 $\mu$ m 8mm distal from the tip. Maximum needle penetration in the tissue is 6mm. A certain variation in the diameter is expected, since this instrument is highly sensitive to environmental conditions changes, such as temperature, humidity, dust, etc.

### **3.2.2 Animal handling**

Male Wistar Han rats weighing 240-260 grams were used (Charles River, Italy). Animals were housed in a temperature- (20-22°C), light- (12 h light/dark cycle) and humidity- (55-65%) controlled environment, with ad libitum commercial rodent pellets and water provided. After surgery the animal were individually housed. Locomotor activity and basal health conditions were monitored twice a day for each animal. After completely recovering animals were housed in groups proportional to the size of the cage. This work complied with national legislation for animal handling.

### **3.2.3 Surgery**

Anesthesia was induced with a mix of 87 mg/kg ketamine and 13 mg/kg xylazine injected intraperitoneally (i.p.) and then maintained with isoflurane. Animals were mounted into a stereotaxic device (Narishige, Japan) with an incisor bar set at -5mm. A midline incision was made and two small holes were drilled in the skull in correspondence with the dorsal and ventral hippocampal dentate gyri (DG). The

coordinates were calculated from bregma according to “A Stereotaxic Atlas of the Rat Brain” [Pellegrino et al., (2nd edition), 1979].

Dorsal DG coordinates (tav. 39):

- Anterior-Posterior: -1.7mm
- Medio-Lateral: -1.2mm
- Dorso-Ventral: +3.9mm;
- ventral DG (tav. 49):
- Anterior-Posterior: -3.4mm
- Medio-Lateral: -4.7mm
- Dorso-Ventral: +6.5mm.

The borosilicate needle, pre-treated with ether and washed with 70% ethanol, was mounted in a pipette holder (WPI, USA) connected to a 50 $\mu$ l Hamilton microsyringe with clear PTFE tubing (Fig. 11).

The Hamilton microsyringe was mounted on a programmable infusion pump and, to avoid damage of the neuronal area, a low controlled rate of liquid infusion was chosen. The injection system was washed with ethanol, sterile water and then filled with sterile physiological solution.

Each viral vector was diluted to the final viral titer of choice with sterile PBS and 0.01% Trypan blue (Sigma). Approximately 8 $\mu$ l of viral solution were drawn up and a bubble of air was used to separate the viral solution from the saline solution. The tip was then lowered into the dorsal or ventral hippocampus and the selected volume of viral vector was injected using the infusion pump at the desired flow rate. The injector remained in place for an additional 1 minute following infusion. Animals were housed in a warm cage until recovery from surgery.



Fig. 11. In house injection system with glass micropipette used for viral vectors injection.

### **3.2.4 Trypan blue visualization**

To check the infusion coordinates, rats infused with a Trypan blue solution (0.05% in physiological solution, Sigma, Italy) were sacrificed through decapitation. The brain was quickly removed and slowly frozen in isopentane at -80°C and conserved at -80°C for 3-4 hours. The brain was then mounted with OCT Embedding matrix (Vetrotecnica, Italy) and placed into a cryostat (Leika, UK) at -18°C for 1 hour. 20µm sections were cut and attached to polarized glass slides (Super Frost Plus, Vetrotecnica, Italy); then quickly immersed in 1g/l Hematoxylin solution (Sigma) to stain the nuclei and immediately visualized under phase contrast microscope. A qualitative evaluation of anatomical damage, using commonly accepted anatomical criteria for the structure of the adult rat hippocampus, was carried out on hematoxylin stained slices.

### **3.2.5 TaqMan analysis**

Animals were deeply anesthetized with ether and decapitated. The brain was quickly removed under RNase-free conditions and the hippocampus from each cerebral hemisphere was collected and placed in a Eppendorf tube containing microbeads (QBiogene, Italy) in 800µl RNA-Later solution (Qiagen, Italy) and incubated at 4°C for 24 hours. The RNA-Later solution was removed and the samples were frozen in cold isopentane and stored at -80°C until processed. The tissue was homogenized with a Ribolyzer (Hybaid, Italy) at speed 6 for 20 seconds followed by 1 minute incubation on ice. This procedure was repeated twice. The samples were then centrifuged at 5000xg for 10 minutes at 4°C. The RNA was extracted using the RNeasy midi kit, following the manufacturer's instructions with an additional DNase I treatment to remove any genomic DNA carryover (all Qiagen, Italy). Purified total RNA was eluted in RNase-free water and stored at -80°C. Quality control evaluation of RNA samples was performed by spectrophotometric analysis (260nm/280nm ratio  $\geq 1.9$ ) (Ultraspec 1000, Pharmacia Biotech) and visual inspection of rRNA integrity (28s and 18s) with the Agilent 2100 Bioanalyzer (Agilent Technologies). Total RNA (500ng) was converted into single stranded cDNA with the Invitrogen Super Script II RNase H Reverse Transcriptase (RT) following the manufacturer's instructions (all Invitrogen Italy). For each sample 2 RT+ and 1 RT- reactions were performed respectively, with or without the enzyme as internal controls. The final product was directly used for TaqMan analysis. The analysis was performed with the Applied Biosystem method (Applied

Biosystem, Italy), using the TaqMan® Universal PCR Master Mix in a 96 well format with the ABI PRISM 7900 sequence detector. Each sample was run in duplicate and the copy number was evaluated using a standard curve of a serially diluted solution of rat genomic DNA (Clontech). GAPDH copy number for each sample was used to normalize P2X2 and P2X7 mRNA levels.

For Ad5 genome quantisation, the DNA was isolated from the injected samples using a Qiagen DNA/RNA midi kit allowing parallel extraction of DNA and total RNA following the manufacturer's instructions (Qiagen, Italy). DNA was eluted in water and stored at -20°C. The concentration was determined by spectrophotometric analysis (Ultraspec 1000, Pharmacia Biotech). Quantification was performed by TaqMan analysis with 250ng DNA in each well, using rat genomic DNA as a negative control and calculating the copy number using several dilutions of the plasmid pAd5-destination vector-hU6-P2X7-4.

### **3.2.6 Histology and immunohistochemistry**

Animals were deeply anesthetized with a mixture of 87mg/kg ketamine and 13mg/kg xylazine prior to intracardial perfusion with 200ml of physiological solution followed by 100ml/100gr of 4% PFA in PBS. Brains were removed and placed in 4% PFA for 1 hour at 4°C, followed by 20% sucrose in 4% PFA for 48 hours at 4°C for cryoprotection. The brain was then slowly frozen in isopentane at -80°C and conserved at -80°C (all reagents from Sigma). For animals injected with GFP expressing virus, sections were collected anteriorly and posteriorly to the injection site to determine the anatomical boundaries of hippocampal GFP expression. 30µm-thick sections, obtained with a cryostat (Leica, UK), were soaked in PBS, positioned on a polarized glass slide, left overnight (ON) to dry at RT and then stored at 4°C. GFP expression was visualized with the Leica DMRA2 fluorescence microscope (Leica, Italy) and slices were then processed for GFP and GFAP or Microtubule Associated Protein 2 (MAP2) staining. The slides were washed in PBS 10 minutes at RT and then washed in 0.3% Triton in PBS for a further 10 minutes. After 2 quick rinses in PBS, each section was incubated with a filtered solution of 10% BSA in PBS for 30 minutes at RT. Each section was subsequently incubated overnight at 4°C with the primary antibody diluted 1:100 in PBS in a humid chamber (primary antibodies used were mouse anti-GFP MAB3580 [Chemicon Inc., UK], rabbit anti-GFAP G3893 [Sigma, Italy], anti-MAP2 AB5543 and

AB5622 [Chemicon Inc., UK] both diluted 1:100). Slides were washed 5 minutes in PBS, incubated for 30 minutes at RT in 0.3% Triton in PBS, then quickly washed 2 times in PBS and incubated with secondary antibody for 3 hours at RT in the dark (FITC anti-mouse diluted 1:50 and Texas Red anti-rabbit diluted 1:100, both from Jackson Lab., USA). Slides were subsequently washed 2 x 10 minutes in PBS and incubated with 1µg/ml DAPI in PBS in the dark with agitation for 15 minutes to stain cell bodies (Sigma, Italy). The slides were quickly washed 3 times in PBS and mounted with a glass coverslip, using an aqueous mounting medium (Gel/mount, Biomed). All the images were visualized with the Leica DMRA2 fluorescence microscope with the FW 4000 software (Leica, Italy) and captured with the Leica DFC300 FX video camera, maintaining the same parameters of acquisition for level of magnification, batch of animals and type and amount of virus injected. These images underwent a qualitative analysis (for GFP detection, emission of green fluorescence and for IHC studies emission of red or green fluorescence).

Variations of this protocol were tested with the P2X7 primary antibody from Alomone (APR-004), using dilutions from 1:50 to 1:200, changing incubation times, solutions and secondary antibody but no staining was observed, opposite to what was reported in the literature (Kukley et al., 2004).

### **3.2.7 Non radioactive in situ hybridization**

#### **3.2.7.1 Probe preparation**

A digoxigenin labelled RNA probe targeting rat P2X7 was produced starting from a pcDNA3 (Invitrogen) plasmid carrying the 3540bp fragment derived from the EMBL submission X95882, having the addition of the EcoR1 linkers to both ends. After linearization of 5µg plasmid with the appropriate restriction enzyme (NcoI for the antisense probe [Promega] and SacII for the sense or control probe [New England BioLabs]) in a 30µl restriction mixture, the volume was increased to 200µl with water and then DNA solution was extracted with an equivalent volume of phenol, followed by 2 extraction with chloroform/phenol (1:1 v/v). Plasmids were ethanol precipitated at -20°C o.n., centrifuged at the maximum speed for 30min at 4°C, dried for 15 min and dissolved in 10 µl of RNase-free water. These templates were used for the synthesis of digoxigenin labelled riboprobes, using the SP6/T7 DIG-RNA labelling kit (Boehringer) according to the manufacturer's instructions. The probes were extracted with ethanol,

dissolved in 50µl sterile RNase free water (DEPC) with 1µl RNase inhibitor and stored at -80°C in aliquots.

### **3.2.7.2 Perfusion and tissue processing**

Adult Wistar-Han (300 grams roughly) rats were deeply anesthetized with a mix of ketamine 87mg/kg and xylazine 13mg/kg and perfused through the ascending aorta first with a physiological solution followed by 4% PFA in phosphate buffer saline (PBS) pH 7.4 (Sigma, Italy). After perfusion, brains were removed from the cranial cavity, postfixed and cryoprotected at least overnight at 4°C in a solution of 4% PFA/20% sucrose in PBS. Brains were stored at 4°C in this solution up to 6 months. Brains were slowly frozen in isopentane at -80°C and serial 40µm thick slices were cut at the cryostat (Leica). Free-floating sections were processed for in situ hybridization starting with a post-fixation for 3hrs in 4% PFA/PBS at RT or were stored up to 12 months in a solution of 4% PFA/PBS at 4°C.

To preserve the integrity of RNA probes and mRNAs in the tissue, all the solutions were prepared with ultrapure water (upH<sub>2</sub>O) treated with 0.1% diethylpyrocarbonate for 6hrs (DEPC- upH<sub>2</sub>O) and then autoclaved for 1hr at 120°C. Glassware and pipette plastic tips and disposable plasticware were sterile or autoclaved for 1hr at 120°C. Powder-free gloves were worn during all steps and were continuously changed.

### **3.2.7.3 Hybridization**

Prior to the hybridization, slices underwent a permeabilization procedure carried out in polystyrene/polyester baskets (Sigma) inserted in 12-wells plastic tissue culture plates (Costar). Free-floating slices were washed twice in 0.1% tween 20 in 1 X PBS (PBST) at RT for 5min and quickly washed in H<sub>2</sub>O, then the slices were permeabilized with 2.3% sodium-meta periodate (Sigma) in H<sub>2</sub>O at RT for 5min and quickly washed in H<sub>2</sub>O. After this step, the sections were incubated in 1% sodium borohydride (Sigma) in 0.1 M Tris-HCl buffer pH 7.5 at RT for 10min, washed twice in PBST for 3min at RT. Then the slices were digested with 8µg/ml proteinase K (Boehringer-Mannheim) in PBST at RT for 10-20min and washed twice in PBST at RT for 5min. After digestion the tissue sections were fixed in 4% PFA/PBS at RT for 5min and washed 3 times in PBST at RT for 10min.



Pre-hybridization was carried out at 55°C for 60-90min in baskets inserted in plastic multiwell plates (12-wells, Costar) in the pre-hybridization solution containing: 20mM Tris-HCl (pH 7.5), 1mM EDTA, 1x Denhardt's solution, 300mM NaCl, 100mM dithiothreitol, 0.5mg/ml Salmon sperm DNA, 0.5mg/ml polyadenylic acid and 50% formamide (all reagents from Sigma, Italy). Slices were then transferred into the hybridization solution additioned with 10% dextransulphate and 50-100ng/ml digoxigenin labeled riboprobes. The riboprobes were added to the hybridization buffer with RNase-free pipette-tips to avoid the risk of RNase degradation of the probes. In situ hybridization was carried out overnight (at least 16hrs) in multiwell plates at 55°C without agitation.

#### **3.2.7.4 Post-hybridization and detection**

After hybridization the sections were washed twice in 2X saline sodium citrate, 0.1% Tween 20 (SSCT)/50% deionized formamide at 55°C for 30min, 20min in 2X SSCT at 55°C and twice in 0.2 SSCT at 60°C for 30min. Slices were then processed for immunodetection with an anti-DIG antibody F(ab)<sub>2</sub> fragment conjugated with alkaline phosphatase (Boehringer, Italy), diluted 1:500 in PBST containing 10% fetal calf serum (FCS) at 4°C overnight. After this incubation the sections were washed four times in PBST at RT for 10min, then incubated in the developing buffer (0.1M Tris-HCl buffer, 0.1M NaCl, 0.05MM MgCl<sub>2</sub>, 1mM levamisol) at RT for 5min and finally incubated in a cromogen solution composed by the developing buffer containing nitro blue-terazolium (NBT) (Boehringer) and 5-bromo-4-chloro-3-indolyl-phosphate (BCIP) (Boehringer, Italy). The reaction was generally carried out ON at 4°C or for 2-6hrs at RT and was stopped by rinsing the sections in stop-solution (10mM Tris-HCl pH 8, 1mM EDTA). Sections were then mounted in water on glass slides coated with 0.5% gelatin (Merck), dried for 30min in oven at 55°C, then immersed 30sec in methanol, 30sec in a mixture of methanol/xylene (1:1) and finally were immersed 3min in xylene and mounted in DPX-mount (BDH).

#### **3.2.8 Oligo radioactive in situ hybridization**

One oligonucleotide targeting rat P2X<sub>7</sub> was selected from 3 different oligo sequences for radioactive in situ hybridization experiment in previous in house studies, since it produced the strongest and most specific signal. These sequences were designed

and checked with bioinformatics software and selected since they presented no or low potential hairpin formation, 3' complementarity or potential self-annealing sites. Since the oligo concentration needed for the experiment is 150ng/μl, they were first diluted in H<sub>2</sub>O in order to generate the 10X stock and then diluted at the desired concentration for the experiment.

For the radioactive labelling of the selected oligonucleotide with <sup>33</sup>P-dATP, the enzyme terminal deoxynucleotidyl transferase (Invitrogen) was used after addition of the oligo (150ng/μl) and of the radioactive nucleotide (Perkin Elmer, USA). The reaction was then incubated 1-2 hours at 37°C. The labelled oligo was purified with the miniQuickSpin column (Roche, Italy) following the manufacturer's instruction. To determine the amount of radioactive ligand incorporated, 1 μl of the purified solution was measured with the γ-counter instrument.

For the hybridization experiment, the hybridization buffer (HB) was prepared in the following way: SSC 4X (Gibco), 50% deionized formamide, 1X denhardt solution, PBS 1X, tRNA 0.25 mg/ml, DTT 0.2M, dextrane sulphate 0.1 g/ml, EDTA 10mM pH 8, sarcosyl 10 mg/ml (all reagents from Sigma), ssDNA 0.5 mg/ml (Roche DNA-Mbgrade) and water.

For each animal 2 slides were used containing 4 brain slices each: the slides were prepared by cutting the frozen brain with a cryostat (Leica) with a slices width of 14μm and then stored at -80°C until usage. For each slide 650 μl of HB containing the radioactive oligonucleotide were used. The final concentration of the radioactive oligo in the hybridization buffer was 5000 CPM/μl. The slides were incubated with the HB and radioactive oligo solution at 42°C ON, in a humid sealed chamber. After incubation and discard of the radioactive solution, the slices were washed 2 x 5 minutes in 2X SSC at RT, 3 x 20 minutes in 0.5X SSC at 55°C and 1 x 5 min 1X SSC at room temperature. Then they were dehydrated in ethanol solutions (EtOH): 2 minutes in EtOH 70%, 2 minutes in EtOH 80% and 2 minutes in EtOH 95%. At the end the slices were air dried and exposed to a Fuji Imaging Plate for 20 days together with a <sup>14</sup>C standard for the quantification. P2X7 mRNA level in the DG injected with the AAV- or Ad5-shRNA vectors, was quantified by image analysis software system AIS 4.

### **3.3 STATISTIC ANALYSIS**

Statistical analysis of the data was carried out using a one-way ANOVA and a Dunnett's post-hoc test. Probability values less than 0.01 were considered significant.

### **3.4 TAQMAN PRIMER AND PROBE AND OLIGO SEQUENCES**

P2X2:

For GGACCTGGGAAGGCAGAGAC,  
Rev GGGCTAAAGCAAGACGCCTG,  
Probe TGTGACTGGGAAACAGAAACCTGTGCA.

P2X4:

For CCAACACCTCTCAGCTTGGATT,  
Rev GGTTCACGGTGACGATCATGT,  
Probe CAGCTCAGGAGGAAAACCTCCCTCTTCATCAT.

P2X7:

For GCCCCTTATCAGCTCTGTGC,  
Rev CCTCCGTGACATTCTCTGTCAC,  
Probe CACCAAGGTCAAAGGCGTTGCAGA.

Ad5 genome:

Forward: TTG CGT CGG TGT TGG AGA,  
Reverse: AGG CCA AGA TCG TGA AGA ACC,  
Probe: CTG CAC CAC ATT TCG GCC CCA C .

Oligo P2X7:

5-CAT GTG CAA GAT CCA CTT GAT GGT GCC GTA ATT CAC GCT CTG GAT  
C-3.

## **4. RESULTS**

## **4.1 SHRNA GENERATION AND VALIDATION *IN VITRO***

To suppress expression of rat P2X<sub>2</sub>, P2X<sub>4</sub> and P2X<sub>7</sub> receptors, four siRNA constructs for each target (named P2Xs-1 to 4) were designed using a commercial web algorithm (Ambion). These siRNAs were then screened for activity by cell transfection and TaqMan analysis. Initially, the rat pheochromocytoma PC12 cell line and a sub-clone, PC12NS1, were selected, since the P2X<sub>2</sub> and P2X<sub>4</sub> receptors were reported to be expressed in both cells by TaqMan analysis, while P2X<sub>7</sub> mRNA was detected only in the PC12NS1 cells. At first the PC12NS1 cells were transfected with the targeting siRNAs, using a positive control (Cy3-labelled siRNA against cyclophilin) and a negative control, i.e. a siRNA sequence designed not to anneal to any mRNA. The transfection was achieved with the Gemini surfactant GSK250910 with a modified version of the reverse transfection protocol (see the Material and Method section). After 24 hours the transfection was repeated and 72 hours later the cells were lysed for TaqMan analysis. siRNA transfection efficiency was determined through evaluation of Cy3-labelled siRNA delivery using a fluorescence microscope. The transfection was repeated three times but in this first attempt no significant knockdown was detected, despite a 90% delivery of siRNAs into the PC12NS1 cells. In order to address this problem, PC12 cells were then transfected using the same conditions and different sets of TaqMan primers to evaluate P2X mRNA levels. These second set of primers were designed to amplify the mRNA region targeted by the siRNA, to facilitate the detection of P2X mRNA suppression. In the PC12 cells a maximum knockdown of P2X<sub>2</sub> mRNA of 50% was detected with the P2X<sub>2</sub>-1 siRNA sequence and a maximum suppression of 50% of P2X<sub>4</sub> mRNA using the P2X<sub>4</sub>-1 sequence (Table 2). These results suggested that primer sequences used for evaluation of the mRNA level were critical and that it is important to use primers annealing near the siRNA targeted region. This may depend upon the fact that siRNA drives the degradation of the target mRNA starting from the annealing region. Flanking regions of the mRNA could still be present in the cell, even if not translatable, and detected by TaqMan analysis. The PC12NS1 cell transfection was then repeated and the target gene mRNA levels analyzed using the new TaqMan primer sets, but no specific gene suppression was detected. These results suggest a problem related to the type of cells used such as the potential presence of a less efficient RNA interference machinery.

siRNA sequences in PC12 cells	% Change from control
P2X2-1	51
P2X2-2	44
P2X2-3	43
P2X4-1	50
P2X4-2	38
P2X4-3	44

Table 2. Level of P2X2 and P2X4 knockdown in PC12 cells compared to control after siRNA transfection (yellow pValue $\leq$  0.01 after ANOVA analysis).

Since P2X7 and P2X4 expression is high in rat astrocytes, the siRNAs were then transfected into these primary cells, using the same delivery agent. As shown in Fig. 12 good siRNA delivery was achieved ( $\approx$ 80% of cells transfected), measured by Cy3-siRNACyclo delivery and good gene suppression (Table 3) one day following transfection.

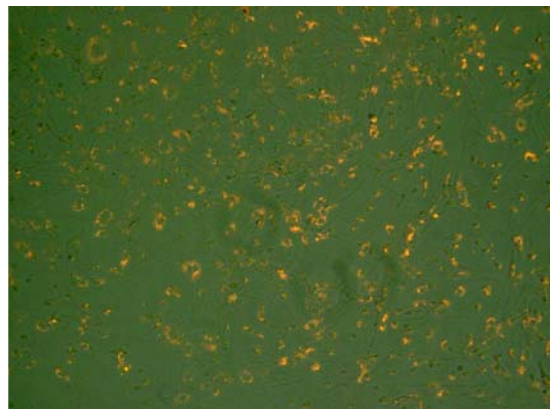


Fig. 12. Cy3-siRNA delivery in astrocytes 3 days after transfection with Gemini GSK250910, 3.5 $\mu$ g/ml (4x magnification).

siRNA sequences in astrocytes	% Change from control
P2X4-1	33
P2X4-2	39
P2X4-3	60
P2X7-1	7
P2X7-2	49
P2X7-3	6

Table 3. % of P2XRs knockdown in astrocytes compared to control after siRNA transfection (yellow pValue $\leq$  0.01 after ANOVA analysis).

This first analysis allowed active siRNA sequences to be identified. In order to achieve prolonged gene suppression *in vivo*, long term siRNA expression in the cell was obtained by using shRNA-expressing viral vectors since the shRNA is cleaved intracellularly to produce the active siRNA. As described in the Material and Method section, the shRNA cassettes were produced starting from the active siRNA sequence by cloning the double strand shRNA construct into the pENTRAU6 plasmid, downstream of the human U6 promoter. Since previous in house studies have not always confirmed a correlation between the activity of siRNAs and shRNAs, the shRNA sequences were tested prior to constructing and producing the final shRNA-viral vector. Hence the pENTRAU6 plasmids, carrying the shRNA cassettes, were transfected into recombinant or co-transfected cells and astrocytes and the P2X mRNA levels determined by TaqMan analysis.

Initially cell lines expressing both recombinant rat P2X4 and P2X7 receptors were transfected with the shRNA plasmids, using Gemini GSK30064 as the delivery agent. In the P2X4 recombinant cells the shRNA plasmid transfection was toxic, provoking a high level of cellular death. Significant gene suppression was observed in the P2X7 cells transfected with the shRNA-pENTR plasmid, albeit there was a certain level of cellular loss (Fig. 13, Table 4). The toxicity may suggest that recombinant cell lines are more sensitive to the transfection agents than normal cell lines.

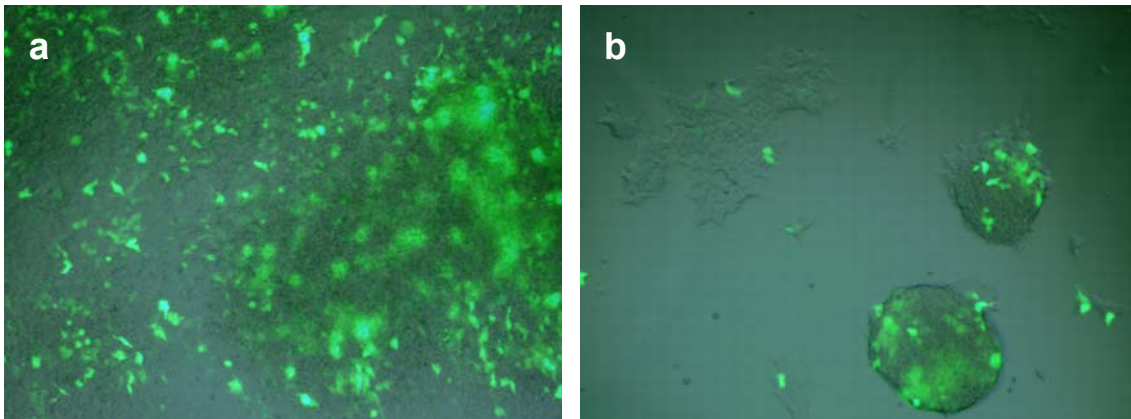


Fig. 13. GFP expression in P2X7 (a) and P2X4 (b) recombinant cells 3 days after transfection with GFP encoding plasmid using GSK30064 8ng/ul (4x magnification).

	<b>HEK-P2X7</b>
<b>Name of shRNA plasmids</b>	<b>% Change from control</b>
P2X7-1	<b>70</b>
P2X7-2	<b>76</b>
P2X7-3	13
P2X7-4	17

Table 4. % of P2X7 knockdown compared to control in HEK-P2X7 recombinant cells (yellow pValue  $\leq$  0.01 after ANOVA analysis).

In order to resolve transfection induced toxicity in P2X4 and P2X7 recombinant cell lines, a co-transfection experiment was performed in a human cell line (HEK293A). The cells were transfected with the three different rat P2X receptor expressing plasmids and the pENTR-U6shRNA vectors at both 1:5 and 1:10 ratios. From previous in house studies the 1:10 ratio of target gene expressing vector/ shRNA vector was shown to be optimal to demonstrate mRNA suppression in a plasmid co-transfection experiment. In each ratio a high and statistically significant suppression of each target gene mRNA was achieved (Table 5).



	<b>HEK-P2XRs ratio 1:5</b>	<b>HEK-P2XRs ratio 1:10</b>
<b>name of shRNA plasmids</b>	<b>% Change from control</b>	<b>% Change from control</b>
P2X2-1	99	100
P2X2-3	81	86
P2X2-4	97	99
P2X4-1	92	94
P2X4-3	91	95
P2X4-4	89	91
P2X7-1	98	62
P2X7-2	100	65
P2X7-3	100	96
P2X7-4	100	99

Table 5. % of P2XRs knockdown compared to control in HEK co-transfected cells (yellow pValue $\leq$  0.01 after ANOVA analysis).

To evaluate siRNA activity in cells endogenously expressing P2X receptors, plasmid transfection of PC12 cells and astrocytes was optimized for the delivery of a GFP expressing reporter plasmid, testing 11 different kinds of in house prepared cationic surfactants as well as the commercial Lipofectamine 2K (LP2K). Each type of cell was transfected with different amounts of the various cationic agents, at different cell densities. Using GFP fluorescence as a marker of transfection, only low levels of transfection efficiency was achieved with all type of surfactants in both PC12 cells and astrocytes. LP2K was the best delivery agent (Fig. 14), but a certain amount of toxicity was detected by cellular morphology visualization.

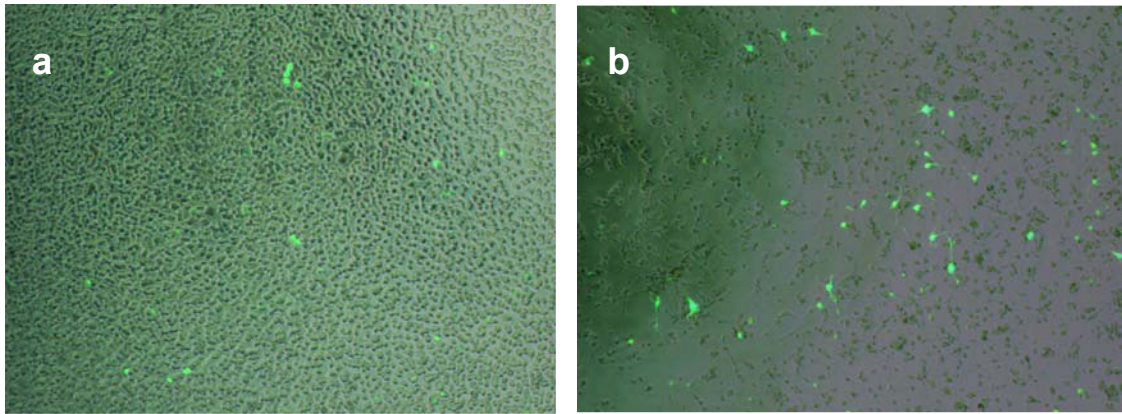


Fig. 14. a: GFP plasmid delivery in PC12 cells with GSK347232A 10ng/ul after 3 days. b: GFP plasmid delivery in astrocytes with LP2K 1.5ng/ul after 3 days (4x magnification).

70% DNA delivery with good cell viability of astrocytes was achieved with an alternative technique, the AMAXA system. Rat astrocytes were transfected with the pENTRAU6-shRNA plasmids. Using TaqMan analysis a significant suppression of P2X4 and P2X7 receptor mRNA was detected in each experiment 3 days after transfection (Table 6). P2X2 mRNA expression was below the level of detection in these primary cells. The experiment was then repeated obtaining slightly different results that could be explained by the variability between different batches of primary cells.

	<b>Astrocytes:experim.1</b>	<b>Astrocytes:experim.2</b>
<b>Name of shRNA plasmids</b>	<b>% Change from control</b>	<b>% Change from control</b>
P2X7-1	70	36
P2X7-2	8	13
P2X7-3	32	40
P2X7-4	62	0
P2X4-1	37	68
P2X4-3	69	75
P2X4-4	49	60

Table 6. P2X7 and P2X4 knockdown compared to control in astrocytes transfected with the pENTR-U6-shRNA plasmids after 3 days (yellow pValue $\leq$  0.01 after ANOVA analysis).

Since the purpose of this study was to achieve the functional suppression of P2X receptors through RNAi, the level of target protein after siRNA delivery needed to be

evaluated. In line with that, a number of commercial antibodies for rat P2X2, P2X4 and P2X7 proteins were tested by Western blot analysis with the specific recombinant or co-transfected cell lysate to select the most appropriate for quantification. The selected antibody was then evaluated on cell lysates from rat hippocampal neurons, rat astrocytes, PC12, PC12NS1, P2X4 and P2X7 recombinant cells or P2X2 plasmid transfected cells using membrane or nuclear fractions (see Fig. 15).

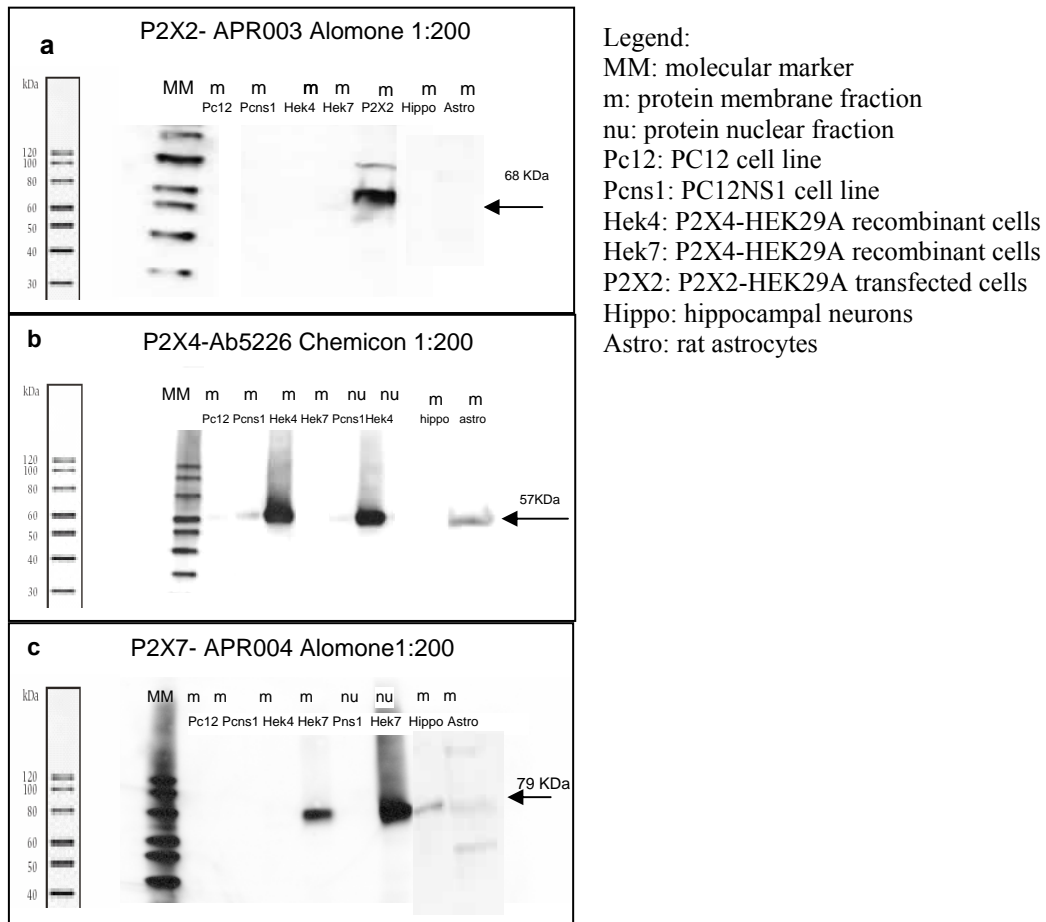


Fig. 15. P2X2 (a), P2X4 (b) and P2X7 (c) protein detection in PC12, PC12NS1, P2X4 and P2X7 recombinant HEK293, P2X2 transfected HEK293, hippocampal neurons and astrocytes membrane or nuclei fraction (the arrow indicates the band and the size corresponding at the P2X protein).

In this assay P2X2 protein was detected only in the HEK293A co-transfected cells while P2X4 protein was detected in recombinant cells, astrocytes and at lower levels in PC12 and PC12NS1 cells. P2X7 protein was detected in recombinant cells and in both hippocampal neurons and astrocytes but multiple bands were detected in the primary cells. The selected antibodies were then used to assay protein knockdown in the

HEK293A co-transfection experiment (Fig. 16). This experiment was repeated twice but the results were variable and not clearly interpretable (data not shown). These results showed that the antibodies selected for Western blot analysis were not adapted to quantify target protein suppression.

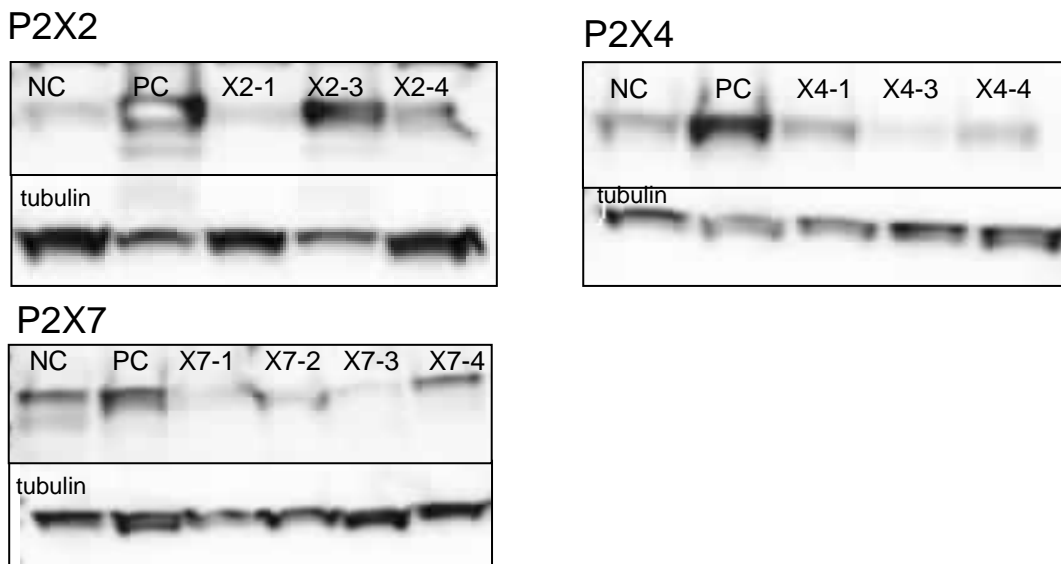


Fig. 16. P2X2, P2X4 and P2X7 protein detection with the relative tubulin expression in P2Xs co-transfected HEK293. The level of tubulin was determined to normalize sample loading [Legend: NC: negative control (shRNA not targeting plasmid), PC: positive control (with only P2Xs plasmid), Xs-1 to 4: pENTR-shRNA plasmids].

From the previous results, the most active shRNA sequences identified for each target gene were as follows: P2X2-1 and P2X2-4 for P2X2, P2X4-1 and P2X4-3 for P2X4 and P2X7-1 and P2X7-4 for P2X7. These shRNA constructs were then tested for their specificity by their ability to suppress expression of the cognate gene but not of the two other P2X genes. HEK293A cells were co-transfected with each P2X expression vector and the selected shRNA vector, using P2X vector/ shRNA vector ratios of 1:1, 1:2 and 1:10, maintaining the total amount of DNA for each ratio constant. For the 1:1 and 1:2 ratios, an shRNA vector against an unrelated rat gene (diamine oxidase, DAO) was also co-transfected as a positive control. From these experiments a non-specific suppression with a few of the shRNA sequences was detected at a 1:10 ratio, where the amount of shRNA plasmid was 10-fold higher than the P2X expressing plasmid. In particular a significant and non-specific suppression of P2X2 mRNA with the P2X7-4 shRNA plasmid and of P2X7 mRNA with the P2X4-3 shRNA plasmid was detected. Regions of homology between the shRNAs and mRNA sequences were investigated, to

test if part of the 19 bases of shRNA sequences can anneal to non-target mRNAs. Up to 9 nucleotides of homology were detected in some of the shRNA sequences for non targeted P2X receptor genes, but no correlation between the amount of homology and the level of non-specific effect was found. Therefore these results can best be explained by non-specific gene suppression caused by increasing amounts of shRNA plasmid compared to gene expressing plasmid. The experiment above gave inconsistent results since the same non-specific mRNA suppression was not detected in all 3 ratios of P2Xs/shRNA plasmid co-transfection. Moreover the co-transfection experiment is an artificial system since the P2X genes are not endogenously expressed in the HEK293A cell line. In order to determine the shRNA specificity for endogenously expressed P2X genes, the shRNA plasmids were transfected into astrocytes, using 2 and 5µg of shRNA plasmids. No significant non-specific effects were measured for P2X4 and P2X7 (Table 7).

<b>Astrocyte pENTR-U6 shRNA transfection</b>			
<b>P2X4-2ug shRNA vectors</b>	<b>% Change from control</b>	<b>P2X4-5ug shRNA vectors</b>	<b>% Change from control</b>
DAO	0	DAO	40
P2X2-1	0	P2X2-1	20
P2X2-4	0	P2X2-4	23
P2X4-1	44	P2X4-1	57
P2X4-3	66	P2X4-3	72
P2X7-1	0	P2X7-1	33
P2X7-4	0	P2X7-4	20
<b>P2X7-2ug shRNA vectors</b>	<b>% Change from control</b>	<b>P2X7-5ug shRNA vectors</b>	<b>% Change from control</b>
DAO	20	DAO	38
P2X2-1	0	P2X2-1	0
P2X2-4	0	P2X2-4	0
P2X4-1	0	P2X4-1	0
P2X4-3	0	P2X4-3	0
P2X7-1	54	P2X7-1	58
P2X7-4	23	P2X7-4	30

Table 7. % of P2X4 and P2X knockdown compared to control in “nucleofected” astrocytes (yellow= pValue≤ 0.01 after ANOVA analysis, red= specific shRNA vectors).

## 4.2 VIRAL VECTOR VALIDATION *IN VITRO*

Since the purpose of this study was to assess the ability of RNA interference to suppress P2X7, P2X2 and P2X4 gene expression *in vivo*, viral vectors containing a U6-shRNA cassette were constructed, starting from U6-shRNA plasmids screened in cultured rat astrocytes and HEK293 cells. Previous in house *in vitro* studies indicated that AAV2/6 and Ad5 viruses preferentially infect neurons and glia, respectively. Hence the AAV2/6 virus was chosen to deliver the P2X2, P2X4 and P2X7 shRNA cassettes to neurons and the Ad5 virus to deliver the P2X7 shRNA cassettes to glia. These AdV and AAV viral vectors were then evaluated for their ability to suppress P2X expression *in vitro* after infection of rat astrocytes and hippocampal neurons, respectively, through TaqMan analysis, Western blot and ion channel activity studies. Different amounts of virus and different post-infection time points were tested.

Two different Ad5-shRNA vectors targeting P2X7 were produced in house. The Ad5 viral vectors, Ad5-P2X7-1 and Ad5-P2X7-4, were validated by infection of rat astrocytes at multiplicity of infection (moi) of 5, 50 and 500, which represents the ratio of virus particles per cell. Since the Ad5 vectors do not express a reporter gene, some astrocytes were infected with a GFP expressing Ad5 vector to measure the level of infection. A high level of GFP expression was observed under fluorescence microscopy in each condition analyzed (see Fig. 17 for an example of infected cells). The P2X7 mRNA levels were assessed 48 hours, 72 hours and 5 days post-infection. P2X4 mRNA levels were also measured at the same time points to evaluate possible non-specific effects of the vectors. As a negative control, an Ad5 vector expressing the shRNA sequence designed not to anneal to any mRNA was used. Ad5-P2X7-4 was the most active and specific vector, achieving a statistically significant maximum suppression of 80% of P2X7 mRNA compared to the negative control at moi 50 after 5 days. P2X4 mRNA level was not modified by the P2X7 viral vectors, indicating the specificity of viral-mediated gene suppression (Table 8). Measuring the level of GAPDH, some toxic effects were seen with the higher moi, as expected, particularly after 5 days. The experiment was repeated with similar results (data not shown).

AdV5	Time point 48hrs		Time point 72hrs		Time point 5ds	
	P2X7%kd	P2X4%kd	P2X7%kd	P2X4%kd	P2X7%kd	P2X4%kd
X7-1 moi 5	15	21	37	0	47	0
X7-4 moi 5	18	3	47	0	33	0
X7-1 moi 50	46	0	56	0	62	0
X7-4 moi 50	54	10	67	0	80	0
X7-1 moi500	59	8	65	0	46	0
X7-4 moi500	63	4	42	0	0	0

Table 8. % of P2X7 mRNA knockdown after Ad5-P2X7-1 and Ad5-P2X7-4 infection, compared to Ad5 negative control (6 replicates in a 96 wells plate for each condition were used) [yellow: significant knockdown after ANOVA analysis ( $p\text{Value} \leq 0.01$ ), red: selected virus].

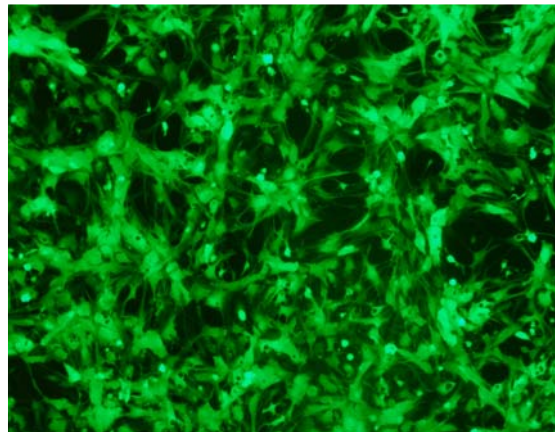


Fig. 17. GFP expression in rat astrocytes after Ad5-GFP infection (50 moi, 72 hrs from infection) (10x magnification).

Western blot analysis was run to determine if P2X7 protein also decreased after Ad5-shRNA infection. Astrocytes were infected with moi 10 and 100 of the same two targeting vectors as above and the negative control vector. Whole cell lysate was collected after 4 days. With 10 moi of the Ad5-P2X7-4 virus, an approximately 60% decrease in P2X7 protein was observed, which was not statistically significant, while the level of P2X4 was unchanged (Fig. 18). The experiment was then repeated but protein reduction was not observed, demonstrating that this antibody in the Western blot and in these experimental conditions is not reliable for protein quantification. As previously shown, staining with the selected antibody for P2X7 in astrocytes revealed several bands, some of which non-specific, and two more intense bands of approximately 70 and 79kDa, probably related to different glycosylated forms of the

protein. A similar staining pattern was reported with a different anti-P2X7 antibody in rat hippocampal membrane fraction (Kim et al., 2001). This antibody was also tested in immunocytochemistry (ICC) staining of rat astrocytes. Despite very strong GFAP staining, a marker of astrocytes, no staining was detected with the anti-P2X7 antibody (Fig. 19). This might have been due by the very low P2X7 expression in individual cells. As previously described, the specificity of the antibody used was questioned due to the observation of a signal in the protein fraction from brains of knock-out animals (Sim et al. 2004).

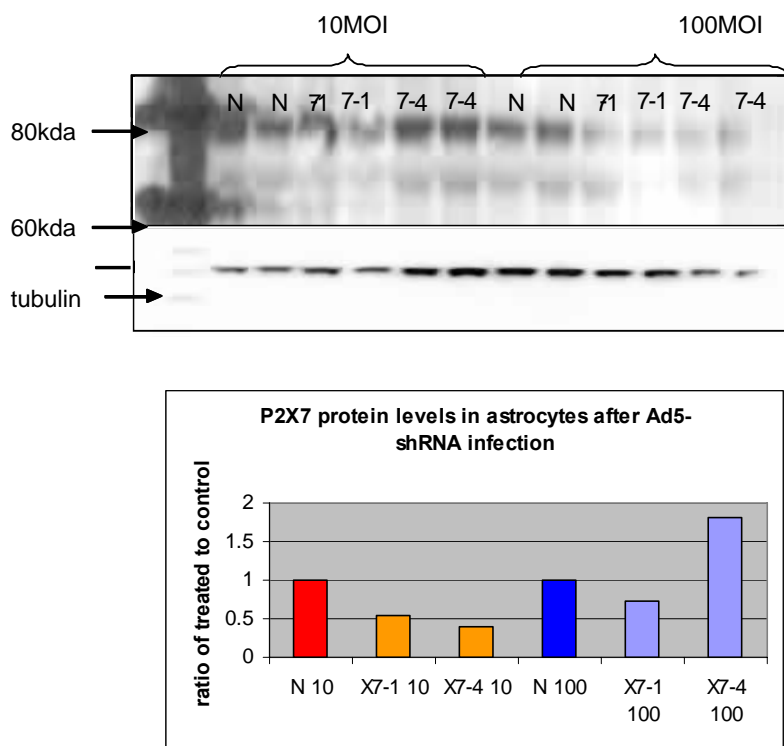


Fig. 18. P2X7 Western blot analysis and P2X7 quantification from AdV infected astrocytes: 2 wells of a 24 wells plate were infected with 10 or 100 moi of the Ad5 vectors. The level of tubulin was determined to normalize sample loading (the two brighter bands are between 60 and 80kDa, the first line represents the molecular marker, N represents the negative control and X7-1 and X7-4 the two targeting vectors).



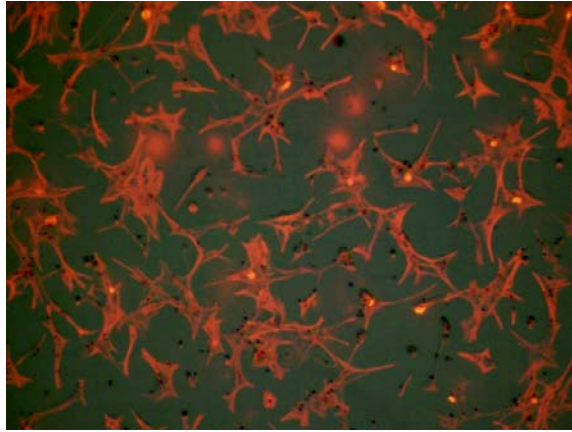


Fig. 19. GFAP staining in rat astrocytes (10x magnification).

To overcome the problem of protein quantification, an assay to measure P2X7 receptor function was set-up. Chakfe and colleagues reported that P2X7 activation in microglial cells provokes IL-1 $\beta$  release after LPS stimulation (Chakfe et al., 2002). Microglial cells were infected with the different vectors and then treated with the selective agonist BzATP (300 $\mu$ M) or ATP. IL-1 $\beta$  levels were quantitated with an ELISA assay. The cells were first infected at moi 100 and 200 of Ad5-P2X7-1 and Ad5-P2X7-4 and 48 hours later were treated with 1 $\mu$ g/ml LPS. 24 hours afterwards, the assay was performed. The results are summarized in Fig. 20.

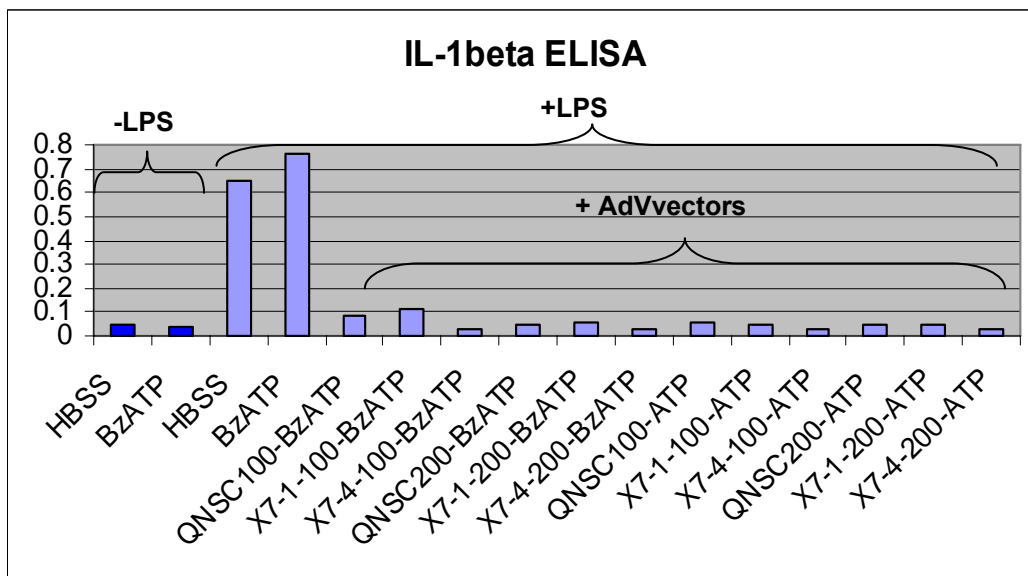


Fig. 20. IL-1 $\beta$  ELISA results (n= 6) (HBSS= saline solution, QNSC= negative control).

A statistically significant decrease in LPS stimulated IL-1 $\beta$  release in the cells infected with Ad5-P2X7-4 compared to the negative control was measured (Table 8). However,

as shown in the graph, an expected toxic effect was observed after viral infection. This preliminary experiment should be repeated with a lower moi of the viral vectors but unfortunately this was not possible due to the unavailability of rat primary microglial cells.

<b>Ad5</b>	<b>% IL1<math>\beta</math> kd</b>
X7-1 100moi	0
X7-4 100moi	49
X7-1 200moi	0
X7-4 200moi	31

Table 9. IL-1 $\beta$  kd (yellow: *p*value  $\leq$  0.01 after ANOVA analysis)

AAV2-based plasmids carrying the shRNA cassettes for the P2X receptors were constructed in house and then packaged into AAV6 capsids by the University of Pennsylvania for generation of high titer of viral vector stocks. The two AAV2/6 vectors targeting P2X2, the three vectors targeting P2X4 and the four vectors targeting P2X7 were screened on cultured rat hippocampal neurons. After 7 days in vitro (DIV) the cells were infected with two different amounts of each virus,  $5 \times 10^3$  viral genome copies per cell (gc/cell) and  $5 \times 10^4$  gc/cell. Five days later the RNA was extracted and P2X gene expression was quantified by TaqMan. Since these vectors expressed GFP, it was possible to quantify the efficiency of viral infection from fluorescence microscopy (Fig. 21).

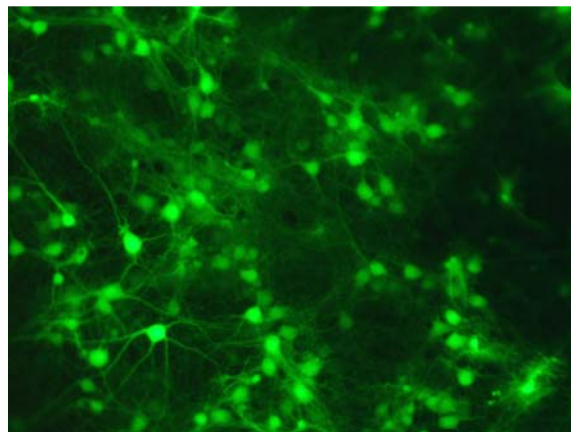


Fig. 21. GFP expression in rat hippocampal neurons after 5 days from infection ( $5 \times 10^4$  gc/cell) (10x magnification).

This first experiment identified the most potent and specific viral vector to suppress target gene expression. The vectors AAV-P2X2-3, AAV-P2X4-3 and AAV-P2X7-3 were selected with a maximum target mRNA knockdown of 90%, 90% and 83%, respectively, which was statistically significant compared to the negative control, without affecting the expression of the other P2X genes (Table 10).

	% P2X2 knockdown		% P2X4 knockdown		% P2X7 knockdown	
	5x10 <sup>4</sup> gc/cell	5x10 <sup>3</sup> gc/cell	5x10 <sup>4</sup> gc/cell	5x10 <sup>3</sup> gc/cell	5x10 <sup>4</sup> gc/cell	5x10 <sup>3</sup> gc/cell
AAV-P2X2-3	89	87	0	0	0	0
AAV-P2X2-4	94	84	18	0	19	40
AAV-P2X4-1	15	27	74	7	0	0
AAV-P2X4-3	0	0	89	18	31	0
AAV-P2X4-4	0	0	58	0	0	0
AAV-P2X7-1	0	25	2	0	51	64
AAV-P2X7-2	28	17	3	0	66	67
AAV-P2X7-3	0	0	12	0	83	59
AAV-P2X7-4	0	0	11	0	22	34

Table 10. AAV vectors screening in rat hippocampal neurons for P2X knockdown: 4 wells of a 24 wells plate were infected for this analysis (yellow: *p*value ≤ 0.01 after ANOVA analysis, red: selected virus).

These vectors were tested again on cultured rat hippocampal neurons at 7 DIV at 5x10<sup>4</sup> gc/cell. Four days and five days after infection RNA was isolated for TaqMan analysis and the total protein content was extracted for Western blot. TaqMan results were consistent with the previous experiment (Table 11).

AAV 5x10 <sup>4</sup> gc/cell-4d	% Change from control		
	P2X2	P2X4	P2X7
P2X2-3	56	6	0
P2X4-3	0	76	0
P2X7-3	0	16	22

Table 11. P2X knockdown data validation with selected AAV virus (yellow: *p*value ≤ 0.01 after ANOVA analysis).

Some variability between the data, in particular for the P2X7 targeting vector, was observed, which might be explained by the different time points tested, by a certain

variability between different hippocampal neuronal cultures and a differential sensitivity to viral vector infection. The results from the Western blot were not unequivocal and reliable (Fig. 22).

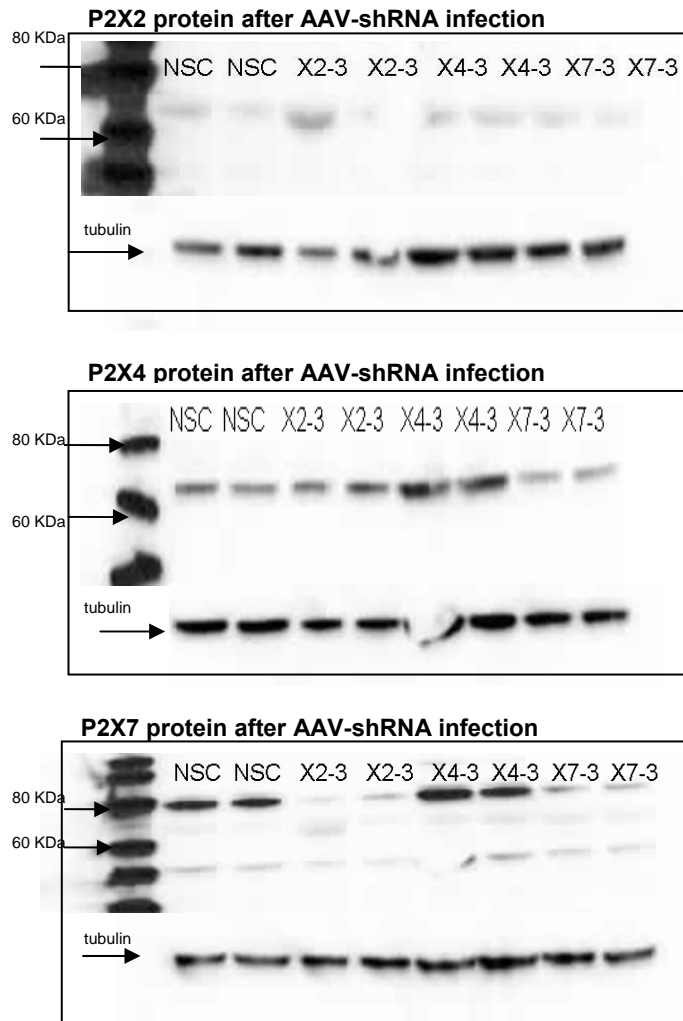


Fig. 22. P2XR Western blot analysis from AAV infected neurons,  $5 \times 10^4$  gc/cell, 5d post-infection: 2 wells of a 24 well plate were used for this analysis. The level of tubulin was determined to normalize sample loading (the first line represents the molecular marker, NSC: negative control virus, Xs-3: shRNAs viral vectors).

In particular multiple bands were detected in the P2X7 Western blot. The 70 and 79KDa bands were reported also by Kim and colleagues but only the 79KDa band was detected in all the samples (Kim et al., 2001). After normalization with tubulin, the P2XRs signals were quantified but no significant protein suppression was measured. Moreover the experiment was repeated with the same samples and a different pattern of staining was detected. This indicates that the antibodies available cannot be used for a reliable quantification of the target protein levels. An ICC experiment was also run with

cultured hippocampal cells, but while good staining was detected with the neuronal-specific  $\beta$ 3-tubulin antibody (Fig. 23), no staining was seen with the P2X antibody. This could reflect the low level of P2X expression in cultured neurons derived from embryos and the low sensitivity of the antibodies used. No functional assays were available in house to measure P2XRs activity in hippocampal neurons infected with the AAV-shRNA vectors.

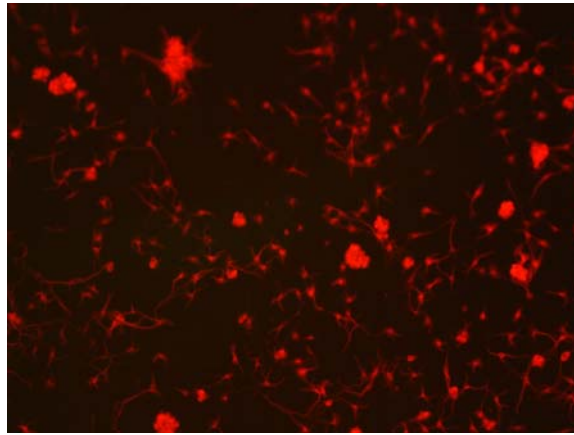


Fig. 23.  $\beta$ 3-tubulin staining of cultured hippocampal neurons (10x magnification).

Specific AAV2/6-shRNA vectors each for P2X2, P2X4 and P2X7 were identified at the end of these *in vitro* experiments together with one active and specific Ad5 vector suppressing P2X7 mRNA expression.

### 4.3 VALIDATION OF VIRAL VECTORS *IN VIVO*

Since the objective of this study was to down-regulate rat P2X receptors *in vivo*, a procedure for shRNA-viral vectors injection into rat brain was optimized. In view of the fact that the strongest patho-physiological evidences of involvement in depression were linked to P2X7, the main focus of the *in vivo* work regarded both AAV- and Ad-shRNA vectors targeting P2X7. The viral vectors were injected into rat hippocampus through a neurosurgical procedure using a stereotaxic device with a microinfusion pump connected to a home-made borosilicate needle. These needles were used because their tips have extremely small external diameter in order to minimize tissue damage. The outer diameter of the tip is roughly 30-50µm while the tip of the more commonly used steel needles measure 200-400µm. This characteristic of the glass needles leads to a negligible amount of mechanical damage at the injection site, with subsequent necrosis and inflammation. This is of particular importance when injecting viral vectors, which can themselves induce an immunological response. Moreover, when investigating gene suppression, it is important to limit external insults that can confound interpretation of the results. In line with that, this system allows the viral vector to be injected into a specific brain area, in this case the dentate gyrus (a subregion of the hippocampus) with high precision and without damaging the brain tissue. The dentate gyrus was selected since it was reported that P2X7 mRNA is expressed throughout the cell body layers of the hippocampus, including the stratum pyramidale in the CA1 and CA3 regions and the granule cell layer (GC). In addition, P2X7 immunoreactivity was observed in the polymorphic layer (PL) of the dentate gyrus (Sperligh et al., 2002). This area is of particular relevance in psychiatric disorders since the hippocampus, which is part of the limbic system, is involved in emotional control, in learning and memory processes and is believed to play a key role in the patho-physiology of both unipolar and bipolar disorders.

Initially a pilot experiment using several animals was performed, in order to optimize the operator experience with the neurosurgical procedure and to determine the exact coordinates for the different injection sites by infusing a physiological solution containing Trypan blue, a colour marker. The coordinates of injection were calculated from bregma according to “A Stereotaxic Atlas of the Rat Brain” [Pellegrino et al., (2nd edition), 1979]. From visualization of Trypan blue in brain slices, it was found that the coordinates of injection chosen were correct and that small differences in animal weight

(200-250 grams) did not alter the position of the injection area in the animal (data not shown).

The AdV vector was initially deeply characterized *in vivo* due to the unavailability of the AAV-shRNA vectors. An injection experiment with Ad5 vectors was performed to evaluate the ability of the viral vector to infect glial cells and to suppress P2X7 mRNA expression *in vivo*. Figure 24 shows the experimental design.

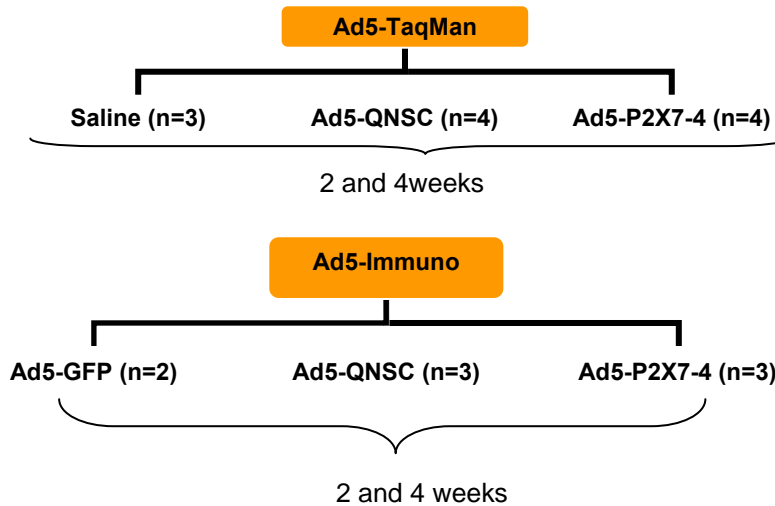


Fig. 24. Ad5 *in vivo* experiment plan.

Each rat received unilateral infusions of vector or saline at a rate of 0.2  $\mu\text{l}/\text{min}$  for a total volume of 4 $\mu\text{l}$  and a total amount of  $1 \times 10^8$  plaque forming units (pfu) for each injection. The amount of virus injected was in line with similar Ad5 experiments *in vivo* in the literature, which reported no immunological response in the rat brain (Xia et al., 2002 and Shine et al., 1997). This experiment was designed to determine if the targeting viral vector, Ad5-P2X7-4, could suppress P2X7 mRNA and protein expression compared to the control vector. Both the dorsal and ventral dentate gyrus were injected to achieve shRNA-virus diffusion in the whole hippocampus. For TaqMan analysis, some of the animals were unilaterally infused with the targeting vector, Ad5-P2X7-4, or the negative control vector, Ad5-QNSC, while other animals were infused only with saline. Two animals per time point were also included as non-operated controls. In addition, quantification of the viral genome in all the injected hippocampi was performed as a positive control for viral vector infusion. Since the Ad5 vectors do not express a marker gene, two animals per group were infused with the Ad5-GFP

expressing vector in order to qualitatively evaluate the anatomical specificity of the infection in these animals through analysis of GFP fluorescence. Two time points were chosen (2 and 4 weeks post-infusion) to investigate target gene suppression and viral vector expression *in vivo*. Following viral vector infusion, the hippocampi were isolated and processed as described in Materials and Methods. Ad5 genome quantitation in the samples infused with the Ad5-P2X7-4 and Ad5-control vector is shown in Fig. 25.

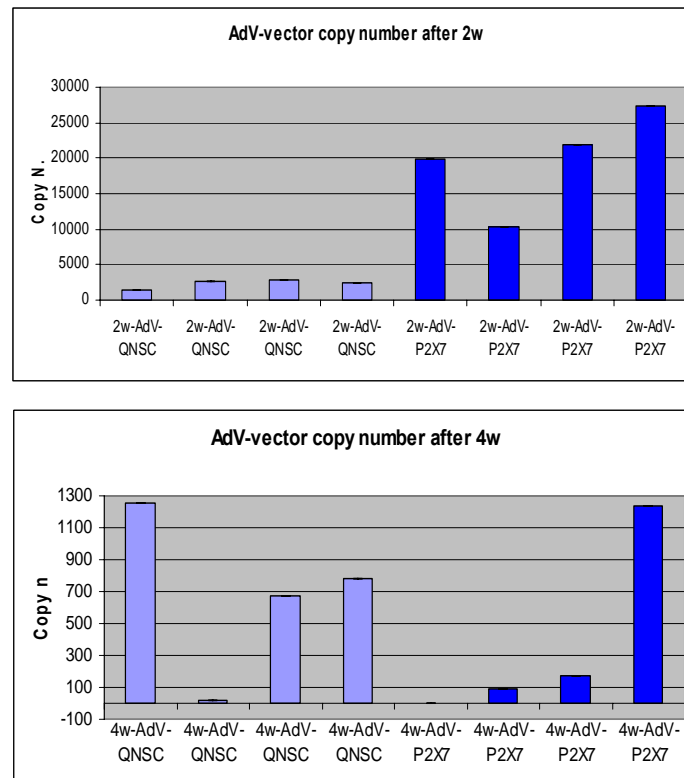


Fig. 25. Ad5 copy number in hippocampi 2 and 4 weeks following infusion *in vivo* with Ad5-P2X7-4 and Ad5-QNSC vectors.

A much higher viral copy number was detected in the hippocampi isolated 2 weeks after viral vector injection, compared to those isolated at 4 weeks. Since these vectors do not replicate and do not integrate into the host genome, the much lower levels of Ad5 genome at 4 weeks might be due to dilution of virus in astrocytes undergoing cell replication. The variability between samples was probably caused by the infusion technique. Since the injection needles can be clogged due to the small diameter of the tip and the high opposing pressure in the tissue, this might have led to different amounts of virus injected in each animal.

Taqman analysis of P2X7 mRNA was performed on all the hippocampi. Expression levels were compared between the injected ipsilateral side and the non-



injected contralateral side from the same animal and between Ad5-P2X7-4 and Ad5-QNSC injected animals to determine if gene expression changed. No significant decrease in P2X7 expression was observed in the hippocampi infused with the Ad5-P2X7-4 compared to the negative control, as initially expected from the *in vitro* results (Fig. 26). An elevated variability in some of the groups was observed, in particular in the Ad5-P2X7-4 injected samples at 2 weeks, probably due to the normal variability between different animals and to the low number of animals analyzed (n=4). Since different amounts of viral vector were detected in each sample, the P2X7 mRNA level was also normalized for the amount of viral genome injected, but no significant decrease was measured after normalization. As a control for specificity, P2X2 mRNA levels were also measured, with no significant difference among the samples (data not shown). No evidence of RNA degradation, which could have affected RNA levels during the analysis *ex-vivo*, was observed from qualitative and quantitative analyses (data not shown).

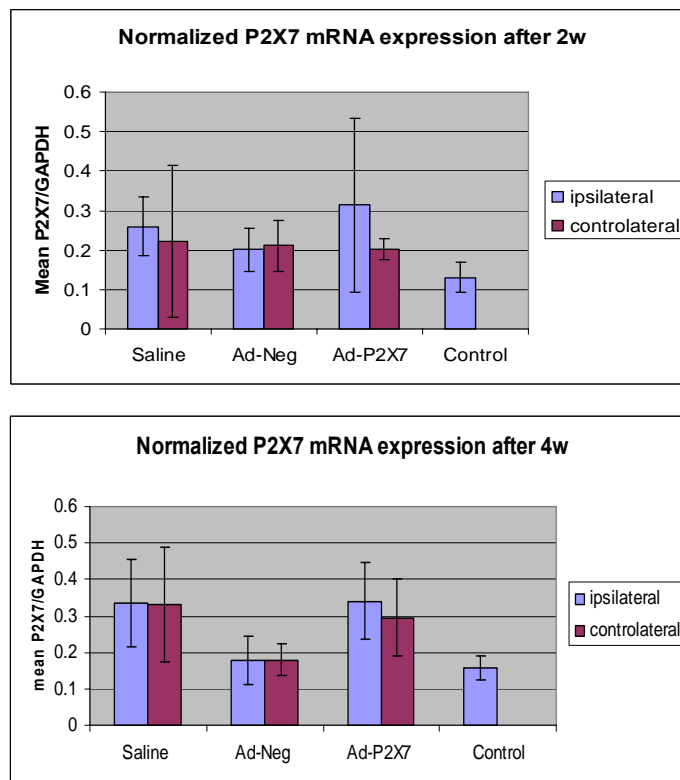


Fig. 26. P2X7 mRNA level 2 and 4 weeks following Ad5 vectors injection in rat hippocampus (GAPDH was used to normalize P2X7 mRNA level).

The brains from animals injected with a GFP-containing viral vector and sacrificed 2 and 4 weeks after injection were processed for direct GFP visualization with fluorescence microscopy and IHC using anti-GFP and anti-GFAP antibodies. GFP fluorescence was localized in both the injection sites (dorsal and ventral DG) with low or no diffusion into the surrounding areas (CA3, CA2, and CA1) and with no fluorescence in the contralateral hippocampus as expected (Fig. 27 and 29). Staining with an anti-GFP antibody confirmed these results (Fig. 28 and 29). The staining was observed for roughly 0.8-1 mm across the injection area in the rostro-caudal axis.

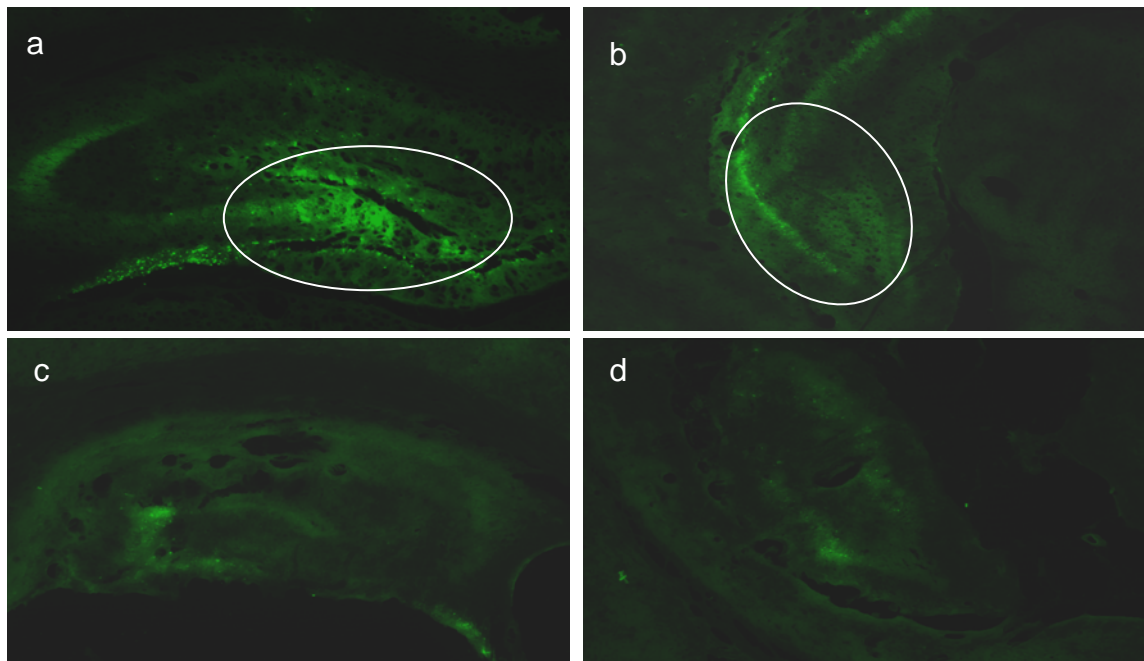


Fig. 27. GFP fluorescence in dorsal DG (a, c) and ventral DG (b, d) 2 and 4 weeks after hippocampal infusion with Ad5-GFP (in the circle is indicated the DG area) (5x magnification).

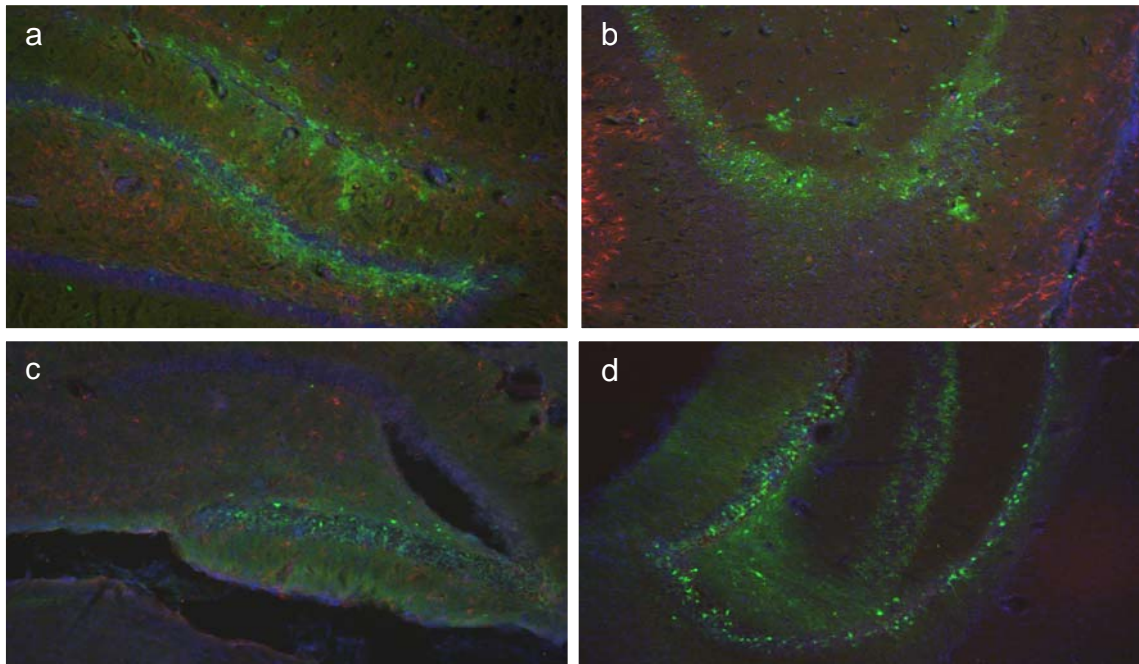


Fig. 28. Dorsal and ventral hippocampus injected with Ad5-GFP after 2 weeks (a, b) and after 4 weeks (c, d) stained for GFAP (red), GFP (green), and DAPI (blue) (10x magnification).

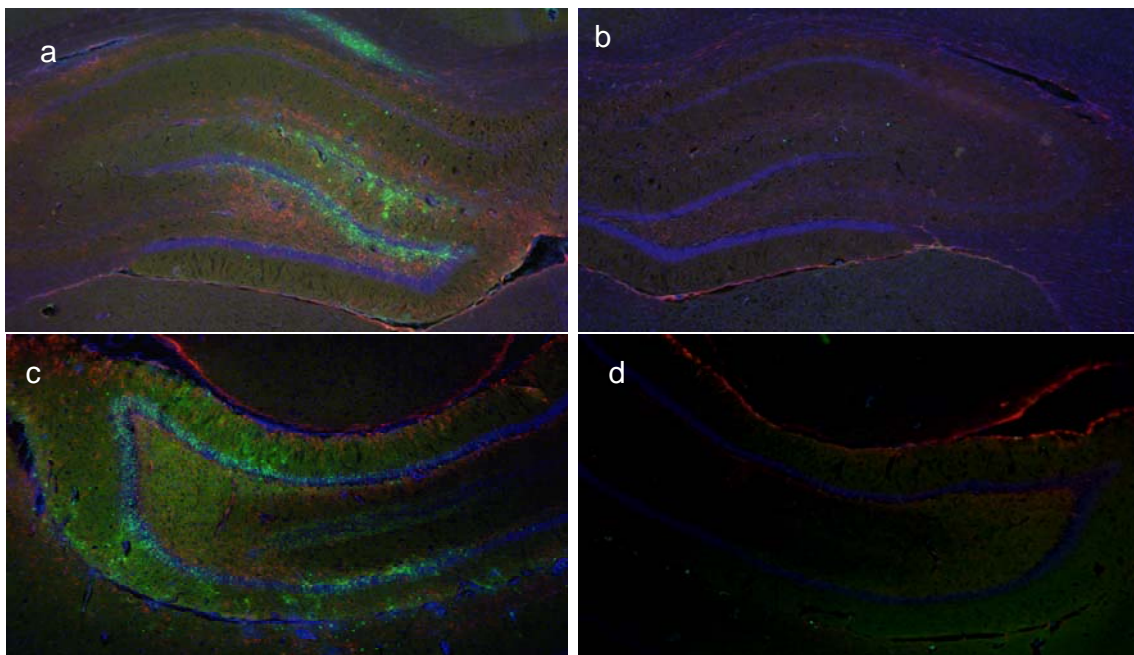


Fig. 29. Dorsal hippocampus ipsilateral (a) and contralateral (b) and ventral hippocampus ipsilateral (c) and contralateral (d) stained for GFP (green), GFAP (red) and DAPI (blue) 2 weeks after Ad5-GFP injection (5x magnification).

Specific to the ipsilateral side, GFP-stained cells showed typical morphology of astrocytes (Fig. 31), while few labelled neurons were seen (Fig. 30). A certain level of

GFAP co-localization with GFP staining was observed (Fig. 31) even if the thickness of the slice (30 $\mu$ m) did not permit resolution of single cells.

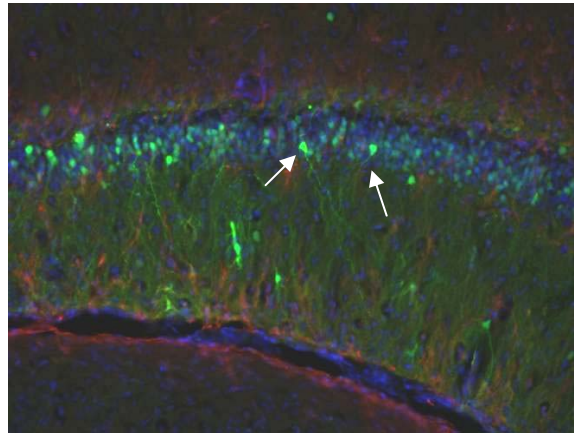


Fig. 30. GFP stained cells looking like neurons in ventral DG pointed by the white arrows (20x magnification).

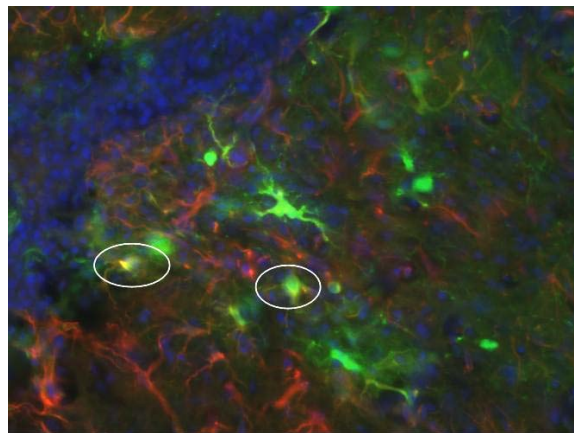


Fig. 31. GFP and GFAP staining in the ventral hippocampus (circled cells indicate GFP and GFAP co-localization) (60x magnification).

From a qualitative observation of the GFAP stained slices, no significant difference in the staining level in the ipsilateral hippocampus compared to the controlateral side was detected, thus excluding astrocytosis provoked by the viral injection (Fig. 32). On the contrary, a lower level of GFP expression was seen in the brains of animals sacrificed 4 weeks after injection compared to the brains of animals sacrificed after 2 weeks (Fig. 27, 28). These results confirm the previous TaqMan quantification of the adenoviral genome at the different time points. Unfortunately it was not possible to stain the slices for P2X7, because the commercial antibody did not

give clear staining even after trying several antibody concentrations and incubation analysis.

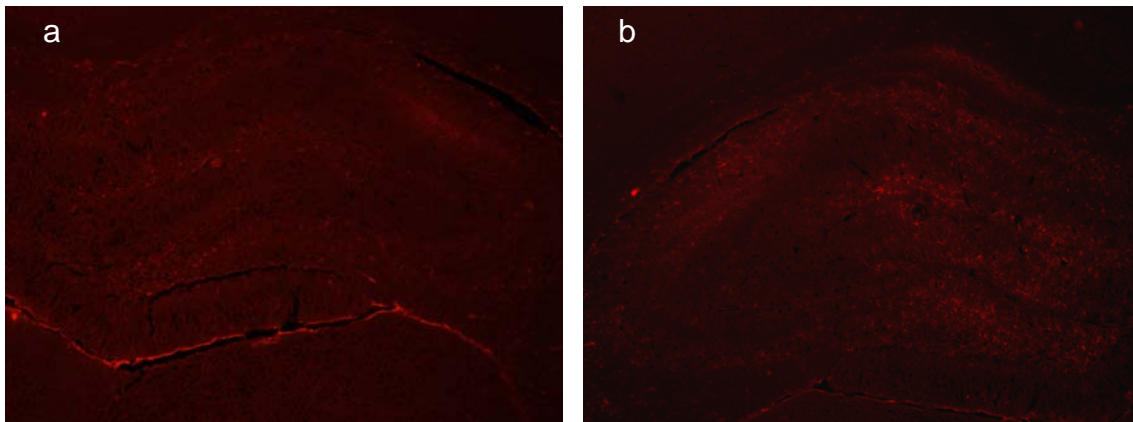


Fig. 32. Contralateral (a) and ipsilateral (b) dorsal hippocampus infused with Ad5-GFP and stained for GFAP (5x magnification).

As previously seen, P2X7 mRNA quantification by TaqMan did not show gene suppression after Ad5-shRNA injection. This result could be explained by the restricted localization of the viral genome in the hippocampus and therefore the impossibility to detect gene suppression when the whole tissue was analyzed. Another pilot study was carried out in order to optimize viral injection by increasing the volume of virus injected and changing the depth of infusion maintaining the same viral titer of the previous study. A total of 6 $\mu$ l of Ad5 vector was injected into the DG at a rate of 0.3 $\mu$ l/min at 2 different depths of injection (3 $\mu$ l at the maximum depth and 3 $\mu$ l at + 0.3mm). This protocol of injection was chosen to maximize the viral diffusion in the injected area. Moreover the Ad5-shRNA vectors were co-injected with the Ad5-GFP virus to qualitatively evaluate the injection. Using this different protocol, a higher level of viral diffusion compared to the previous study was observed in the injected area and GFP expression was confirmed mainly in astrocytes and at lower level in neurons (Fig. 33).



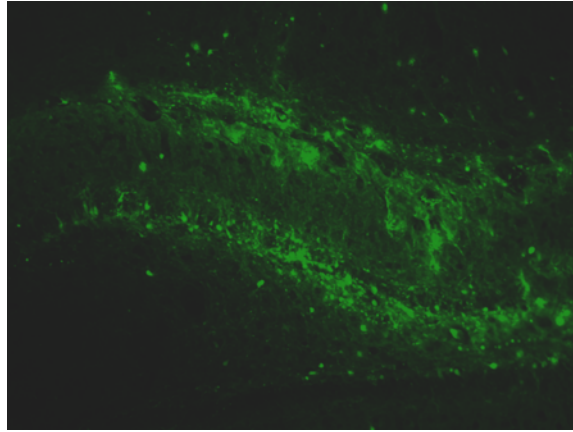


Fig. 33. GFP expression after Ad5-GFP injection in DG at 2 different depths of infusion ( $1 \times 10^8$  pfu) (10x magnification).

The first AAV2/6-P2X7 viral vector injection was also completed. In this experiment  $2.7 \times 10^9$  gc of AAV vectors was injected into the hippocampus with the injection protocol described above for the Ad5 injection. The amount of virus injected was similar or slightly lower to that reported in the literature (see Babcock et al., 2005 and Cao et al., 2004). In any case this was the maximum possible amount of injected virus since the viral titer for both the targeting and negative AAV vectors was quite low. In fact the yields of the AAV2/6 vectors are usually 10 fold lower than the ones of other serotypes. In addition it is not recommended to inject more than  $4 \mu\text{l}$  for each injection point to avoid provoking tissue damage. The AAV injected animals were sacrificed 4 weeks post-injection since the AAV vectors require longer time than Ad5 vectors for maximum transgene expression *in vivo*. The microinfused brains were analyzed for GFP fluorescence and GFP immunoreactivity (GFP-IR), since the AAV vectors co-expressed GFP. GFP-IR was detected in both the granular cell layers and the polymorphic layer of the DG (Fig. 34a). A lower level of GFP expression was also detected in the surrounding areas as in the pyramidal neurons of the CA1, CA2 (Fig. 35a) and CA3 regions and in the mossy fibers (Fig. 35b). No GFP staining was detected in the controlateral non-injected hippocampus (Fig. 36). The group of GFP-expressing neurons were spread over 1–2 mm on a rostro–caudal axis consistent with what reported in the literature (see Babcock et al., 2005). From a co-localization study with the neuronal marker MAP2, GFP was detected in neurons both in the cell body and in the projections (Fig. 34b, 37 and 38). Other slices from the same brains were also stained with the anti-GFAP antibody, a marker of astrocytes, to analyse if there were gross

differences between the injected hemisphere and the non-injected controlateral hemisphere, thus excluding the presence of astrocytosis induced by viral vector injection. No significant differences in GFAP staining were observed after viral injection. These results confirm the previously observed *in vitro* tropism of the AAV2/6 viruses for neurons.

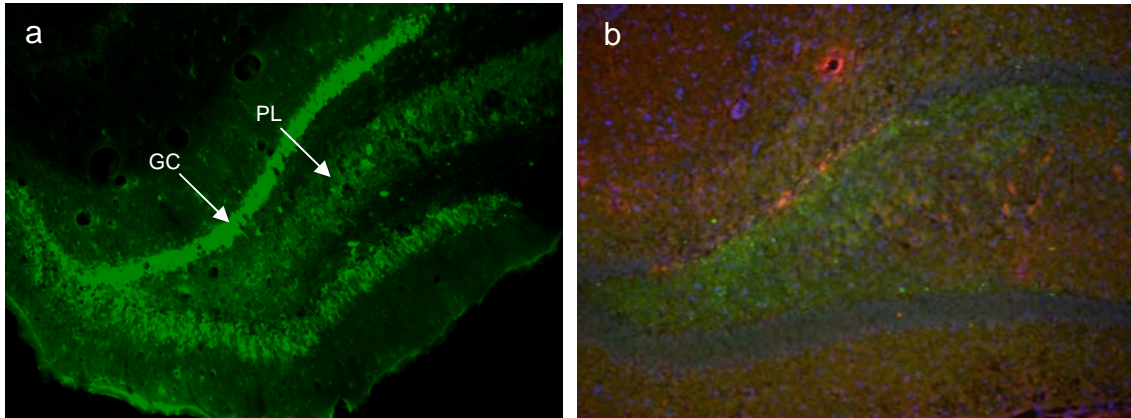


Fig. 34. a: GFP detection in dorsal DG 4w after AAV2/6 injection (10x magnification). b: IHC analysis in dorsal AAV injected DG for GFP (green), MAP2 (red) and DAPI (blue) (10x magnification).

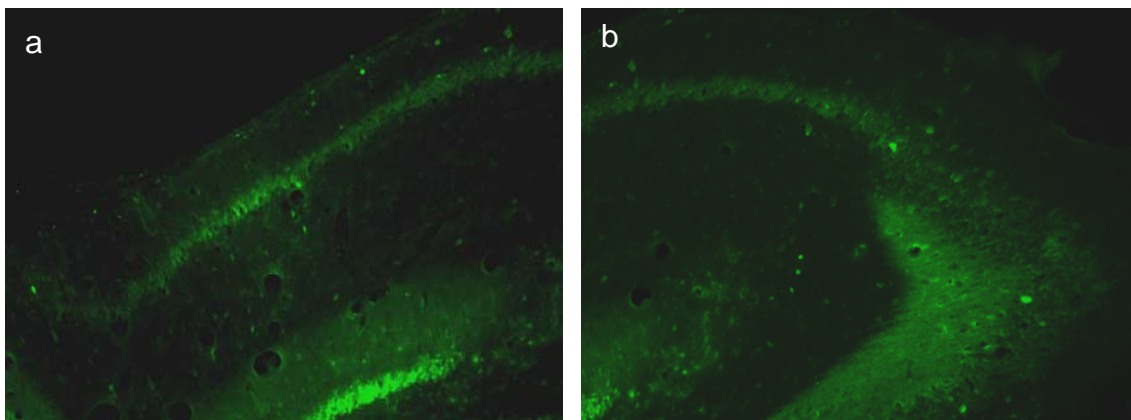


Fig. 35. a: GFP expression in CA1 and CA2 regions after AAV2/6 injection (10x magnification). b: GFP expression in CA3 region after AAV2/6 injection (10x magnification).

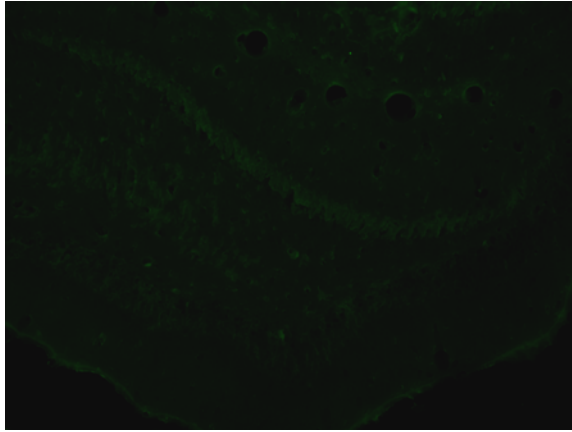


Fig. 36. Controlateral DG after AAV2/6 injection (10x magnification).

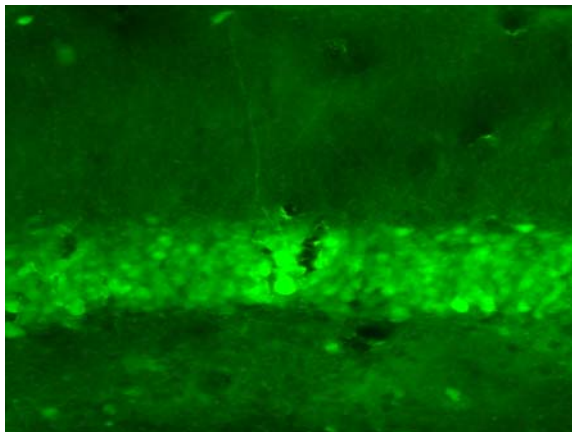


Fig. 37. GFP detection in GC after AAV2/6 injection (20x magnification).

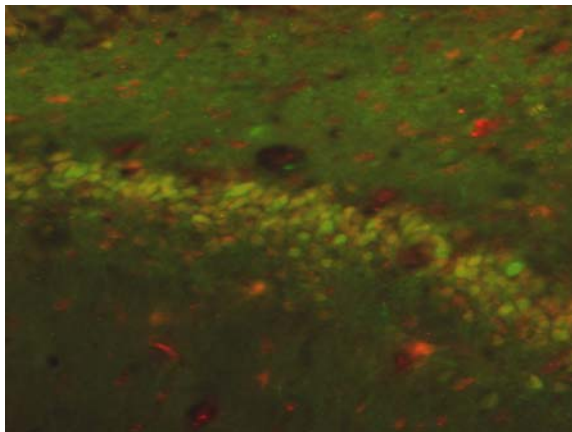


Fig. 38. GFP-MAP2 staining in DG cells injected with AAV after 4 weeks (green: GFP, red: MAP2, yellow: co-localization) (20x magnification).

In order to determine if P2X7 gene expression was reduced around the injection site, in situ hybridization was performed. Both AAV- and Ad5-shRNA injected brains were processed for colorimetric in situ hybridization to quantify P2X7 mRNA directly in the injected area. A non-radioactive colorimetric in situ hybridization protocol was performed with a digoxigenin labelled P2X7 riboprobe. Unfortunately, even if a specific



signal was detected with the antisense probe in the pyramidal and granular cell layer, it was not possible to sufficiently reduce the background signal to accurately quantify mRNA expression, a problem often reported with this technique. Moreover a high level of tissue degradation was observed after the hybridization due to the experimental conditions used (Fig. 39).

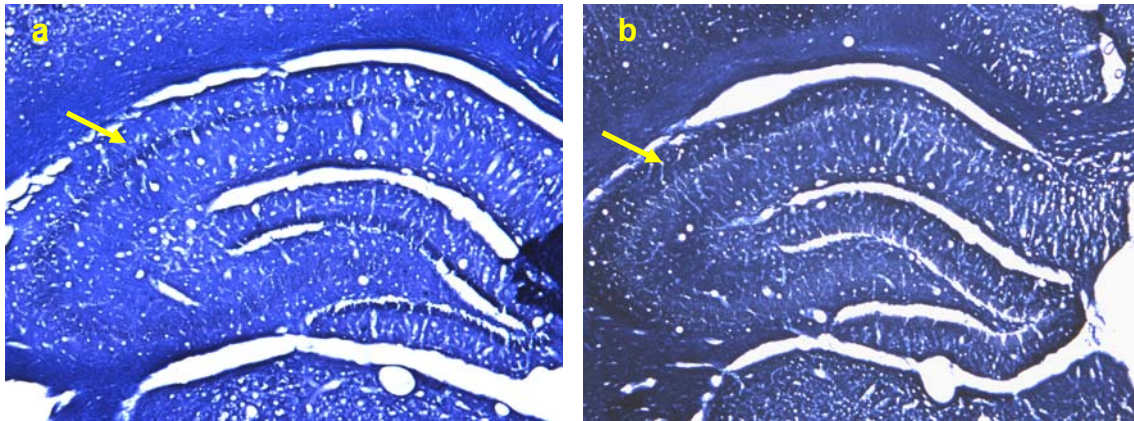


Fig. 39. Dorsal rat hippocampus stained with a digoxigenin-labelled riboprobe for rat P2X7 (left) and with a control sense probe (right): the arrow indicates the presence of the stain or not in the pyramidal cell layer (5x magnification).

Consequently, radioactive in situ hybridization was used. Since this method requires a different sample processing *ex-vivo*, another *in vivo* injection study was performed. Six animals were injected with the AAV2/6- or Ad5-shRNA targeting vector into the dorsal dentate gyrus of one hemisphere and with the negative control virus in the other hemisphere. The Ad5-GFP virus was co-injected with the Ad5-shRNA vectors in order to detect the presence of the adenoviruses in the injected area. After 4 and 2 weeks respectively following injection of the AAV and the Ad5 vectors, the brains were isolated, frozen and cut into 14 $\mu$ m slices. 8 slices from each animal corresponding to the injected area (dorsal DG) were selected for GFP visualization prior to the in situ hybridization analysis. The P2X7 mRNA level in the P2X7 shRNA-injected DG and in the negative control injected DG of each slice was evaluated. 21-22% of mRNA down-regulation with the P2X7-shRNA vector compared to the QNSC-shRNA vector (p-value  $\leq 0.001$ ; ANOVA) was detected in the AAV injected animals. In the Ad5 group, a trend for P2X7 mRNA decrease in the P2X7-shRNA injected DG compared with the QNSC-shRNA injected hemisphere was observed (Fig. 40, 41).

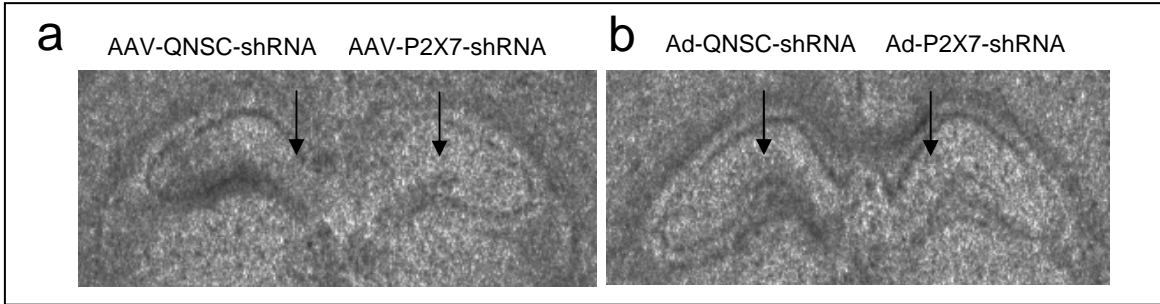


Fig. 40. a: P2X7 mRNA detection in dorsal rat hippocampus 4w after AAV2/6-shRNA injection in the sample 4 (left: AAV-QNSCshRNA and right: AAV-P2X7shRNA). b: P2X7 mRNA detection in dorsal rat hippocampus 2w after Ad5-shRNA injection in the sample 3 (left: Ad5-QNSCshRNA and right: Ad5-P2X7shRNA). The arrows indicate the DG area.

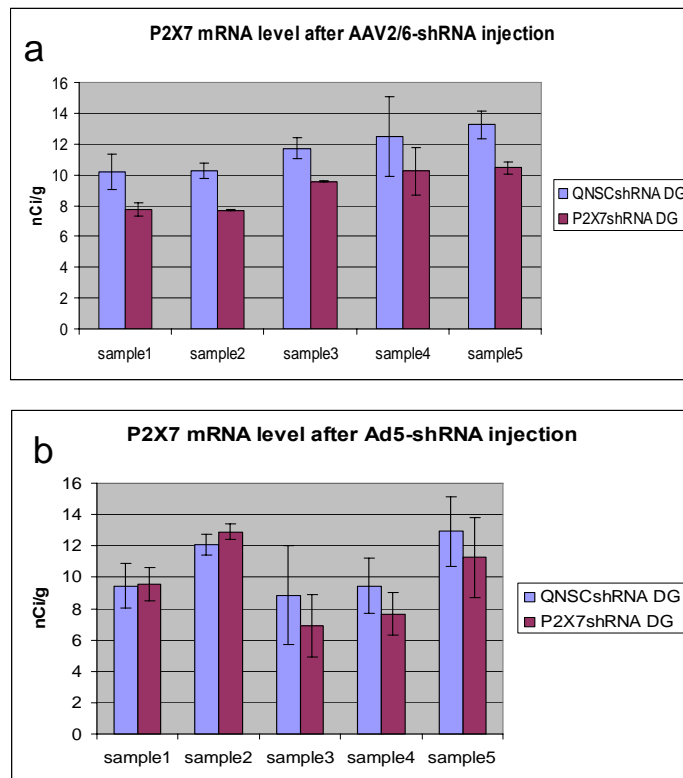


Fig. 41. a: P2X7 mRNA quantification in dorsal rat hippocampus 4w after AAV2/6-shRNA injection (n= 8 slices). b: P2X7 mRNA detection in dorsal rat hippocampus 2w after Ad5-shRNA injection (n= 8 slices). 1 animal per group died prior to the analysis.

In particular in two of the five animals analyzed a P2X7 mRNA decrease was not observed. This was probably caused by a lower amount of virus being injected due to glass needle blocking. In fact in these 2 animals a lower level of GFP expression was observed but it was not possible to accurately quantify it since the brain slices analyzed

were frozen and the tissue morphology was not well preserved. Therefore it was not possible to normalize the P2X7 mRNA level for the amount of virus injected as previously done in the TaqMan analysis. The *in situ* hybridization experiment was repeated with similar results.

In conclusion, *in vivo* studies indicate the ability of the AAV- and Ad-shRNA vectors to suppress the target mRNA expression *in vivo*, in rat hippocampus. Further studies will be necessary to demonstrate the functional suppression of P2X7 receptor after viral vector injection *in vivo* and associated behavioural effects.

## 5. DISCUSSION AND CONCLUSIONS

As discussed in the introduction, P2X receptors are ATP-gated cation channels permeable to sodium, potassium and calcium, which mediate fast excitatory synaptic responses both on autonomic nerve endings and on a limited population of neurons in the CNS. In neurons, both somatodendritically and presynaptically, P2X receptors are involved in the modulation of neurotransmitter release and activation of multiple intracellular signalling pathways. In addition, the P2X7 receptor is expressed on glial cells in many regions of the brain where it plays a role in the release of cytokines. Experimental data suggest an involvement of the P2X7 receptor, and of the P2X2 and P2X4 receptors to a less extent, in psychiatric disorders, including both unipolar and bipolar depression. Expression of P2X7 mRNA is decreased by stress in rodents and this effect is prevented by treatment with the antidepressant paroxetine (Barden et al., 2004). In addition, selectively decreasing P2X7 expression in the hippocampus of mice with an antisense RNA leads to increased immobility in the forced swimming test, a screen used to predict clinical efficacy of antidepressants. Furthermore, a genetic association of the region containing the P2X7 gene with depression was found (Barden et al., 2006). This region additionally contains the P2X2 and P2X4 genes, which may also play a role in the etiology of depression.

To better understand the functional role of P2X2, P2X4 and P2X7 receptors in rat brain and their involvement in the etiology of depression, RNA interference has been used to down-regulate their expression. This approach has important advantages over previous techniques used to manipulate gene expression. Transgenic and knockout mice are limited by developmental effects, genetic compensation, and a lack of regional specificity. These problems can be overcome by conditional transgenic mice to restrict effects in a spatial-temporal manner. However, generating these animals is difficult and time-consuming. Finally, the injection of antisense oligonucleotides into specific brain regions is complicated by their rapid *in vivo* degradation. Even if chemically modified to increase their stability, repeated infusion of oligonucleotides is required to achieve long-term *in vivo* suppression of a target protein. Recently, RNA interference, a sequence-specific suppression of mRNA expression by stretches of homologous double-stranded RNA, has been shown to function across a wide range of organisms, including mammals (Mittal, 2004). Moreover, in addition to its use as a tool for biologists, short

double stranded RNA is thought to play an important role in the regulation of gene expression during development (Bartel, 2004).

RNAi has been widely used to explore the patho-physiology of neuropsychiatric diseases. Several RNAi approaches can be used to reduce gene expression in mammalian brain. As described by Thakker and colleagues, target gene was suppressed by siRNA infusion into the dorsal third ventricle via osmotic minipumps (Thakker et al., 2005). They achieved a widespread suppression of the serotonin transporter gene after a 2-week siRNA infusion. This decrease in mRNA level translated into a widespread reduction specifically in the levels of SERT protein in the brain and in an antidepressant-like behaviour measured in the mouse forced swim test. This behavioural effect was identical to the response obtained from mice that received a selective SERT inhibitor. These results therefore demonstrated the possibility to achieve widespread gene knockdown in the brain with i.c.v. infusions of siRNA to produce a behavioural phenotype. In any event, a large amount of chemically modified siRNA was required. An alternative method of siRNA delivery into the brain is injection of shRNA-viral vectors. Babcock and colleagues (2005) targeted the hippocampal A-Ca<sup>2+</sup>/calmodulin-dependent protein kinase II (A-CaMKII) which has been implicated in spatial learning, neuronal plasticity, epilepsy, and cerebral ischemia. They designed an AAV vector to express a shRNA targeting A-CaMKII driven from the U6 promoter (AAV-shCAM) and the marker protein GFP. The AAV-shCAM vector was microinfused into the rat hippocampus and 4 weeks later A-CaMKII and GFP expression and behaviour were studied. A-CaMKII protein was significantly reduced by shRNA treatment. This suppression of A-CaMKII was associated with changes in exploratory behaviour in the open field task and impaired learning in the Morris water maze (Babcock et al., 2005). These results demonstrate the efficacy of virally-based siRNA constructs targeting neuronal protein expression in the brain.

The final goal of this project was to produce a long term down regulation of P2X receptor expression in rat hippocampus in order to investigate behavioral effects. This required long term expression of the siRNA sequences *in vivo* by using shRNA-expressing vectors. To overcome the problem of poor transfection efficiency of mammalian cells with plasmid-based vectors, viral vectors were generated. Previous in house studies suggested that adeno-associated virus and adenovirus preferentially infect neurons and glial cells *in vitro*, respectively. Since the target cells of this study are hippocampal neuron and glia, AAV and AdV vectors were chosen to deliver the shRNA

cassettes. AdV and AAV possess advantages over other viral vectors such as the ability to infect both dividing and non dividing cells and to persist episomally, increasing the chance for long term expression and avoiding risks related to viral integration into the host cell genome (Walther and Stein, 2000). Moreover these vectors, in particular the AAV, can be safely manipulated and present a low level of toxicity and immunogenicity.

In order to develop the shRNA-expressing viral vectors, several siRNA sequences targeting each gene were designed and validated by means of transfection in the rat pheochromocytoma cell lines PC12 and PC12NS1 and in rat astrocytes using a surfactant as delivery agent. Both PC12 and PC12NS1 cells express the P2XR genes. Astrocytes were chosen since both P2X4 and P2X7 receptors are endogenously expressed in these primary cells. Active and specific siRNA sequences, able to suppress target mRNA expression, were identified. Interestingly siRNA-mediated gene suppression was not measured in the PC12NS1 cells by TaqMan analysis, while the same siRNA sequences were effective in the parental cell line PC12. These results suggest potential differences in the RNAi machinery of the two cell types. The results also demonstrate the need to validate siRNA sequences in several cell types. From the selected siRNA sequences, the U6-shRNA cassettes were produced and cloned into a pENTR plasmid. These plasmids were then screened for their ability to down-regulate the expression level of the target receptor by transfecting astrocytes and recombinant and co-transfected cell lines. Plasmid transfection in astrocytes was not achieved even though several delivery agents and several experimental conditions were tested. This reflects the general low transfection efficiency in primary neuronal cultures using surfactants. Therefore DNA “nucleofection” was used for shRNA-plasmid delivery into astrocytes. Up to 100% mRNA suppression was achieved in co-transfected cell lines while a maximum of 70% of mRNA suppression was obtained in recombinant cell lines and astrocytes. The lower level of P2XR suppression in astrocytes can be explained by the higher resistance of these primary cells to exogenous DNA transfection while recombinant cell lines were more sensitive than normal cell lines to the transfection agents. The specificity of the shRNA-vectors was also tested. In fact a problem often encountered with siRNA-mediated gene suppression is down-regulation of non-related genes. Commercial antibodies were tested and selected for evaluation of protein levels after shRNA-plasmid delivery. Even if several experimental conditions were tested, they were not found to be reliable for a quantitative analysis where the quality of the signal is critical to obtain statistically significant results. This suggests that, depending

on the antibodies available, Western blots is not the optimal method for quantification of protein suppression and that a functional assay, if available, could be more reliable to evaluate target protein knockdown.

Finally, the shRNA cassettes were cloned into viral vectors. Several AAV2-based shRNA vectors were produced for the three different P2X receptors. AAV2-vectors were selected since different experimental reports demonstrated that they can deliver the shRNA cassette to neurons both *in vitro* and *in vivo* and can produce a long-lasting, highly efficient and specific down-regulation of gene expression (Michael et al., 2005). The serotype AAV6 was chosen for vector packaging because it infected neurons *in vitro* at the highest levels among the serotypes available in house. Since P2X7 is also expressed in glial cells, two Ad5-shRNA vectors targeting P2X7 were produced. GFP was co-expressed in the AAV-shRNA vectors to measure the level of infection. An Ad5 vector expressing GFP was also produced since the Ad5-shRNA vectors do not express a marker gene. These viral vectors were initially screened for their ability to infect hippocampal neurons (AAV2/6) and astrocytes (Ad5) and to suppress target gene expression *in vitro*.

An Ad5 vector suppressing P2X7 mRNA expression without affecting P2X4 mRNA levels in cultured rat astrocytes was identified. A maximum of 80% mRNA suppression compared to control was observed. Moreover a high level of astrocyte infection, estimated at around 80%, was measured after AdV-GFP infection without evident signs of toxicity. Analogous suppression of P2X7 protein was not confirmed, because the commercially available antibody was not accurate enough to quantify the specific protein band in a Western blot analysis, even though several experimental conditions were attempted in order to optimize protein detection. Preliminary data demonstrated a decrease in P2X7 function in Ad5-P2X7-4 infected microglial cells compared to control, measured as agonist-induced IL-1 $\beta$  release after LPS treatment. There was a statistically significant functional suppression but a certain level of toxicity in the cells was detected after Ad5 infection.

AAV2/6 vectors suppressing P2X2, P2X4 and P2X7 mRNA expression in cultured rat hippocampal neurons were generated. A high level of target gene suppression (a maximum of 90% suppression compared to the control) was measured by TaqMan analysis without non-specific effects. 80-90% hippocampal neuronal infection was observed using GFP fluorescence, with a certain level of toxicity only after a prolonged viral exposure. No reliable data for protein suppression were obtained

from Western blot analyses and no functional data could be generated due to lack of assays in house.

One active and specific AAV-shRNA viral vector for each receptor and one active and specific AdV-shRNA vector targeting P2X7 were selected from these *in vitro* experiments for *in vivo* investigation. Since a series of preclinical and genetic data suggested a role of P2X7 in the etiology of depression, *in vivo* work was focused on this gene. A viral vector injection procedure in rat brain was optimized in order to achieve the maximum cell infection with AdV and AAV vectors, without causing anatomical damage. For this procedure, home made glass needles were used since in house studies demonstrated their ability to induce a negligible amount of anatomical disorganization and inflammation compared to commercially available steel needles.

The presence of the Ad5 and AAV viral vectors in the injected brain area were demonstrated. The viruses were injected into the dentate gyrus of rat hippocampus since both P2X7 mRNA and protein are reported to be expressed in this region and because hippocampus is believed to play a key role in the patho-physiology of psychiatric disorders. AAV2/6 vectors were detected by GFP expression through direct fluorescence visualization and IHC analysis. After AAV injection into the dorsal DG, GFP was detected both in the granular cell layer and in the polymorphic layer. Moreover GFP expression was detected in the surrounding area such as the pyramidal cell layer in CA1, CA2 and CA3 regions and the mossy fibers, demonstrating the ability of AAV2/6 to infect both granular and pyramidal neurons *in vivo* and of GFP protein to travel anterogradely within neurons, as previously described by Mandel and Muzyczka for the AAV2/1 and AAV2/5 vectors (Mandel and Muzyczka, 2004). In contrast, no staining in the controlateral non-injected hippocampus was observed, indicating that this serotype does not undergo transport to distal sites or retrograde transport as seen for other serotypes such as the AAV2/5 and AAV2/9 (Mandel and Muzyczka, 2004 and Cearley and Wolfe, 2006). From a co-localization study with the neuronal marker MAP2, GFP was detected in neurons both in cell bodies and in projections. Widespread (~1-2 mm) rostro-caudal expression of GFP in the hippocampus 28 days following AAV microinfusion was observed, consistent with literature reports (see Babcock et al., 2005). Despite this encouraging evidence, subsequent in house experiments (unpublished) demonstrated that the AAV6 was not the best serotype to achieve the highest neuronal infection *in vivo*. In these studies other serotypes, in particular AAV8 and AAV9 produced wider infection of rat hippocampus after intracranial injection



compared to the AAV6 (data not shown). Recently Klein and colleagues (2007) reported that the AAV8 and AAV9 vectors produced a higher level of transduced cells compared to other AAV serotypes after microinjection in rat hippocampus. In addition the authors showed that the method of viral vector purification can influence the transduction pattern as well as the results when comparing serotype strengths. Similar studies reported high transduction efficiency with the AAV8, AAV9 and AAV10 vectors in rat brain (Cearley and Wolfe, 2006).

The expression of GFP in the dorsal and ventral hippocampus 2 and 4 weeks after Ad5-GFP viral vector injection was also shown. IHC verified that GFP expression was concentrated in the injection site, within the dentate gyrus, with undetectable diffusion into the surrounding area. The staining was observed for roughly 0.8-1 mm around the injection area in the rostral-caudal axis. The majority of the cells stained were astrocytes, with a minority showing neuronal morphology, confirming previous *in vitro* results. From a qualitative analysis, neither astrogliosis nor mechanical damage was observed in the injected area, thus excluding the presence of inflammation induced by the virus or by the injection method. The intensity of GFP fluorescence, GFP IHC and TaqMan quantification of the Ad5 viral genome demonstrated decreasing levels of viral vector in glia over time. Since the viral vector does not integrate into the nuclear DNA, these results suggest that the viral genome was diluted, possibly through replication of glial cells. In fact it is now well established that astrocytes undergo cell division even under basal conditions and that the hippocampus of normal adult mammalian brain is a region of proliferation of neural progenitor cells (see for example Chirumamilla et al., 2002). A difference in the amount of virus measured in each animal was detected by TaqMan quantification of the Ad5 viral genome, probably due to the infusion technique and potential obstruction of the injection needles due to the small diameter of their tip and opposite pressure in the tissue.

TaqMan analysis was initially chosen to measure target mRNA after viral vector injection. Following Ad5-shRNA viral vector injection in both dorsal and ventral DG, no significant variations in P2X7 mRNA expression were detected in the whole hippocampus, even after normalization for the amount of viral genome detected in each sample. Possibly the amount of virus injected into the whole hippocampus was not sufficient to suppress P2X7 expression, since viral numbers appeared to be diluted. Most likely TaqMan analysis of the whole hippocampus was not sensitive enough to detect a decrease in mRNA expression occurring in a limited part of it. In fact the

shRNA-viral vector was injected only in a restricted region of the hippocampus (dorsal and ventral DG) while the whole hippocampus was processed for TaqMan analysis with a probable dilution effect. Indeed from GFP fluorescence and GFP IHC the virus was detected only in a small region of the whole tissue analyzed. To overcome this problem, a possibility is to specifically isolate the anatomical region corresponding to the injected area, for example through isolation of the apical and caudal regions of the hippocampus. Other methods (not available in house) that can be used for dissection of the injected area are tissue micro-punch dissection and laser-capture microdissection (LCM). This last technique was used by Hommel and colleagues to remove the AAV-shRNA infected cells in the ventral tegmental area which were identified for removal by detection of GFP expression and were subsequently analyzed for target gene suppression. Real-time RT-PCR analysis revealed a significant decrease of the target mRNA in the neurons infected with the targeting AAV-shRNA vector compared with neurons infected with the control shRNA vector isolated by LCM (Hommel et al., 2003). The number of animals used in this *in vivo* experiment (4 per group) was not ideal for a quantitative study, because 6 to 8 replicates are normally needed for TaqMan analysis. Since P2X7 receptor expression is activated in glia after inflammatory events, the viral vector injection could have induced an inflammatory response in the injected area and therefore a P2X7 mRNA increase, thus preventing the possibility to measure target gene suppression. This hypothesis was not confirmed since GFAP staining observed in the injected and not-injected hemisphere was qualitatively similar, excluding the presence of inflammatory astrogliosis in the injected area. Regarding the time points analyzed, 2 weeks or less, rather than 4 weeks after Ad-shRNA injection was found to be a better time point for gene suppression detection. In fact, Xia and colleagues (2002) reported target gene suppression already 4 days after Ad-shRNA injection in rat brain, and Chen and colleagues (2006) measured a time-related decrease in gene suppression, in particular 20 days post-injection compared to 10 days.

After this first experiment, another *in vivo* study with both Adv and AAV injection was performed. A different injection protocol was optimized in order to achieve a higher infusion of the virus into rat hippocampus through injection of the virus at 2 different depths of infusion. Moreover for this study *in situ* hybridization was used to evaluate mRNA suppression. With this technique it is possible to detect the mRNA levels directly within the anatomical region of interest, easily permitting detection of mRNA suppression after shRNA-vector delivery. Initially a colorimetric in

situ hybridization analysis with a digoxigenin labelled P2X7 riboprobe was tried. This method was chosen over the radioactive method since it permits avoiding the special precautions needed for the use, handling and safe disposal of radionucleotides even though it could present several disadvantages over radioactive labeling such as the lower level of sensitivity, the impossibility to perform a quantitative analysis and the frequent non-specific staining (see Wilkinson et al. 1999). Even though experimental conditions such as hybridization, post-hybridization temperature and time, were altered, it was not possible to reduce the background level. In addition, a high damage level of the tissue was observed after analysis, due to the experimental conditions used. Subsequently, a radioactive in situ hybridization analysis with a P2X7 oligonucleotide was performed since it is possible to measure even very low levels of gene suppression and to carry out a quantitative analysis. 20-22% of P2X7 mRNA down-regulation in the AAV-shRNA-P2X7 injected dentate gyrus compared to the control QNSC-shRNA injected DG was measured. The P2X7 mRNA suppression resulted statistically significant ( $p$ -value  $\leq 0.001$ ). This decrease in mRNA level is much lower compared to that measured after cell infection *in vitro*. RNAi-mediated gene silencing *in vivo* is expected to be less than that which can be obtained *in vitro* due to the higher difficulty of siRNA delivery *in vivo*. This is particularly true when the target tissue is brain. First of all this tissue is limited by the BBB that restricts the passive entry of materials from the peripheral circulation. If directly injected into the brain, the shRNA-viral vectors can be diluted in non-targeted regions or inactivated by endonucleases. Moreover, when using needles with limited outer diameter for the microinjection, the viral diffusion into the target area is hindered by high opposing pressure of the tissue and the possibility of clogging the needle. This limited mRNA suppression could also be dependent upon the AAV serotype used as shown following viral vector delivery of GFP. In any case as reported in the literature, a limited decrease in the mRNA level could still be associated with a functional suppression and a behavioral effect (Thakker et al., 2005 and Hommel et al., 2003). For example Hommel and colleagues measured  $\approx 23\%$  of target gene mRNA suppression by RT-PCR after AAV-shRNA injection into the ventral tegmental area. This localized gene knockdown was associated with a statistically significant behavioral change. This seems to suggest that the reduction in the P2X7 mRNA in the DG injected with the targeting AAV shRNA vector is associated with a reduction in the P2X7 receptor function.

In the Ad5 group, a trend for P2X7 mRNA down-regulation in the P2X7-shRNA injected DG was observed, but it was not statistically significant. The number of animals used in this study was not optimal for a statistical analysis. In particular in 2 out of the 5 animals analyzed a decrease in mRNA level was not observed. This could be dependent on a lower amount of viral vector injected due to the obstruction of the glass needle. In fact with in situ hybridization it was not possible to accurately quantify the amount of virus injected, as previously done with TaqMan. The amount of virus injected was qualitatively determined by GFP expression since the AAV-shRNA vectors expressed the GFP protein and the AdV-shRNA vector was co-injected with the AdV-GFP vector. From a qualitative analysis a difference in the GFP staining in these 2 animals was observed but it was not possible to determine it accurately and to normalize the P2X7 mRNA level for the amount of viral genome injected. Since the brain slices were frozen for the radioactive in situ hybridization, the morphology of the slices analyzed was not well defined. Therefore it was not possible to quantify GFP expression.

The present study demonstrates that microinfusion of AAV-shRNA-P2X7 in the dentate gyrus resulted in a small but statistically significant suppression of rat hippocampal P2X7 mRNA expression, while a similar trend even if not statistically significant was obtained with the AdV-shRNA injection. The AAV serotype used in this study may not be the best one to achieve neuron infection *in vivo*, even though an elevated infection of hippocampal neurons was obtained *in vitro*. Moreover it was demonstrated that the glass needle injection method was able to infuse viral vectors into restricted brain areas without inducing anatomical damage and inflammation. A certain level of variation in the amount of virus injected was observed in some animals due to the extremely small external diameter of the needle tip and the possibility to clog it. In any case this problem could be overcome through quantification of the virus injected in each sample and normalization of the target mRNA or protein level for the amount of virus detected. Future studies are needed to evaluate functional P2X7 suppression *ex vivo* with the P2X7-shRNA vectors, such as measuring channel activity after shRNA-vector injection. In addition, a phenotypic effect in a behavioral test such as the forced swimming test could be evaluated.

In conclusion, in this project viral vector-mediated RNA interference was explored for the suppression of target genes both in cultured cells and in the rat brain. Active and specific AAV- and AdV-shRNA vectors able to suppress target gene

expression in neuronal cells were generated and validated both *in vitro* and *in vivo*. Unfortunately it was not possible to measure the level of the target protein after shRNA vector delivery either *in vitro* or *in vivo* since the commercially available antibodies did not result in a clear stain in the Western blot analysis. Phenotypical assays measuring a decrease in the activity of the target gene after shRNA-vector delivery are ideal for siRNA validation, but are not always available depending on the target gene function. In this study a functional assay for the P2X7 receptor in microglial cells was set up that allowed detecting a significant P2X7 functional decrease in the cells infected with the targeting Ad5-shRNA vector compared to the control vector. On the other hand, no functional assays were available in house to measure P2X receptors function in neurons. Compared to other approaches available, such as siRNA infusion into the brain via osmotic minipumps, this method requires more time for the development, production and validation of the shRNA-viral vectors *in vitro* prior to *in vivo* delivery. Nonetheless, with this method it is possible to achieve a long term suppression of gene expression in neuronal cells since the viral vector, in particular the AAV vector, is expressed after an extended period. In fact the transduction volume after intracranial injection with the AAV vectors was shown to be constant two weeks post-injection compared with two months post-injection for several serotypes, indicating that transgene expression remained invariable over a long period of time (Taymans et al., 2006). Moreover with this method it is possible to obtain a localized viral vector infection and siRNA expression allowing the investigation of the effects of target gene suppression in the specific area of interest. Some technical conclusions can be drawn by this study. The detection method chosen for gene knockdown evaluation must be selected appropriately, since it could be difficult to detect gene suppression occurring in the limited area of viral vector injection. Moreover the protocol of injection and the amount and serotype of virus used for the delivery of the shRNA cassette play a key role in the success of the overall experiment.

## 6. REFERENCES

- Akaneya, Y., Jiang, B., and Tsumoto, T. (2005) RNAi-induced gene silencing by local electroporation in targeting brain region. *J Neurophysiol* 93, 594– 602.
- Armstrong, J.N., Brust, T.B., Lewis, R.G. and MacVicar, B.A. (2002) Activation of presynaptic P2X7-like receptors depresses mossy fiber–CA3 synaptic transmission through p38 Mitogen-Activated Protein Kinase. *The Journal of Neuroscience*, 22(14): 5938-5945.
- Aston, C., Jiang, L. and Sokolov, B.P. (2005) Transcriptional profiling reveals evidence for signaling and oligodendroglial abnormalities in the temporal cortex from patients with major depressive disorder. *Molecular Psychiatry*, 10(3):309-22.
- Atkinson, L., Batten, T.F., Moores, T.S., Varoqui, H., Erickson, J.D., Deuchars, J., (2004) Differential co-localisation of the P2X7 receptor subunit with vesicular glutamate transporters VGLUT1 and VGLUT2 in rat CNS. *Neuroscience* 123, 761–768.
- Babcock, A.M., Standing, D., Bullshields, K., Schwartz, E., Paden, C.M., Poulsen, D.J. (2005) In vivo inhibition of hippocampal Ca<sup>2+</sup>/Calmodulin-dependent protein kinase II by RNA interference. *Mol Ther.: J. Am. Soc. Gene Ther.* Jun;11(6):899-905.
- Barden, N. at al., European Patent Application, Bulletin 2004/43.
- Barden, N., Harvey, M., Gagne, B., Shink, E., Tremblay, M., Raymond, C. et al. (2006) Analysis of single nucleotide polymorphisms in genes in the chromosome 12Q24.31 region points to P2RX7 as a susceptibility gene to bipolar affective disorder. *American Journal of Medical Genetics Part B (Neuropsychiatric Genetics)* 141B:374–382.
- Bartel, D.P. (2004) MicroRNAs: genomics, biogenesis, mechanism, and function. *Cell* 116, 281-297.
- Bennett, M.R. (2007) Synaptic P2X7 receptor regenerative-loop hypothesis for depression. *Aust N Z J Psychiatry*, Jul;41(7):563-71.
- Brummelkamp, T.R., Bernards, R., Agami, R. (2002) A system for stable expression of short interfering RNAs in mammalian cells. *Science*. Apr 19;296(5567):550-3.
- Burger, C., Gorbatyuk, O.S., Velardo, M.J., Peden, C.S., Williams, P., Zolotukhin, S. et al. (2004) Recombinant AAV viral vectors pseudotyped with viral capsids from serotypes 1, 2, and 5 display differential efficiency and cell tropism after delivery to different regions of the central nervous system. *Molecular Therapy*, Aug;10(2):302-17.

- Burnstock, G. (1996) P2 purinoceptors: historical perspective and classification. *Ciba Foundation Symposium* 198 p1-34.
- Burnstock, G. (2001) Purinergic signalling in development. *Handbook of experimental Pharmacology*, Vol 151/I. Purinergic of pyrimidinergic signalling I. Springer-Verlag Berlin, p 89-127.
- Cabrini, G., Falzoni, S., Forchap, S.L., Pellegatti, P., Balboni, A., Agostini, P. Et al. (2005) A His-155 to Tyr polymorphism confers gain-of-function to the human P2X7 receptor of human leukemic lymphocytes. *J Immunol.*, Jul 1;175(1):82-9.
- Cao, L., Jiao, X., Zuzga, D.S., Liu, Y., Fong, D.M., Young, D., et al. (2004) VEGF links hippocampal activity with neurogenesis, learning and memory. *Nat Genet* 36, 827–835.
- Carmell, M.A., Zhang, L., Conklin, D.S., Hannon, G.J., and Rosenquist, T.A. (2003) Germline transmission of RNAi in mice. *Nat Struct Biol* 10, 91–92.
- Cearley, C.N. and Wolfe, J.H. (2006). Transduction characteristics of adeno-associated virus vectors expressing cap serotypes 7, 8, 9, and rh10 in the mouse brain. *Mol Ther* 13: 528–537.
- Chakfe, Y., Seguin, R., Antel, J.P., Morissette, C., Malo, D., Henderson, D. and Seguela, P. (2002) ADP and AMP induce Interleukin-1 $\beta$  release from microglial cells through activation of ATP-primed P2X7 receptor channels. *The Journal of Neuroscience*, 22(8): 3061-3069.
- Chen, Y., Chen, H., Hoffmann, A., Cool, D.R., Diz, D.I., Chappell, M.C., Chen, A.F., Morris, M. (2006) Adenovirus-mediated small-interference RNA for in vivo silencing of angiotensin AT1a receptors in mouse brain. *Hypertension*. Feb 47(2): 230-7.
- Chirumamilla, S., Sun, D., Bullock, M.R., Colello, R.J. (2002) Traumatic brain injury induced cell proliferation in the adult mammalian central nervous system. *Journal of Neurotrauma*, 19(6); 693–703.
- Chou, J., Kern, E.R., Whitley, R.J. and Roizman, B. (1990) Mapping of herpes simplex virus-1 neurovirulence to  $\gamma$ 134.5, a gene nonessential for growth in culture. *Science* 250: 1262-6.
- Crooke, S.T. (2000) Potential roles of antisense technology in cancer chemotherapy. *Oncogene*; 19:6651-9.
- Cunha, R.A., Ribeiro, J.A. (2000) ATP as a presynaptic modulator. *Life Sciences* 68; 119–137.
- Davies, W. (2005) Knockdown not knockout. *Drug Discov Today* 10, 157– 158.

Deuchars, S.A., Atkinson, L., Brooke, R.E., Musa, H., Milligan, C.J., Batten, T.F., Buckley, N.J., Parson, S.H., Deuchars, J. (2001) *The Journal of Neuroscience*, 21(18): 7143-7152.

Di Virgilio, F., Borea, P.A., Illes, P. (2001) P2 receptors meet the immune system. *Trends Pharmacol. Sci.* 22, 5–7.

Dorn, G., Patel, S., Wotherspoon, G., Hemmings-Mieszczak, M., Barclay, J., Natt, F.J., et al. (2004) siRNA relieves chronic neuropathic pain. *Nucleic Acids Res* 32, e49.

Elbashir, S.M., Lendeckel, W., Tuschl, T. (2001) RNA interference is mediated by 21- and 22-nucleotide RNAs. *Genes Dev.* 15, 188-200.

Erb, L., Liao, Z., Seye, C.I. and Weisman, G.A. (2006) P2 receptors: intracellular signaling. *Pflugers Arch - Eur J Physiol* 452: 552–562.

Federici T., Boulis N. (2007) Gene therapy for peripheral nervous system diseases. *Curr Gene Ther.* Aug;7(4): 239-48.

Ferrari, D., Chiozzi, P., Falzoni, S., Dal Susino, M., Collo, G., Buell, G., Di Virgilio, F. (1997) ATP-mediated cytotoxicity in microglial cells. *Neuropharmacology* 36, 1295–1301.

Fire, A., Xu, S., Montgomery, M.K., Kostas, S.A., Driver, S.E. and Mello, C.C. (1998) Potent and specific genetic interference by double-stranded RNA in *Caenorhabditis elegans*. *Nature*. 1998 Feb 19;391(6669):806-11.

Fumagalli, M., Brambilla, R., D’Ambrosi, N., Volonte, C., Matteoli, M., Verderio, C., Abbracchio, M.P. (2003). Nucleotide-mediated calcium signaling in rat cortical astrocytes: role of P2X and P2Y receptors. *Glia* 43, 218–303.

Grosshans, H., Slack, F.J. (2002) Micro-RNAs: small is plentiful. *J Cell Biol.* Jan 7;156(1):17-21.

Gurney, M.E., Pu, H., Chiu, A.Y., Dal Canto, M.C., Polchow, C.Y., Alexander, D.D., et al. (1994) Motor neuron degeneration in mice that express a human Cu,Zn superoxide dismutase mutation. *Science* 264, 1772– 1775.

Harper, S.Q., Staber, P.D., He, X., Eliason, S.L., Martins, I.H., Mao, Q., et al. (2005) RNA interference improves motor and neuropathological abnormalities in a Huntington’s disease mouse model. *Proc Natl Acad Sci U S A* 102:5820–5825.

Hassani, Z., Lemkine, G.F., Erbacher, P., Palmier, K., Alfama, G., Giovannangeli, C., et al. (2005) Lipid-mediated siRNA delivery down-regulates exogenous gene expression in the mouse brain at picomolar levels. *J Gene Med* 7, 198– 207.



- Hommel, J.D., Sears, R.M., Georgescu, D., Simmons, D.L. and DiLeone, R.J. (2003) Local gene knockdown in the brain using viral-mediated RNA interference. *Nat Med* 9, 1539–1544.
- Hoyer D. (2007) RNA interference for studying the molecular basis of neuropsychiatric disorders. *Curr Opin Drug Discov Devel*, Mar;10(2):122-9.
- Illes, P. and Ribeiro, J.A. (2004) Neuronal P2 Receptors of the Central Nervous System. *Current Topics in Medicinal Chemistry* 2004, 4, 831-838 831.
- Khakh, B.S., Gittermann, D., Cockayne, D.A., Jones, A. (2003) ATP modulation of excitatory synapses onto interneurons. *J. Neurosci.* 23, 7426–7437.
- Kim, M., Spelta, V., Sim, J., North, R.A., Surprenant, A. (2001) Differential assembly of rat purinergic P2X7 receptor in immune cells of the brain and periphery. *J. Biol. Chem.* 276, 23262–23267.
- Klein, R.L., Dayton, R.D., Tatom, J.B., Henderson, K.M. and Henning, P.P. (2007) AAV8, 9, Rh10, Rh43 Vector gene transfer in the rat brain: effects of serotype, promoter and purification method. *Molecular Therapy*; 16-1, 89-96.
- Kochanek, S., Clemens, P.R., Mitani, K., et al. (1996) A new adenoviral vector: replacement of all viral coding sequences with 28 kb of DNAindependently expressing both full-length dystrophin and  $\beta$ -galactosidase. *Proc Natl Acad Sci U S A* 93: 5731-6.
- Köles, L., Furst, S., Illes, P. (2005). P2X and P2Y receptors as possible targets of therapeutic manipulations in CNS illnesses. *Drug News Perspect*, Mar;18(2):85-101.
- Konishi, Y., Stegmuller, J., Matsuda, T., Bonni, S. and Bonni, A. (2004) Cdh1-APC controls axonal growth and patterning in the mammalian brain. *Science* 303, 1026–1030.
- Kukley, M., Stausberg, P., Adelman, G., Chessell, I.P., Dietrich, D. (2004) Ecto-nucleotidases and nucleoside transporters mediate activation of adenosine receptors on hippocampal mossy fibers by P2X7 receptor agonist 20-30-O-(4-benzoylbenzoyl)-ATP. *J. Neurosci.* 24, 7128–7139.
- Li, C., Parker, A., Menocal, E., Xiang, S., Borodyansky, L., Fruehauf, J.H. (2006) Delivery of RNA interference. *Cell Cycle* 5:18, 2103-2109, 15 September.
- Lingor, P., Michel, U., Scholl, U., Bahr, M. and Kugler, S. (2004) Transfection of “naked” siRNA results in endosomal uptake and metabolic impairment in cultured neurons. *Biochem Biophys Res Commun* 315, 1126–1133.

- Lucae, S., Salyakina, D., Barden, N., Harvey, M., Gagné, B., Labbé, M. et al. (2006) P2RX7, a gene coding for a purinergic ligand-gated ion channel, is associated with major depressive disorder. *Hum Mol Genet.* Aug 15;15(16):2438-45.
- Makimura, H., Mizuno, T.M., Mastaitis, J.W., Agami, R. and Mobbs, C.V. (2002) Reducing hypothalamic AGRP by RNA interference increases metabolic rate and decreases body weight without influencing food intake. *BMC Neurosci* 3, 18.
- McQuillin, A., Bass, N.J., Choudhury, K., Puri, V., Kosmin, M., Lawrence, J. et al. (2008) Case-control studies show that a non-conservative amino-acid change from a glutamine to arginine in the P2RX7 purinergic receptor protein is associated with both bipolar- and unipolar-affective disorders. *Mol Psychiatry*, Feb 12.
- Michael, U., Malik, I., Ebert, S., Bahr, M., Kugler, S. (2005) Long-term in vivo and in vitro AAV-2-mediated RNA interference in rat retinal ganglion cells and cultured primary neurons. *Biochemical and Biophysical Research Communications*, 326; 307-312.
- Mirnics, K., Middleton, F.A., Marquez, A., Lewis, D.A. and Levitt, P. (2000) Molecular characterization of schizophrenia viewed by microarray analysis of gene expression in prefrontal cortex. *Neuron* 28, 53– 67.
- Morsy, M.A., Caskey, C.T. (1999) Expanded-capacity adenoviral vectors– the helper-dependent vectors. *MolMed Today*; 5: 18-24.
- Napoli, C., Lemieux, C., and Jorgensen, R.A. (1990) Introduction of a chimeric chalcone synthase gene into petunia results in reversible co-suppression of homologous genes in trans. *Plant Cell* 2, 279–289.
- Neary, J.T., Kang, Y., Willoughby, K.A., Ellis, E.F. (2003) Activation of extracellular signal-regulated kinase by stretch-induced injury in astrocytes involves extracellular ATP and P2 purinergic receptors. *J Neurosci.* Mar 15;23(6):2348-56.
- Nikkah, G., Cunningham, M.G., Jodicke, A., Knappe, U., Bjorklund, A. (1994) Improved graft survival and striatal reinnervation by microtransplantation of fetal nigral cell suspensions in the rat Parkinson model. *Brain Res.* 633: 133-143.
- Nörenberg, W., Illes, P. (2000) Neuronal P2X receptors: localisation and functional properties. *Naunyn-Schmiedeberg's Arch Pharmacol* 362 :324–339.
- North, R.A. (2002) Molecular Physiology of P2X Receptors. *Physiol Rev* 82: 1013–1067.

- Numakawa, T., Yagasaki, Y., Ishimoto, T., Okada, T., Suzuki, T., Iwata, N. et al. (2004) Evidence of novel neuronal functions of dysbindin, a susceptibility gene for schizophrenia. *Hum Mol Genet* 13, 2699–2708.
- Ocker, M., Neureiter, D., Lueders, M., Zopf, S., Ganslmayer, M., Hahn, E.G., Herold, C., Schuppan, D. (2005) Variants of bcl-2 specific siRNA for silencing antiapoptotic bcl-2 in pancreatic cancer. *Gut*; 54:1298-308.
- Panenka, W., Jijon, H., Herx, L.M., Armstrong, J.N., Feighan, D., Wei, T., Yong, V.W., Ransohoff, R.M. and MacVicar, B.A. (2001) P2X7-like receptor activation in astrocytes increases chemokine monocyte chemoattractant protein-1 expression via mitogen-activated protein kinase. *J. Neurosci.* 21, 7135–7142.
- Pankratov, Y.V., Lalo, U.V., Krishtal, O.A. (2002). Role for P2X receptors in long-term potentiation. *J Neurosci.*, Oct 1;22(19):8363-9.
- Pfeifer, A., Ikawa, M., Dayn, Y., and Verma, I.M. (2002) Transgenesis by lentiviral vectors: lack of gene silencing in mammalian embryonic stem cells and preimplantation embryos. *Proc Natl Acad Sci U S A* 99, 2140– 2145.
- Rainov, N.G. and Kramm, C.M. (2001) Vector Delivery Methods and Targeting Strategies for Gene Therapy of Brain Tumors. *Current Gene Therapy*, 1, 367-383 367.
- Ratcliff, F., Harrison, B.D. and Baulcombe, D.C. (1997) A similarity between viral defense and gene silencing in plants. *Science* 276, 1558–1560.
- Ratray, M. and Michael, G.J. (1999) Oligonucleotide probes for in situ hybridization. In *In situ hybridization: a practical approach*. By D. G. Wilkinson. Published in 1999 by Oxford University Press.
- Roberts, J.A., Vial, C., Digby, H.R., Agboh, K.C., Wen, H., Atterbury-Thomas, A., Evans, R.J. (2006) Molecular properties of P2X receptors. *Pflugers Arch - Eur J Physiol* 452: 486–500.
- Rubinson, D.A., Dillon, C.P., Kwiatkowski, A.V., Sievers, C., Yang, L., Kopinja, J., et al. (2003) A lentivirus-based system to functionally silence genes in primary mammalian cells, stem cells and transgenic mice by RNA interference. *Nat Genet* 33, 401–406.
- Rubio, M.E., Soto, F. (2001) Distinct Localization of P2X Receptors at Excitatory Postsynaptic Specializations. *The Journal of Neuroscience*, 21(2): 641-653.
- Sharp, P.A. (1999) RNAi and double-strand RNA. *Genes Dev.* Jan 15;13(2):139-41.

Shine, H.D., Wyde, P.R., Aguilar-Cordova, E., Chen, S.H., Woo, S.L., Grossman, R.G., Goodman, J.C. (1997) Neurotoxicity of intracerebral injection of a replication-defective adenoviral vector in a semipermissive species (cotton rat). *Gene Ther.* Apr;4(4):275-9.

Sim, J.A., Young, M.T., Sung, H.Y., North, R.A., Surprenant, A. (2004) Reanalysis of P2X7 receptor expression in rodent brain. *J. Neurosci.* 24, 6307–6314.

Skaper, S.D., Facci, L., Milani, D. et al. (1990) Culture and use of primary and clonal neural cells. In: Conn PM (ed.). *Methods in Neurosciences*, Vol. 2. San Diego: Academic Press; pp. 17–33.

Sperlagh, B., Kofalvi, A., Deuchars, J., Atkinson, L., Milligan, C.J., Buckley, N.J. and Vizi, E.S. (2002) Involvement of P2X7 receptors in the regulation of neurotransmitter release in the rat hippocampus. *Journal of Neurochemistry*, 81, 1196–1211.

Sperlagh, B., Vizi, E.S., Wirkner, K., Illes, P. (2006) P2X7 receptors in the nervous system. *Progress in Neurobiology* 78 327–346.

Surprenant, A., Rassendren, F., Kawashima, E., North, R.A., Buell, G. (1996) The cytolytic P2Z receptor for extracellular ATP identified as a P2X receptor P2X7. *Science* 272, 735–738.

Taymans, J.M., Vandenberghe, L.H., Haute, C.V., Thiry, I., Deroose, C.M., Mortelmans, L. et al. (2007). Comparative analysis of adeno-associated viral vector serotypes 1, 2, 5, 7, and 8 in mouse brain. *Hum Gene Ther* 18: 195–206.

Thakker D.R., Hoyer D. and Cryan J.F. (2006) Interfering with the brain: Use of RNA interference for understanding the pathophysiology of psychiatric and neurological disorders. *Pharmacology & Therapeutics* 109, 413 – 438.

Thakker, D.R., Hoyer, D. and Cryan J.F. (2006). Interfering with the brain: use of RNA interference for understanding the pathophysiology of psychiatric and neurological disorders. *Pharmacology & Therapeutics* 109, 413 – 438.

Thakker, D.R., Natt, F., Husken, D., Maier, R., Muller, M., van der Putten, H., et al. (2004) Neurochemical and behavioral consequences of widespread gene knockdown in the adult mouse brain by using non-viral RNA interference. *Proc Natl Acad Sci U S A* 101, 17270– 17275.

Thakker, D.R., Natt, F., Husken, D., van der Putten, H., Maier, R., Hoyer, D., et al. (2005) siRNA-mediated knockdown of the serotonin transporter in the adult mouse brain. *Mol Psychiatry* 10, 782–789.

Van den Haute, C., Eggermont, K., Nuttin, B., Debyser, Z., and Baekelandt, V. (2003) Lentiviral vector-mediated delivery of short hairpin RNA results in persistent knockdown of gene expression in mouse brain. *Hum Gene Ther* 14, 1799–1807.

Ventura, A., Meissner, A., Dillon, C.P., McManus, M., Sharp, P.A., Van Parijs, L., et al. (2004) Cre-lox-regulated conditional RNA interference from transgenes. *Proc Natl Acad Sci U S A* 101, 10380–10385.

Verdel, A., Jia, S., Gerber, S., Sugiyama, T., Gygi, S., Grewal, S.I., et al. (2004) RNAi-mediated targeting of heterochromatin by the RITS complex. *Science* 303, 672–676.

Verderio, C., Matteoli, M. (2001) ATP mediates calcium signaling between astrocytes and microglial cells: modulation by IFN-gamma. *J. Immunol.* 166, 6383–6391.

Vianna, E.P., Ferreira, A.T., Naffah-Mazzacoratti, M.G., Sanabria, E.R., Funke, M., Cavalheiro, E.A., Fernandes, M.J. (2002) Evidence that ATP participates in the pathophysiology of pilocarpine-induced temporal lobe epilepsy: fluorimetric, immunohistochemical, and Western blot studies. *Epilepsia* 43 (Suppl 5), 227–229.

Walther, W. and Stein, U. (2000) Viral vectors for gene transfer. *Drugs*. Aug; 60 (2): 249-271.

Wasserman, M. J., Corson, T.W., Sibony, D., Cooke, R.G., Parikh, S.V., Pennefather, P.S., Li, P.P., Warsh, J.J. (2004) Chronic lithium treatment attenuates intracellular calcium mobilization. *Neuropsychopharmacology*. Apr;29(4):759-69.

Whittemore, S.R., Zhang, Y.P., Shields, C.B., Morassutti, D.J., Magnuson, D.S.K. (2002) Optimizing stem cell grafting into the CNS. *Methods Mol. Biol.* 198: 319-326, Humana Press.

Xia, H., Mao, Q., Eliason, S.L., Harper, S.Q., Martins, I.H., Orr, H.T., et al. (2004) RNAi suppresses polyglutamine-induced neurodegeneration in a model of spinocerebellar ataxia. *Nat Med* 10, 816–820.

Xia, H., Mao, Q., Paulson, H.L., and Davidson, B.L. (2002) siRNA-mediated gene silencing in vitro and in vivo. *Nat Biotechnol* 20, 1006– 1010.

Xiao, X., Li, J., Samulski, R.J. (1998) Production of high-titer recombinant adeno-associated virus vectors in the absence of helper adenovirus. *J Virol* 72: 2224-32.

Xie, F.Y., Woodle, M.C. and Lu, P.Y. (2006) Harnessing in vivo siRNA delivery for drug discovery and therapeutic development. *DDT* Volume 11, Number 1/2.

Zhang, Y., Boado, R.J., and Pardridge, W.M. (2003) In vivo knockdown of gene expression in brain cancer with intravenous RNAi in adult rats. *J Gene Med* 5, 1039–1045.